Detection of Mental Task related EEG for Brain Computer Interface Implementation (using SVM classification approach)

by

Tsu-Hui Angel Lin

Submitted to the Department of Electrical Engineering
in partial fulfillment of the requirement for the degree of

Master of Science

at the

UNIVERSITY OF CAPE TOWN

March 2007

Signature of author..... Signed by candidate .....
Department of Electrical Engineering
March, 2007

Statement of Originality

I know the meaning of plagiarism and declared that all work in this document, save for that which is properly acknowledged, is my own.

In memory of Hsu Pi-Shia Lin, my loving grandmother

Acknowledgements

The author wishes to thank the following:

- The project supervisor, Dr. L. John for his guidance throughout this thesis.
- The project supervisor, Professor J. Tapson for his guidance throughout this thesis.
- The National Research Foundation of South Africa for the financial support.
- Professor J. Greene, for many useful suggestions on the classification method.
- The EEG research group, in particular E. Muluh, for the assistance with data acquisition.
- Family and friends for their encouragement.
- Clark, for his persistent editing and loving support.

Abstract

Brain computer interface (BCI) technology provides a method of communication and control for people with severe motor disabilities. This thesis explores the application of Fast Fourier transform and support vector machine (FFT-SVM) to the problem of mental task detection in EEG-based brain computer interface (BCI) implementation.

Two sets of EEG data were gathered from 5 right handed subjects participating in 7 different tasks in which resting with eyes open, eyes closed, and mental arithmetic are real tasks and listening to music, left and right hand movements are imagining tasks. The first data set was gathered using the 128 channel Geodesic Sensor Net (GSN) EEG device, the second uses the single-channel ModularEEG device. The data was analyzed with the proposed detector, and the feasibility of different mental tasks, channel locations, and single channel modularEEG device for BCI implementation was investigated.

The proposed detector consists of data pre-processing, feature extraction, and classification stages. Data was preprocessed offline with MATLAB to remove artifacts by visual inspection, and segmented into one-second epochs. The absolute Fast Fourier transform from 8-30Hz frequency components were found feasible to use as EEG features for mental task detection. A linear support vector machine classifier was applied to the features for classification.

The classification results for the GSN recorded data sets shows that FFT-SVM classifier correctly classified above 80% of data in most of the tasks, and above 90% in 2 out of 5 untrained subjects for imagined music, mental arithmetic and imagined movement tasks in at least one channel. The (Fp1-Fp2) ModularEEG results were similar to the (Fp1-Fp2) GSN results and yield good classification accuracy (above 80% in 3 out of 5 subjects). ModularEEG were also rated as causing less fatigue, compared to the GSN system. This suggests that ModularEEG is a good candidate for BCI implementation.

Table of contents

List of figures

List of Tables

Terminology

Abbreviations

Medical

EEG - Electroencephalogram
ECG - Electrocardiogram
EOG - Electrooculogram
EMG - Electromyogram
ERD - Event related desynchronization
ERS - Event related synchronization
ERP - Event related potential

Systems

BCI - Brain computer interface
GSN - Geodesic Sensor Net
MOD - ModularEEG device

Mathematical

SVM - Support Vector machine
FFT - Fast Fourier transform
SI - Separability Index

Scalp regions

F - Frontal
Fp - Pre-frontal
C - Central
P - Parietal
O - Occipital
T - Temporal

Chapter 1 Introduction

1.1 Background

Since the early 1940's, computers have become an increasingly useful tool to human beings. From calculations to simulations, communication and eventually entertainment, computers have played an important role in daily lives. Despite their seemingly infinite functionality, computers today require human control in order to perform the desired tasks. Over the past years, a number of human computer interfaces have been developed, such as the keyboard, mouse, drawing tablet, speech recognition software and tracking interfaces. Some of these interfaces are intuitive, and some are less so. The fact that all these designs require some form of physical input prevents their use by people with certain disabilities. For example, a paraplegic person will not be able to use a mouse nor a keyboard.

With the proliferation of advanced technology, researchers and computer users are looking for new ways for humans to interface with computers. In recent years, attempts to achieve communication based on the analysis of electrical brain signals have begun. The intention was to help people with severe motor disabilities to communicate by providing them with a new supporting tool for communication and control. Advances in machine learning, signal processing, and hardware equipment have made possible the development of brain computer communication systems, or Brain-Computer Interfaces (BCI). A BCI is a system that acquires and analyzes brain (neural) signals with the goal of providing a direct communication channel between the brain and the computer, without going through the usual pathway of peripheral nerves and muscles [1, 2].

Several techniques exist for recording brain activities, such as electroencephalography (EEG), functional magnetic resonance imaging (fMRI) [3] and magnetoencephalography (MEG) [4, 5]. Where EEG makes use of scalp, cortical or depth electrodes for recording, fMRI measures the haemodynamic response related to neural activity in the brain with a large circular magnet scanner, and MEG detects the faint magnetic field that emanates from head using a magnetic detection coil bathed in liquid helium for recording. All of these techniques have the potential to implement a BCI system. Among the current monitoring

methods, scalp recorded EEG is an attractive choice for BCI implementation, as it is non-invasive, low cost, and relatively simple to implement.

Human brainwave patterns vary greatly amongst people, and even for the same person at different times. While one particular method of BCI control may work very well for some users, it may not work at all for the others. No generic implementation of BCI has yet been developed to suit everybody yet. In order to increase the accessibility to BCI systems, a variety of BCI systems has been developed so that the users can choose to use the one that enables them to achieve best controllability. Examples of existing BCI systems are the Mu-wave cursor control system [6], Thought Translation Device (TTD) [7], Event related synchronization/de-synchronization cursor control [8], P3 character recognition [9, 10] and Adaptive Brain computer interface [11].

One implementation of BCI, out of the many, is the mental activity based BCI system. In this type of BCI control, users concentrate on different mental tasks associated with different device commands. The ideal system would perform online detection of user's spontaneous brainwave signals and link these to respective device commands during an initial training phase. The user would then be able to execute different commands by concentrating on the appropriate mental tasks [1, 2].

This thesis focuses on the detection of mental activity using scalp EEG for this type of BCI system implementation. The bulk of the work was on the exploration of various mental activities, and possible scalp locations for brain signal acquisition and classification in BCI system.

1.2 Objectives

As indicated in the previous section, this thesis is involved with the classification of EEG for detection of various mental tasks -- a key step to building a direct brain computer interface system. More specifically, the aims of this research are to:

- Explore the possible mental tasks that are detectable from scalp EEG
- Develop analysis methods for classifying the EEG data, using a linear Support Vector Machine classifier.
- Search for the possible single-channel scalp locations for detection of mental activity related EEG, for use in BCI systems.

- Investigate the possibility of implementing a single-channel BCI system with pre-frontal EEG, using low-resolution ModularEEG hardware [12].

1.3 Scope and limitations

This thesis is limited to the use of scalp EEG and a linear Support Vector Machine classifier for the detection of mental activity. The purpose of this research was to establish whether such a method is feasible and to investigate the issues involved. All experimental datasets were collected from right-handed male subjects by the author using the 128-channel Geodesic Sensor Net [13] device and the ModularEEG hardware.

Comparison of the different EEG devices for BCI implementation was not done in this research.

1.4 Plan of development

Chapter 2 begins with a brief overview of Electroencephalography (EEG) and its issues relevant to the BCI system, and ends with a brief overview of current BCI systems. Chapter 3 introduces the components of a mental task detection system and the methods used in this project. Chapter 4 describes the experimental approach to building a classification method for detection of mental tasks. Chapter 5 and 6 present the results as well as the discussion of results from the classification method. Conclusions and recommendations for future work appear in the final chapters.

Chapter 2 Electroencephalography

The aim of this chapter is to introduce the basic concept of electroencephalography and its role in brain computer interface systems.

2.1 The electroencephalogram

The electroencephalogram (EEG) is the neurophysiologic measurement of the electrical activity of the brain by recording from electrodes placed on to the scalp. It was first measured by Hans Berger in 1929 [14]. It is a graphical representation of the difference in voltage between two scalp locations plotted over time [15].

EEG originates from the synaptic activity of neurons inside the cortex. The individual neurons communicate by sending tiny electrochemical signals to one another, causing the neurons to become polarized and depolarized. Although the resulting electric potentials of a single neuron are far too small to be detected from the scalp, when thousands of these neurons are acting together in a synchronous manner, it produces signals of the magnitude of a few microvolts, which is detectable by an EEG device. Details on brain and neuron structures can be found in Appendix C.1 and C.2.

The human head consists of conductive tissues and skull, which can be modeled as a volume conductor. The process of current flow from the activating neurons, through the tissues towards the recording electrodes is called the volume conduction. This process causes distribution of potentials to spread across the scalp, and allows the EEG to be captured. EEG is therefore a two-dimensional projection of the 3 dimensional activity inside the brain [15]. An example of a multi-channel EEG recording is shown in figure 2.1.

Clinically, electroencephalographers correlate brain functions as well as dysfunctions and diseases with certain patterns of EEG traces on an experimental basis. Because EEGs are usually difficult to evaluate in their raw form, various pre-processing techniques are applied to the EEG before evaluation. Spectral analysis is one of the most popular methods of analyzing EEG. Due to the oscillatory characteristic of EEG, normal EEG signals usually

appear as rhythmical signals and different rhythms usually correspond to different brain states. EEGs are commonly classified into five rhythms according to their frequency range: alpha, beta, theta, delta and gamma. Table 2.1 summarizes the properties of these EEG rhythms, and figure 2.2 shows an example of these rhythms.

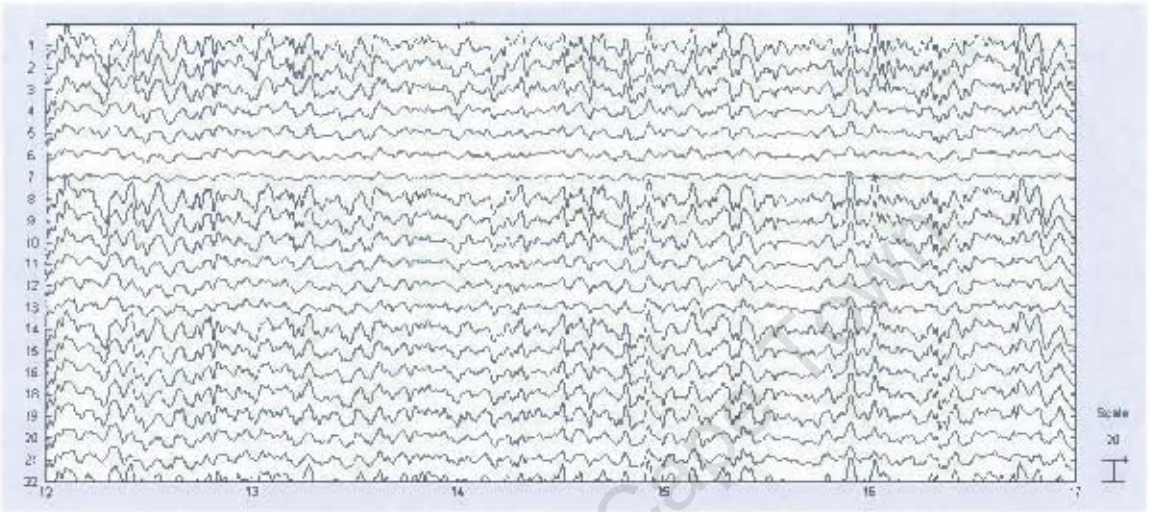

Figure 2.1: An example of a multi-channel EEG recording. The y-axis specifies which channel the waveforms were recorded from, and the x-axis shows the time in seconds.

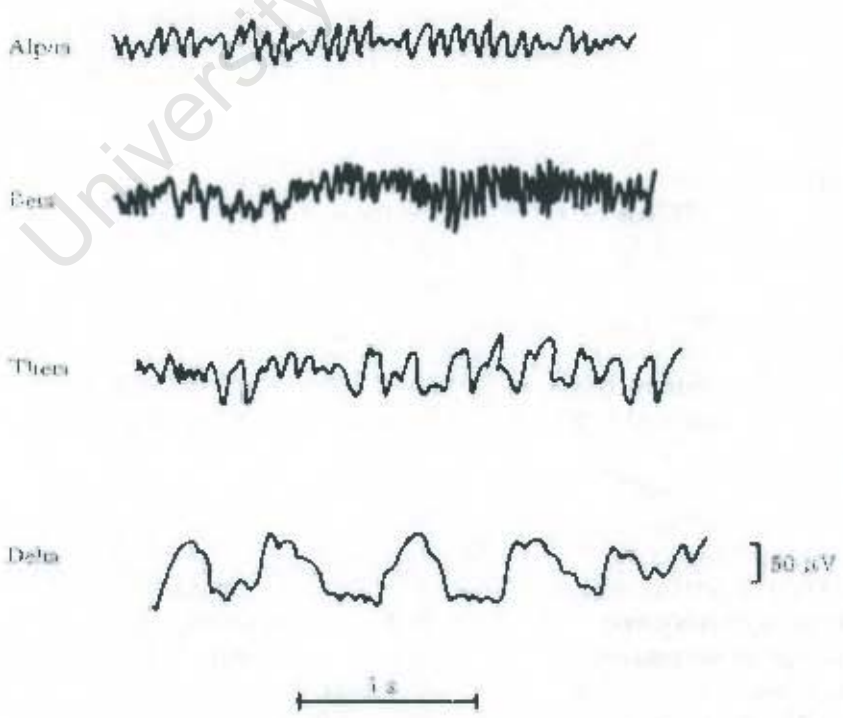

Figure 2.2: Brainwave component frequencies [16]

Table 2.1: Brainwave types with their associated mental states (summarized from [16])

Brainwave type	Frequency range	Associated mental states
Delta	0~4 Hz	deep sleep
Theta	4~7Hz	drowsiness, light sleep
Alpha	8~13 Hz	relaxed, calmed, alert state consciousness
Beta	14~30 Hz	active busy, anxious, thinking, concentrating
Gamma	40+ Hz	high mental activities

2.2 EEG hardware

A typical EEG recording system consists of the following components [17], shown in figure 2.3:

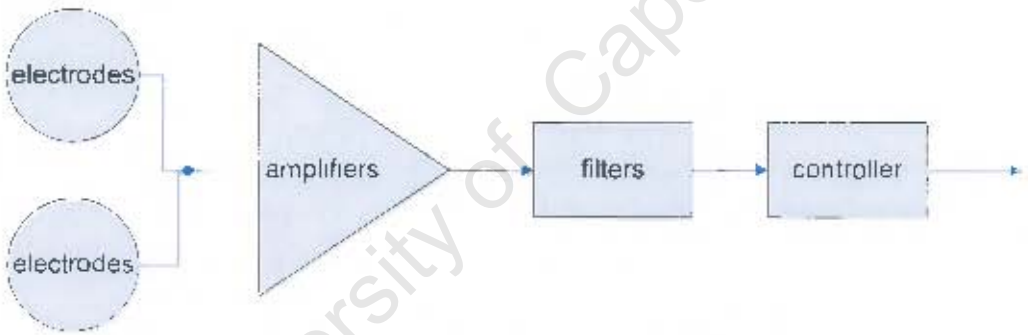

Figure 2.3: Diagram showing the components of a recording system

Electrodes

Permanent electrodes are usually made of silver or gold, as shown in figure 2.4. These button or cup shaped electrodes are applied to a clean scalp or forehead with some conducting solution, gel or paste. The electrodes and the conducting solution serve as a metal-electrolyte interface with the skin, where a flow of ions in the brain due to electric current is converted into a flow of electrons in the electrode. Typical conducting solutions used are sodium or potassium chloride. The metal plated electrodes are glued to the scalp, and are therefore more tolerant to movements and they stay in good condition for long term monitoring [16].

Disposable adhesive electrocardiogram (ECG) electrodes, shown in figure 2.5, are an alternative to the metal electrodes. The disposable electrodes are much cheaper, more convenient and hygienic when compared to the metal electrodes, but suffer from lower sensitivity and tolerance towards movements. Disposable electrodes generally last for less than 72 hours.

Figure 2.4: permanent gold plated electrodes

Figure 2.5: disposable ECG electrode

Amplifiers

EEG signals are very weak (20-100 microvolt) and have high source impedance, therefore differential amplifiers are used to amplify the signal into the range where they can be digitized accurately. Differential amplifiers must have high common-mode rejection ratios (at least 100dB) and high input impedance (at least 100Mohms), in order to minimize loading effects and the distortion of the signal [17].

Filters

Low pass filters remove 50/60Hz electrical noise caused by mains hum before recording. When information of interest lies at frequencies above this line noise, a notch filter is able to remove a narrow band around 50/60Hz, but it can result in phase distortion [17].

Controller

Channels of analog signals are repeatedly sampled at a fixed time interval (sampling rate) and converted to the digital format with an analog-to-digital (A/D) converter. The resolution of the system is determined by the smallest amplitudes that can be sampled. The converter

is interfaced with a recording unit, which functions to communicate to other devices for display or storage of data [17].

2.3 EEG artifacts

In EEG recordings, artifacts are potential shifts that do not originate from the brain. They can be grouped into two categories: artifacts which arise from physiological movement as well as other electrophysiological sources inside the body; and artifacts which result from noise and interference from outside the body. It is just as important to have knowledge about the artifacts as it is about EEG, as artifacts may be mistakenly interpreted as EEG due to similarity in their wave patterns.

The most commonly seen artifacts are described below [18, 19], and an example of some contaminated EEGs are shown in figure 2.6:

Eye blink and eye movement (Electrooculogram - EOG) artifacts

The human eye can be seen as a fixed dipole with a positive pole at the cornea and negative pole at the retina. Eye blinks or other movements produces electrical potentials around the eyes known as electrooculogram (EOG) signals, which propagate over the scalp causing significant artifacts in EEG recordings. EOG amplitudes are usually below 4 Hz and have much larger amplitudes than the amplitudes of the EEG, so they usually drown the EEG signals completely.

Muscle movement (electromyogram - EMG) artifacts

Electromyogram (EMG) signals are electrical potentials generated by skeletal muscles. The movement of muscles also causes artifacts in the EEG, especially those close to the recording electrodes (e.g., the frontalis, orbicularis oculi, and temporalis muscles). EMGs have a broad frequency range of 0-500 Hz, with dominant energy being in the 20-200Hz range. An example of the frequency spectrum of EMG is shown in figure 2.7. Movements such as swallowing, tongue movements, and breathing will cause low frequency artifacts around 1 Hz.

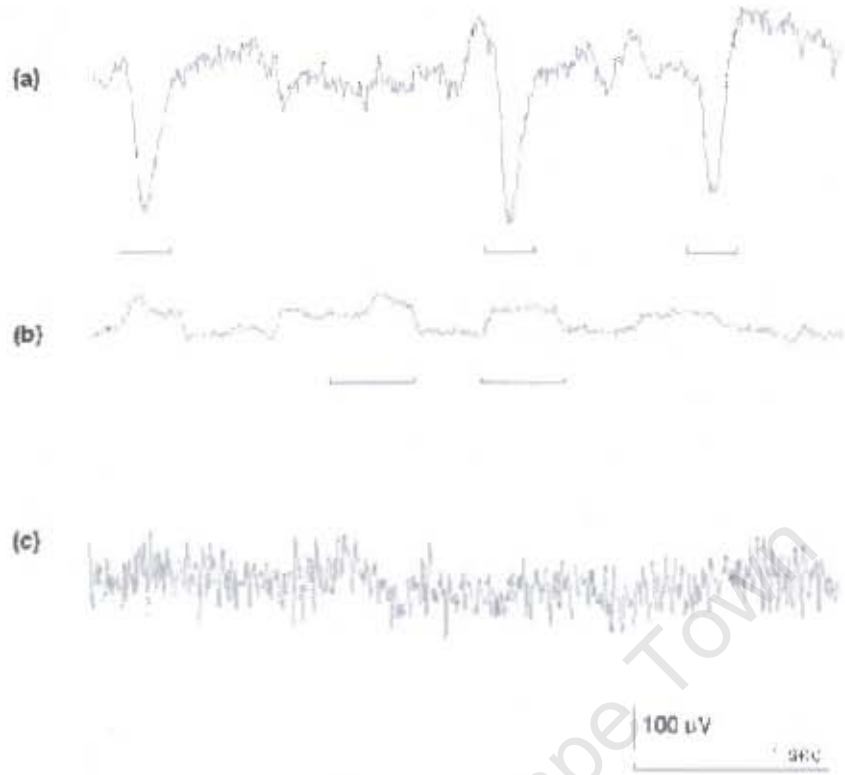

Figure 2.6: Examples of (a) eye blink artifact, (b) horizontal eye movement artifact and (c) muscle artifact in EEG [18].

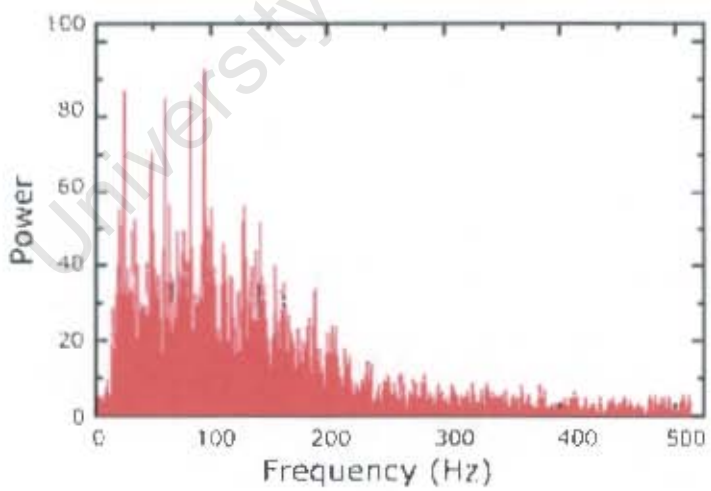

Figure 2.7: Frequency spectrum of the EMG signal detected from the Tibialis Anterior muscle during a constant force isometric contraction at 50% of voluntary maximum [20].

Sweating

Another source of biological artifacts is change of skin resistance due to sweating. This causes potential drifts in the EEG, which may be misinterpreted as slow brain activity.

Electrical interference

External electrical signals may cause unwanted noise in EEG. The most common source of noise is the 50/60Hz mains hum due to power distribution lines and nearby electronic equipment.

Bad electrode contact and movement of wires

The electrodes and connecting wires transmit measured EEG to the EEG device. Artifacts arise when there is a brief change of contact between the electrode and skin, or when the connecting wires were moved and not electrically shielded.

2.4 Electrode nomenclature and montages

In the first International EEG congress in 1947, it was recognized that there should be a standard method of placing electrodes. The study of possible electrode placement methods was done by H.H. Jasper, who proposed the 10-20 electrode placement system [21]. The system uses known neuro-anatomical landmarks for determining the reference points. The electrodes are placed at 10% and 20% of a measured distance between the reference points. Since then the 10-20 system was adopted as the standard for clinical EEG.

Later, the advancement of multi-channel EEG hardware and the advancement of topographic methods to study spontaneous EEG necessitated the standardization of a larger number of channels. In 1985, the 10-20 system was extended to the 10-10 (or 10%) system, increasing the original 21 electrodes to 74 [22]. The 10-10 system is further extended to the five percent electrodes system, containing up to 345 electrode locations [23]. Currently, laboratories studying EEG use even larger numbers of electrodes: measuring EEG with 32, 64, 128 and 256 channels has become quite common [24].

Figure 2.8 illustrates the electrode nomenclature for the 10-20 system. The naming convention of the electrode locations matched with the underlying anatomy of the brain: Fp –

pre-frontal, F – frontal, P – parietal, T – temporal, C – central, and O – occipital, and 'z' refers to electrodes placed at the midline. Additional electrodes (for higher resolution recording) are usually placed between these electrodes, which followed the same naming convention.

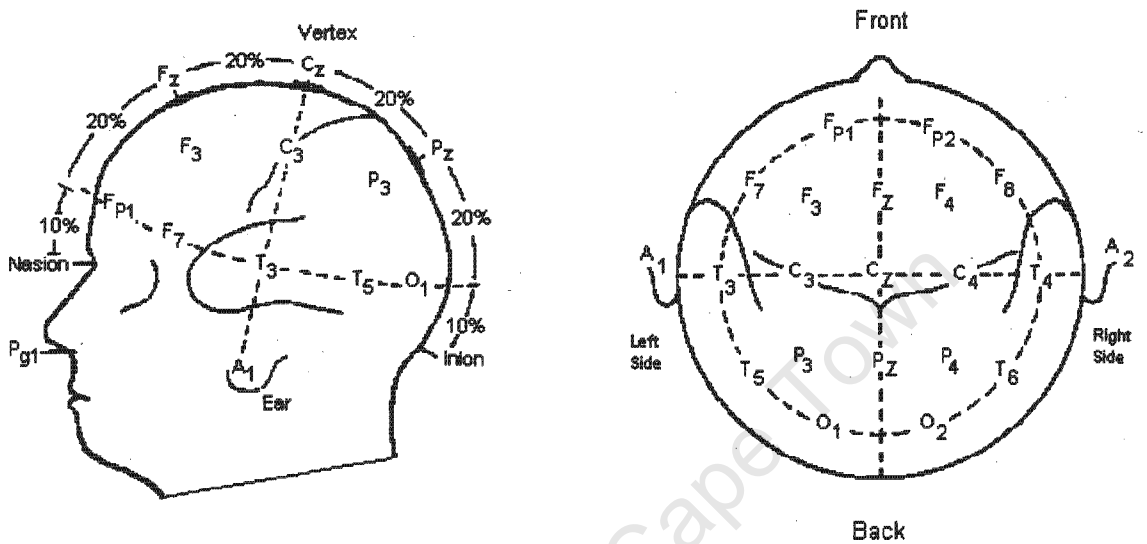

Figure 2.8: The 10-20 International system of electrode placement [25].

Each EEG channel measures the potential difference between two points on the scalp. The arrangement of the electrodes is referred to as a montage. There are three types of montage:

- Bipolar montage – electrodes are arranged in pairs, and each channel measures the potential difference between the pair of electrodes.

- Unipolar or referential montage – the potential differences between each electrode and a common reference electrode are measured. The reference electrode usually has the least relevant activity. Several different reference electrodes for uni-polar recordings were mentioned in the literature. They are the vertex (Cz), left or right mastoids (A1, A2), linked mastoids ((A1 + A2)/2), linked ears, ipsilateral ear, contra-lateral ear, C7 reference and tip of nose.

- Reference free montage – the potential difference between each electrode and a common value is measured. The common value is usually calculated from the rest of the electrodes. Examples are common average reference, weighted average reference and source derivation.

Bipolar montages can be derived from unipolar or reference free montages, by subtracting one unipolar channel from the second to give the bipolar measurement of the pair of electrodes, but not vice versa. Selection of the reference electrode in a unipolar montage is important as EEG distortion may result if the reference electrode channel has high activity. The reference free montage does not have the referencing problem; however, any large amplitude artifacts may cause fluctuation in the reference value, hence causing distortion to the EEG.

2.5 Brain computer interface technology

A brain-computer interface (BCI), sometimes called a neural interface or brain-machine interface, is a system that acquires and analyzes brain (neural) signals with the goal of creating a communication channel directly between the brain and the computer [1, 2]. Such a channel has potentially a number of uses:

- To build an assistive device for communication and control for disabled people.
- To diagnose and monitor neurological disorders.
- To improve man-machine interaction.

For many years, people have speculated that EEG or other measures of brain activity may provide this new channel. Over the past decades, the advancement of computing technology has enabled EEG to be analyzed in real time, and therefore enabled productive BCI research to begin. Many of these research projects [6-9] concentrated on the development of new communication tools for people with severe motor disabilities, so that patients can interact with computers or other systems and hence, communicate directly with the external world using their brain.

2.5.1 Present day BCI systems

BCI research includes non-invasive approaches that use standard scalp recorded EEG as well as invasive approaches that use cortical or depth recording [2]. This thesis will investigate non-invasive approaches using scalp recorded EEG.

Scalp EEG based BCI systems fall into four groups, based on the EEG signal features they use:

Visual evoked potentials

Visual evoked potentials (VEP) are EEG potentials measured at the visual cortex, which are produced by visual stimuli. Commonly used visual stimuli are flashing lights or checkerboards on a video screen that flicker between black on white or white on black or other pairs of contrasting colours. EEG activity will increase in the visual cortex at the stimulating frequency. Hence, by detecting the frequency of the VEP, the direction of the user's eye gaze can be determined, and hence the user's intended action (e.g. where user desires to move a mouse cursor). VEP is an inherent response, so no user training is necessary. [2]

P300 event related potentials

P300 is an event related potential in EEG, typically maximal at the parietal cortex, causing a positive peak at around 300 ms after the stimuli [2]. It is a response modulated by auditory, visual, somatosensory task relevant stimuli. For a stimulus that is unexpected (i.e. a distracter) in the context of the task, P300a is generated. The P300 is a higher cognitive potential that is modulated by attention. An example of P300 BCI is by Farwell and Donchin [9]. The user faces a 6 x 6 grid containing letters, numbers or commands. Each row or column flashes in 125 ms intervals. The user makes a selection by counting the number of times the row or columns containing the desired commands flashes. The user's P300 amplitude will be higher for the rows and columns containing the desired command.

Slow cortical potentials

Slow cortical potentials (SCP) are slow potential shifts of the EEG in the cortex, and usually occur for 0.5-10 s. Birbaumer's team has shown that people can learn to self-regulate their

SCPs by producing either cortical positivity or negativity according to the task requirement, and thus control movement of an object on the computer screen [2, 7]. This type of BCI requires user training, and biofeedback is needed to train the user.

Mu and beta rhythms

Mu and beta rhythms are 8-12, and 18-26 Hz spontaneous EEG activities that are predominant in an awake person at the sensory motor cortex when they are not engaged in processing sensory inputs or motor outputs. When there are movements or preparation for movement, mu and beta rhythms decrease. Wolpaw and McFarland have shown that by imagining left or right hand movement, users are able to produce changes in EEG activity in the sensory motor cortex, that can be used for a 2 dimensional cursor control [6].

BCIs are also grouped into dependent and independent BCI. Dependent BCI does not use the normal output pathway of the brain to send messages, but the activity in those pathways is needed to generate changes in the EEG which could be detected by the computer and translated into messages [2]. VEP based BCI systems are examples of dependent BCI. On the other hand, independent BCIs do not depend on the normal pathways, nor any activity in these pathways to send messages. They use brain activity generated by the user directly to send messages. Mu-rhythm and SCP based BCI systems are independent BCIs.

Because independent BCIs do not use any of the muscular pathways to communicate, they create a completely new channel directly between the brain and the computer, which has much greater theoretical interest to researchers then dependent BCIs. In addition, in the case of severely paralyzed patients who may lack nearly all normal output pathways, independent BCIs would be more useful [2]. The problem with an independent BCI however, is that it does not work for everyone. Some methods may work well for some users but not at all for other people. This is due to the inter-subject variability of EEG. It is therefore better to have a variety of control methods, so that the users have options to choose, and use the ones where they are able to achieve best controllability.

Currently there are six mental task based BCI systems developed around the world, summarized in table 2.2. Feature extraction, classification and training are discussed in the next chapter.

2.5.2 Parts of a BCI system

BCI systems, like all other communication and control systems, have an input, an output, components that translate input signals into output signals, and protocols for determining the operation. A general BCI system consists of three modules, shown in figure 2.9.

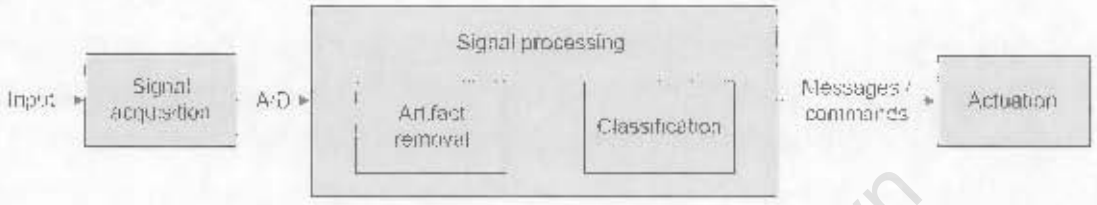

Figure 2.9: Diagram showing modules of a BCI system.

The signal acquisition module captures EEG from the scalp with some EEG hardware, and sends the digitized EEG signal to the signal-processing module. The signal processing module then filters the EEG, removes artifacts, and classifies the EEG into device commands. The Actuation module will receive commands and use them to control assistive devices such as a mouse cursor.

2.5.3 Other factors influencing EEG activity for BCI control

Other mental states or processes that may affect one's ability to maintain control of one's EEG signal include [1]:

- Concentration/focus
- Frustration
- Emotional states (e.g. depression)
- Relaxation
- Fatigue
- Distractions / interruptions
- Motivation / desire
- Intentions
- Other thoughts

Table 2.2: Summary of mental task based BCI systems around the world (modified from [26])

System	Group	Mental tasks/EEG trials	Electrodes	Features, classification algorithm	Application, number of subjects	Training time
Mu-wave cursor control [6]	Wadsworth Center, Albany, USA	mu and beta rhythm modulation	sensorimotor cortex, C3 and C4,	• power in mu- and beta band. • linear classifier	• 2-D cursor control • 4 subjects	Weeks
ERS/ERD cursor control [8]	University of Technology Graz, Austria	imagine left and right hand and foot movement	sensorimotor cortex, bipolar C3-C3' and C4-C4'; 27 electrodes over central areas	• power in alpha and beta band, autoregressive coefficients • Linear discriminate analysis, hidden Markov models	• virtual keyboard, cursor movement • 4 subjects	Days
Thought Translation Device (TTD) [7]	University of Tubingen, Germany	control of slow brain potential	Fz, Cz, Pz	• low pass filtering • Thresholding	• on/off switch • 8 subjects	Months
Adaptive Brain Interface [11]	European Union JRC	relax, imagination of left and right hand movement, cube rotation, subtraction, word association	F3, F4, C3, Cz, C4, P3, Pz, P4	• power in 2Hz wide bands from 8-30Hz • Neural network	• Asynchronous control of mobile robot, virtual keyboard • 15 subjects	Days
	EPFL Switzerland [27]	imagined left and right finger movement, mental counting, object rotation	Fp1, Fp2, F7, F3, F4, F8, T3, T4, C3, C4, T5, P3, P4, T6, O1, O2	• several type of feature vectors • online kernel based algorithm	• 2D object positioning • 6 subjects	Days
	Neil Squire Foundation Canada [28, 29]	recognition of movement imagination against other mental activities	bi-polar recordings: F1-FC1, Fz-FCz, FC2-C2	• bi-scale wavelength analysis • one nearest neighbour classifier	• switch • 7 subjects	Weeks

2.6 Known EEG characteristics for different mental tasks

EEG changes in response to different mental tasks have been widely studied in neuroscience and physiology. Some EEG spectral changes with respect to eyes closed condition, listening to music, mental arithmetic, and imagined movement are summarized below:

Eyes closed

In Srinivasan's experiment [30] for characterizing the spatial structure of alpha component, it was found that alpha power was significantly high at the posterior region of the brain when eyes are closed compared to when eyes are open. See figure 2.10 for topographical maps for average alpha power of 23 adults and 20 children in Srinivasan's experiment.

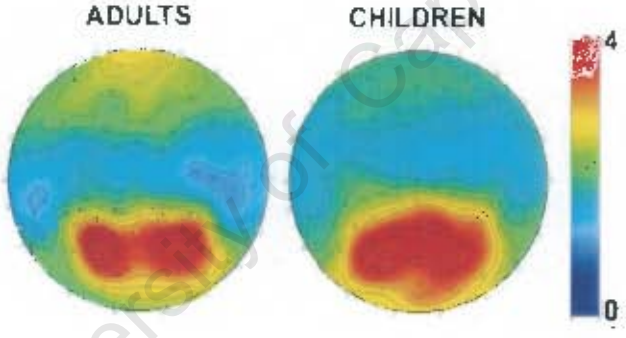

Figure 2.10: Topographic map of averaged alpha power (μV^2) in eyes closed conditions [30]

Maltez et al. [31] compares the variability of power in different frequency bands during resting conditions with cycles of eyes open (5s) followed by eyes closed (5s) repeated for 10mins. Experiment with 57 subjects has shown that, towards the end of the experiment, there were a decrease in alpha and beta power, and an increase in delta and theta power. This observation suggests that EEG frequency estimates varies over time for resting conditions.

Listening to music

The EEG responses from listening to music documented in the literature are diverse and sometimes contradictory. This indicates that EEG responses to music are not easily

predicted, and may depend on the mental state of the subject and the experimental paradigms. Subject could have varied in gender, musical skill level, inherent hearing characteristics, emotional state during recordings, and musical preference.

Ramos and Corsi-Cabrera [32] studied the effect of classical music, silence, and the sound of an infant crying on the EEG spectra of 14 amateur classical musicians. The results indicated that relative theta power increased in response to classical music (rated as a "pleasant" stimulus by subjects), but decreased in response to the sound of an infant crying (rated as an "unpleasant" stimulus by subjects). The study also reported that relative beta power did not change across the three conditions.

In contrast to the findings of Ramos and Cori-Cabrera, Nakamura et al. [33] reported a significant increase in beta power, over the posterior two third of the scalp for listening to music versus resting conditions.

Altenmuller et al. [34] investigated the EEG changes of 16 right-handed students when the students are listening to 4 different type of music: jazz, rock-pop, classical music and environmental sounds. It was found that positive emotional attributions were accompanied by an increase in left temporal activation, and negative emotional attributions by a more bilateral pattern with preponderance of the right fronto-temporal cortex. No differences related to the four stimulus categories could be detected. The study concluded that the EEG response was primarily a measure of the subject's emotional response to the music, instead of a measure of the cognitive awareness of the actual music. Yuan et al. [35] also concluded that changes in the EEG power spectrum when listening to music were closely related to emotions.

Sulimov et al. [36] compared EEG spectral changes during resting and listening to music. It was found that there is an increased of alpha power in the parietal and occipital areas of both hemispheres when the subjects are listening to music.

Pavlygina et al. [37] compared EEG spectral changes when the subjects are resting with eyes open, versus listening to classical and rock music, with varying sound volume. It was found that EEG spectral changes during listening to music are affected by the type and the sound volume of music. When the subjects are listening to moderate classical music, the most prominent changes were in the upper alpha (10.25-13 Hz), beta and gamma bands, with the highest spectral changes in beta and gamma band at the temporal (T4 and T6) area.

On the contrary, when listening to moderate and strong rock music, prominent changes are in the theta and lower alpha (8.25-10 Hz) band, with the highest spectral changes in the beta and gamma bands of the right temporal, central and parietal (T4, C4 and P4) areas. It was also found that these spectral changes from listening to rock music persist for at least 5 minutes after the music as stopped.

Mental arithmetic

Alpha attenuation with mental arithmetic calculation in an eyes-closed state was reported in the original human EEG publication by Berger [14]. Similar results have since been reported by a number of investigators including Glass [38] and Glass and Kwiatkowski [39].

In addition to alpha attenuation (with eyes closed mental arithmetic) Glass and Kwiakowski [39] also reported beta attenuation. It was discovered that the alpha attenuation due to the visual stimulus from opening the eyes is much greater than the attenuation due to mental arithmetic. Volavka et al. [40] also found beta increase in the parietal-temporal channels during mental arithmetic while the subject's eyes were closed.

In the eyes open mental arithmetic scenario, Fernandez et al. [41] have found significant differences in the delta and theta components in right posterior channels and in the beta component in the frontal channels. Recently, Yamaguchi [42] also reported notable increases in parieto-occipital beta using an eyes open paradigm.

Imagined movement

Imagined movement related EEG has been studied by many research groups. Pfurtscheller et al, McFarland et al. and Neuper et al. [43-45] have all reported alpha and beta frequency changes in the sensorimotor scalp areas (C3, C4) during imagined movement tasks.

Alpha and beta changes in the sensory motor cortex are referred to as the mu and beta rhythm in the literature. A number of mu and beta rhythm based BCI's have been developed over the last three decades, specifically using the imagined movement paradigm [2].

A mu rhythm based predictor, reported by Peltoranta and Pfurtscheller [46], was applied to a single subject, and was capable of achieving a 85%-90% discrimination accuracy between left and right index finger movement.

McFarland et al. [43] reported mu and beta rhythm variation with both real and imagined hand movement. A single representative combination of mu and beta variation in response to imagined left and right index finger movement was illustrated by Babiloni et al. [47], this were also able to discriminate between the two imagined movements with an accuracy ranged between 69% and 97% using 9 electrodes, with 5 different subjects.

Chapter 3 Approach to mental task detection

In this chapter, previous approaches to mental task detection using EEG for BCI implementation are discussed. Approaches reviewed are within the framework of a generalized mental task detection system consisting of data pre-processing, feature extraction and classification. Emphasis was given to methods that are relevant to the author's approach in later chapters, which forms the signal-processing module of a mental task based BCI system.

3.1 Components of a detection system

Most mental task detection systems can generally be divided into 3 main stages as shown in figure 3.1. These main stages are outlined below:

- Data pre-processing – Continuous EEG data are screened for artifacts, and contaminated data are removed manually or automatically. High pass or low pass filters are usually applied to raw data to remove unwanted high and low frequency noise prior to screening of biological artifacts. The clean data is then segmented into smaller epochs, usually by a sliding window, before further processing.

- Feature extraction – EEG data are mapped into an appropriate feature space, and features that provide good representations for different mental tasks are selected for classification.

- Classification – the extracted EEG features are classified into the different mental tasks. Sometimes it is also useful for the classification results to show the degree of confidence of the classification.

Figure 3.1: Diagram showing components of a mental task detection system

3.2 Data pre-processing methods

3.2.1 Artifact removal

Artifacts are a major challenge in classification of EEG as they cause EEG signals to distort and may even drown the signals completely (e.g. large movements). It is therefore crucial that they are removed before further processing. There are various methods for EEG artifact removal, discussed below [19]:

Filtering

Low frequency artifacts such as eye blinks, eye movement, sweating, and swallowing can be removed to some extent with a 4Hz low pass filter. However, these artifacts generally have much larger amplitudes than EEG, which cause distortion to the EEG that filters cannot remove. Low frequency artifacts also overlap with the delta wave, and filtering will lead to reducing of the delta component of EEG.

High frequency artifacts such as muscle activity can be removed to some extent with a 40Hz low pass filter. However, muscle artifacts have a broad frequency range, with most of the energy between 20~200 Hz (see figure 2.7), which sometimes overlap with beta waves. In that case, filters will not be able to remove them without removing beta components. Because EMG power increases with muscle tension, when dominant EMG frequencies have low power, we could assume that the non-dominant frequency bands have so little power that they will not distort EEG signals.

50Hz mains hum electrical noise is removed with a 50 Hz notch filter or a low pass filter, since EEG signals of interest are usually below 40 Hz. Obviously, a 60Hz notch filter is used in countries where the mains frequency is 60Hz.

Rejection

EEG data epochs contaminated with artifacts can be manually or automatically corrected. Manual artifact rejection requires human labor and artifact identification may be biased. Automatic methods are much faster and more precise; however they may not be as accurate as manual methods, and it is often difficult to set rejection rules for recognizing all different type of artifacts. The success of artifact rejection depends on the quality of detection, and the application for which it is used. For example, applications that involve much movement, such as monitoring of sportspeople's EEGs, will cause unacceptable loss of data. In other applications such as a brain computer interface, its use can be adequate.

Subtraction

This method is only used for removal of EOG artifacts, and is based on the assumption that measured EEG is a linear combination of EEG and EOG. A separate channel is dedicated to measure EOG, and original EEG is recovered by subtracting measured EOG from EEG, using appropriate weights. The disadvantage of the method is the need for an additional EOG channel enclosing the eye muscles, which may be uncomfortable for users, and may adversely affect users' mental activity performance under investigation.

ICA blind source separation

Independent component analysis (ICA) is a relatively recent method for blind source separation. Contaminated EEG data is separated into independent components, components with artifacts are rejected, and the remaining components are merged again to produce artifact free EEG. This method has been shown to perform very well in removal of EOG artifacts, without loss of EEG data [48, 49]. However, ICA requires multi-channel EEG recording, as it assumes that the number of EEG sources equals the number of recording channels. In the case of a BCI system using only a few channels, ICA would not be possible.

Artificial neural networks

EEG data contaminated with different types of artifacts are pre-recorded, segmented into short segments and used to train neural networks for recognition of these artifacts. When EEG data are fed into the network, the trained network detects contaminated epochs that match up with the artifact EEG, and reject the epoch automatically [50, 51].

The success of this method depends on the quality and number of training sets for different kind of EEG artifacts. Larger training sets usually gives better classification results.

3.2.2 Epoch extraction

Epoch extraction refers to the division of continuous signals into shorter segments of data that are processed separately for classification. For obtaining spontaneous EEG features in the frequency domain, such as the weightings of specific spectral bands, equal length epochs are extracted using a sliding window. For obtaining event-related EEG features such as voltage amplitude over the sensory motor cortex from motor imagery, EEG changes are time locked, hence equal length epochs are extracted at a specific time prior to, at the time of, or after the event. Epochs are then averaged to enhance signal to noise ratio before feature extraction.

3.3 Feature extraction methods

Feature extraction is the mapping of the EEG epochs into a feature vector space that is suitable for classification. This process is an integral part of BCI systems as it reduces the amount of processing resources required to represent complex EEG data accurately, and also simplifies the task of discriminating between pattern classes of the original signal. Careful consideration has to be given to this process as selected features have significant influence on the complexity of the classifier. If features contain the relevant information that is highly representative of the different pattern classes, then classification may be a simple task. If, however, the selected features do not capture enough information to distinguish between the different classes, then reliable classification would be difficult to achieve. Features that contain overlapping information may also be undesirable as additional unnecessary information could confuse the classifier or overdetermine the problem [18]. The choice of optimal feature extraction method is dependent on the subject and the mental activity to be detected.

The purpose of the feature extraction process in BCI systems is to extract EEG features that (optimally) encode the user's message. Usually the extracted features are of lower dimensionality than the original signal. A number of feature extraction procedures have been used in mental task based BCI systems. They include spatial filtering, voltage amplitude measurements, Surface Laplacian (SL), and spectral analysis [2]. Some features are in time domain, frequency domain, or both. It is important to ensure that BCI features

are not contaminated with artifacts, as sometimes artifact signals may correlate with the user's intent, and be incorrectly selected as signal features.

Initial selection of signal features may be based on standard guidelines from known locations and temporal and spectral characteristics of EEG supplemented by operator inspection of initial topographical and spectral data from each user [2]. These methods can also be replaced by automated feature selection methods. Commonly used features for mental task detection are described below.

Time domain features

Voltage amplitude measurements of slow cortical potentials (SCP), and event-related potentials (ERP) are time domain features used for BCI control (e.g. the Thought Translation Device, Tubingen, Germany) [7]. The EEG data is first filtered to obtain the frequency components of interest in the time domain. The negative and positive potential shifts of the extracted component are features for classifications into a binary response, e.g. yes/no, accept/reject.

Frequency domain features

EEG signals are rhythmic in nature with characteristic spectral properties. Therefore, spectral estimates of EEG are sometimes a better representation of EEG for classification purposes. Spectral features of EEG can be obtained using Fast Fourier Transform (FFT) [52], or autoregressive (AR) [53] based and wavelet [54] based spectral estimates. Both amplitude and power estimate of frequency bands have been used for BCI control. Mu and beta rhythms measured from the sensory motor cortex are examples of spectral features used in mental imagery BCIs [6, 55].

Other feature selection methods

EEG is also represented with autoregressive (AR) coefficients, by windowing EEG and using an AR feature extraction method to extract AR coefficients. Studies have shown that four coefficients are sufficient in representing several voluntarily modulated EEG signals [56].

Scalp Surface Laplacian (SL) is an alternative way of viewing EEG. It is a measurement of the local current density flowing through the skull into the scalp. SL-transformed data were computed by estimating the power spectral density of windowed epochs. [47]

The common spatial patterns (CSP) method is used in multi-channel EEG feature extraction and channel selection. The idea is to use a linear transform to project multi-channel EEG data into a low-dimensional spatial subspace with a projection matrix. The resulting matrix reflects directions of the most pronounced difference in variance between the two classes of data [57].

The distinction sensitive learning vector quantization (DSLVQ) method is a supervised learning algorithm for feature selection. The method uses a weighted distance function to modify the influence of each feature according to its contribution to correct/incorrect classification of the system. Pfurtscheller's group used DSLVQ on EEG spectral components to select the most relevant frequency components for discrimination between left and right motor imagery [45].

Adaptive Gaussian Representation (AGR) coefficients are also used to represent EEG features for discrimination of mental tasks in BCI [58].

3.4 Classification methods

Once the appropriate EEG features are selected, they are presented to the classifier for classification to discriminate between different mental tasks. Extant BCIs use a variety of classifiers that measure the membership of a feature vector with respect to each mental activity by means of machine learning approaches. Both linear and non-linear classifiers have been studied in the literature for this application, including Linear Discriminant Analysis (LDA), Hidden Markov Classifier, z-scale base Discriminant Analysis (ZDA), artificial neural networks (ANN), support vector machines (SVM), and the extreme learning machine (ELM). Some classifiers such as SVMs are used for feature elimination as well, by discarding features that give poor classification results [59]. See table 2.2 in chapter 2 for a summary of the features and classifiers used in various mental task based BCI systems.

In more recent studies, the SVM have been used more commonly for mental task classification, as SVM have been shown to outperform many classification algorithms in many problems, including BCI [60, 61]. SVMs learn a classification function from training

data, and do not require pre-defined rules to function as a classifier. As a complete set of rules for accurately discriminating EEGs from different mental tasks cannot be easily determined, SVM becomes an attractive method to classify EEG patterns.

Given the promising results from studies that use SVM to classify EEG, it was decided that this research should further investigate the application of SVM to classify EEG.

3.4.1 Support Vector Machines

Support Vector Machines (SVM) are supervised learning systems that uses a hypothesis space of linear functions in a high dimensional feature space, trained with a learning algorithm from optimization theory that implements a learning bias derived from statistical learning theory [62]. SVM was introduced by Vapnik [63] and co-workers, and formulates a computationally efficient way of learning 'good' separating hyperplanes in high dimensional feature space, by controlling the hyperplane margin measures [62].

The simplest model of SVM is the maximal margin classifier. It works for data that are linearly separable in the feature space, and forms the building block of the more complex SVM's. The maximal margin classifier minimizes the classification error by separating the data with a maximal margin hyperplane. The mathematical theory of the SVM is described below, following the same treatment from the SVM book by Christianini [62] and technical report by Gunn [64].

The optimal separating plane

Any type of data that can be represented as a vector in n dimensions and classified by a hyperplane in $n-1$ dimensions. Consider a two-class classification problem, separating a set of training vectors belonging to two separate classes.

$$D = \{(x_1, y_1), \ldots, (x_l, y_l)\}, \; x \in R^n, y \in \{-1, 1\} \qquad (3.1)$$

With a hyperplane,

$$f(x) = \langle w, x \rangle + b \qquad (3.2)$$

Where $(w,b) \in R^n \times R$ are the parameters that control the function and the decision rule is given by $\mathrm{sgn}(f(x))$, and $\mathrm{sgn}(0) = 1$. See figure 3.2: the hyperplane is the solid line, with the positive region above and negative region below. The quantities *w* and *b* are referred to as the *weight vector* and *bias*, terms borrowed from the neural network literature [62]

Many weight vectors can represent the same hyperplane, so we can rescale the weights to $(\lambda w, \lambda b)$, for $\lambda \subset R^1$, without changing the classification decisions. It is appropriate to consider a canonical hyperplane, where parameters *w*, *b* are constrained by

$$\min_i |\langle w, x_i \rangle + b| = 1 \qquad (3.3)$$

A canonical hyperplane therefore has the distance $\frac{1}{\|w\|}$ to its nearest data point. The set of vector is optimally separated if the separating hyperplane separates it without error and with a maximum separation margin between the two classes of points, see figure 3.3. If the weight vector *w* realizes a functional margin of 1 on the positive point x+ and negative point x-, it implies that

$$\langle w, x^+ \rangle + b = +1,$$

$$\langle w, x^- \rangle + b = -1.$$

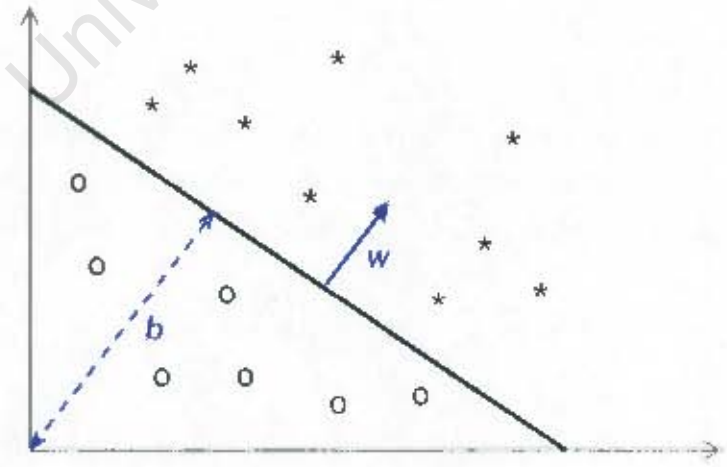

Figure 3.2: A separat ng hyperplane (w,b) for a two-dimensional training set

This can be rewritten as

$$y_i\left[\langle w, x_i\rangle + b\right] \geq 1, \quad i = 1, \ldots, l \tag{3.4}$$

We can then normalize w to compute the geometric margin γ,

$$\begin{aligned} \gamma &= \min_{x_i, y_i = -1} \frac{\left|\langle w, x_i\rangle + b\right|}{\|w\|} + \min_{x_i, y_i = 1} \frac{\left|\langle w, x_i\rangle + b\right|}{\|w\|} \\ &= \frac{1}{\|w\|}\left(\min_{x_i, y_i = -1} \left|\langle w, x_i\rangle + b\right| + \min_{x_i, y_i = 1} \left|\langle w, x_i\rangle + b\right| \right) = \frac{2}{\|w\|} \end{aligned} \tag{3.5}$$

Hence, the hyperplane that has the maximum margin is the one that minimize $\frac{1}{2}\|w\|^2$. It is independent of b, because changing b will shift the plane in the direction normal to itself.

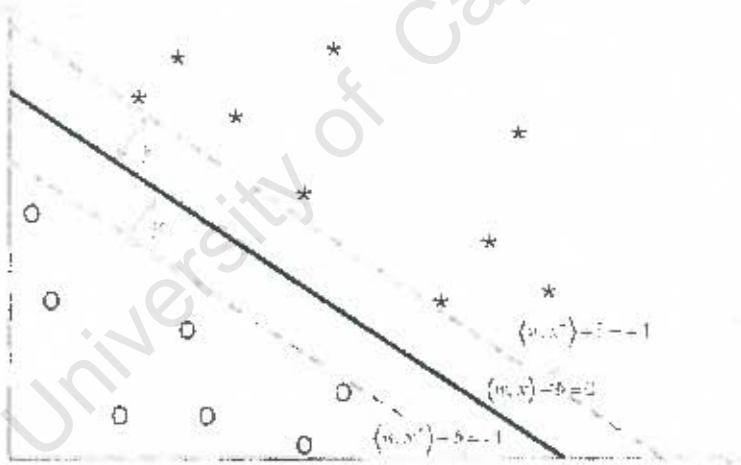

Figure 3.3: The margin of a training set

The hyperplane (w, b) that solves the optimization problem is

$$\begin{aligned} &\text{Minimize}_{w,b} \langle w \cdot w \rangle, \\ &\text{Subject to,} \quad y_i\left[\langle w, x_i\rangle + b\right] \geq 1, \quad i = 1, \ldots, l \end{aligned} \tag{3.6}$$

The saddle point of the Lagrangian gives a solution to this. The optimization problem is transformed into its corresponding dual problem. The primal Lagrangian is

$$L(w,b,\alpha)=\frac{1}{2}\langle w\cdot w\rangle-\sum_{i=1}^{l}\alpha_i\left[y_i\left(\langle w_i\cdot x_i\rangle+b\right)-1\right] \qquad (3.7)$$

Where α are the Lagrange multipliers, $\alpha \geq 0$. Differentiating with respect to w and b gives:

$$\frac{\partial L(w,b,\alpha)}{\partial w}=w-\sum_{i=1}^{l}y_i\alpha_i x_i=0, \quad , \frac{\partial L(w,b,\alpha)}{\partial b}=\sum_{i=1}^{l}y_i\alpha_i=0$$

This relation shows that the hypothesis can be described as a linear combination of the training points, re-substituting the relations obtained back to the primal gives the corresponding dual form,

$$\begin{aligned}L(w,b,\alpha)&=\frac{1}{2}\langle w\cdot w\rangle-\sum_{i=1}^{l}\alpha_i\left[y_i\left(\langle w_i\cdot x_i\rangle+b\right)-1\right]\\&=\frac{1}{2}\sum_{i,j=1}^{l}y_iy_j\alpha_i\alpha_j\langle x_i\cdot x_j\rangle-\sum_{i,j=1}^{l}y_iy_j\alpha_i\alpha_j\langle x_i\cdot x_j\rangle+\sum_{i=1}^{l}\alpha_i \qquad (3.8)\\&=\sum_{i=1}^{l}\alpha_i-\frac{1}{2}\sum_{i,j=1}^{l}y_iy_j\alpha_i\alpha_j\langle x_i\cdot x_j\rangle\end{aligned}$$

with constraints,

$$\begin{aligned}&\alpha_i\geq 1, \quad i=1,\ldots,l\\&\sum_{i=1}^{l}\alpha_i y_i=0\end{aligned} \qquad (3.9)$$

Solving the equations (3.8) with constraints (3.9), determines the Lagrange multipliers, and the optimal weight vector $w=\sum_{i=1}^{l}y_i\alpha_i x_i$ gives the maximal margin hyperplane.

The value of b does not appear in the dual problem, so it is calculated from the primal constraints: [62]

$$b^* = -\frac{\max_{y_i=-1}\left(\langle w^* \cdot x_i \rangle\right) + \min_{y_i=1}\left(\langle w^* \cdot x_i \rangle\right)}{2} \tag{3.10}$$

The hard classifier is then,

$$F(x) = \operatorname{sgn}\left(\langle w^*, x \rangle + b\right) \tag{3.11}$$

Alternatively, a soft classifier may be better used to interpolate the margin, because it will be able to classify testing points that are within the margin [64].

$$F(x) = h\left(\langle w^*, x \rangle + b\right) \quad \text{where} \quad h(z) = \begin{cases} -1 : z < -1 \\ z : -1 \le z \le 1 \\ +1 : z > 1 \end{cases} \tag{3.12}$$

The Karush-Kuhn-Ticker [62] complementarity conditions state that the optimal solutions α, (w,b) must satisfy

$$\alpha_i \left(y_i \left[\langle w, x_i \rangle + b \right] - 1 \right) = 0, \quad i = 1, \ldots, l \tag{3.13}$$

This implies that only points x_i which satisfy

$$y_i \left[\langle w, x_i \rangle + b \right] = 1 \tag{3.14}$$

will have non-zero Lagrange multipliers. Hence in the expression for weight vector only those points are involved, and they are termed *support vectors* (*sv*). If the data are linearly separable, the support vectors would lie on the margin and hence the number of support vectors would be small, see figure 3.4. Consequently, the hyperplane is determined by a small subset of the training points, and removing other points would make no difference to the resulting hyperplane. Therefore *sv* contains all the information needed for classification and may be used to summarize large datasets.

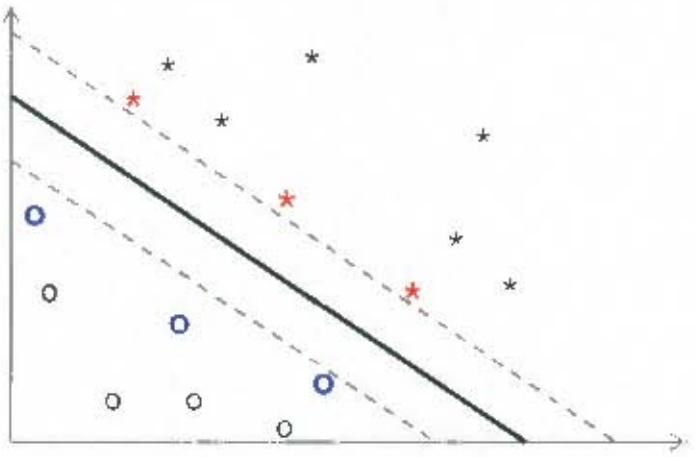

Figure 3.4: A maximal margin hyperplane with its support vectors highlighted

The generalized optimal separating plane

In general, if the data are noisy, there will be no linear separation in the feature space. There are two approaches to generalizing this problem: margin distribution, or use a more complex function to describe the decision boundary. The choice depends on prior knowledge of the problem and an estimate of the noise of the data.

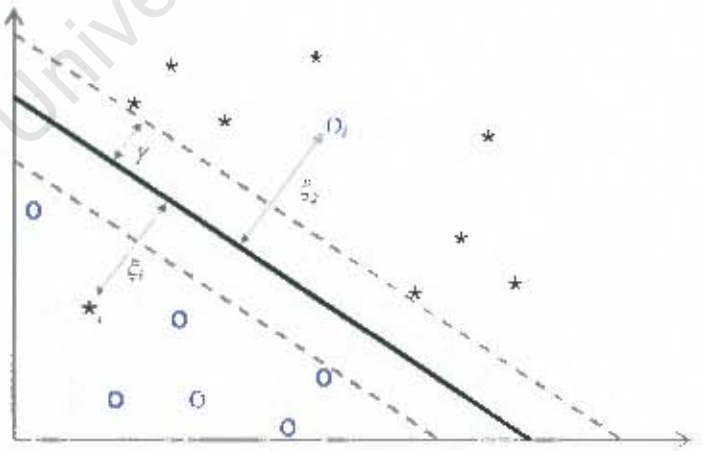

Figure 3.5: The slack variable for a non-linearly separable problem

In the case of margin distribution, an additional cost function associated with misclassification is introduced, see figure 3.5. The margin slack variable ξ is a measure of the classification error, $\xi > 0$. It allow the margin constraints to be violated subject to

$$y_i\left[\langle w, x_i\rangle + b\right] \geq 1 - \xi_i, \quad i = 1,\ldots,l \tag{3.15}$$

The optimal generalized hyperplane is realized by the weight vector that minimizes the function

$$L(w,\xi) = \frac{1}{2}\langle w \cdot w\rangle + C\sum_i \xi_i \tag{3.16}$$

Where C is a given value, and is determined by trial and error. The solution of the problem is given by the saddle point of the Lagrangian

$$L(w,b,\xi,\alpha,\beta) = \frac{1}{2}\langle w \cdot w\rangle + C\sum_i \xi_i - \sum_{i=1}^{l}\alpha_i\left(y^i\left[w^T x^i + b\right] - 1 + \xi_i\right) - \sum_{i=1}^{l}\beta_i\xi_i, \tag{3.17}$$

The corresponding dual function is calculated by differentiating with respect to w, and b,

$$\frac{\partial L}{\partial \beta} = 0 \quad \Rightarrow \quad \sum_i^l \alpha_i y_i = 0$$

$$\frac{\partial L}{\partial w} = 0 \quad \Rightarrow \quad w = \sum_i^l \alpha_i y_i x_i$$

$$\frac{\partial L}{\partial \xi} = 0 \quad \Rightarrow \quad \alpha_i - \beta_i = C$$

And resubstituting the relations back to the primal equation to obtain the new dual objective function: [62]

$$L(w,b,\xi,\alpha,\beta) = \sum_i \alpha_i - \frac{1}{2}\sum_{i,j=1}^{l} y_i y_j \alpha_i \alpha_j \langle x_i \cdot x_j\rangle \tag{3.18}$$

The solution of the problem is

$$\alpha^* = \arg\min_{\alpha} \frac{1}{2}\sum_{i,j=1}^{l} y_i y_j \alpha_i \alpha_j \langle x_i \cdot x_j \rangle - \sum_{k=1}^{l} \alpha_k \qquad (3.19)$$

With constraints

$$0 \le \alpha_i \le C \qquad i = 1,\ldots,l$$

$$\sum_{j=1}^{l} y_i \alpha_i = 0$$

This solution is the same as the maximum margin case described previously, except that the bounds of the Lagrange multiplier are modified; however, the value of C has to be determined, which reflects the amount of noise in the data, and it is usually in the range of 0.001 ~ 10.

3.5 Training

The performances of BCI systems are affected by the quality of EEG signals fed into the system. Thus, the quality of mental practice, degree of imagined effort, and the ability to control thoughts may have major effects on the performance of mental task based BCI systems. In addition to utilizing the signal processing methods, some researchers have investigated the effect of subject training in BCI control. Studies have suggested that training may help subjects to produce more discernible EEG patterns associated with specific mental tasks, by practicing performing these mental tasks regularly, with biofeedback [5, 65]. Training can be with or without biofeedback. Biofeedback training systems use visual (graphics) or audio (sound) feedback to make the trainee aware of what brainwave patterns are present. The feedback system can be set up to reinforce or reduce a particular set of brainwave patterns.

Studies have shown that subject training can improve EEG control and classification accuracy of the EEG patterns for imagined hand movement tasks over the primary motor cortex and frontal area [66].

Chapter 4 Methodology

This chapter describes the experimental setup procedures and analytical method for building a mental task detection system.

The objectives of the experiment are to:

- Explore the possible mental tasks that are detectable from scalp EEG.
- Search for possible single channel scalp locations and EEG frequency bands for detection of mental activity related EEG.
- Investigate whether channel locations and EEG frequency bands for mental task detection are subject specific.
- Investigate the feasibility of building a single channel BCI system using ModularEEG hardware.

4.1 EEG experiment setup

Two sets of EEG data were gathered from subjects participating in 7 different tasks in which resting with eyes open, eyes closed, and mental arithmetic are real tasks and listening to music, left and right hand movements are imagining tasks. The first data set were gathered using the 128 channel Geodesic Sensor Net (GSN) EEG device [13], and the second uses the single-channel ModularEEG device [12]. See Appendix A and B for specification of these devices.

The reason for having two different sets of data is to facilitate the comparison between EEG collected from different devices. The GSN device captures EEG data over the whole scalp, and enables the investigation of scalp locations that are most responsive to EEG changes between specific mental tasks. The ModularEEG device is a relatively lower cost, more portable device as compared to the GSN system, which makes it a viable candidate for BCI implementation.

In this thesis, the electrode locations close to Fp1 and Fp2 above the eye were compared to determine whether single channel recording with ModularEEG is feasible for BCI implementation, as using a single channel is an attractive element for a BCI system.

4.1.1 Participants

Five right-handed subjects were recruited for the study, their mean age being 23 +/- 1 years. All subjects signed consent forms, and were paid for their participation. The International Federation of Clinical Neurophysiology (IFCN) clinical EEG recording standards is a standard that is commonly adopted in clinical EEG recording [67]. The standard requires certain conditions to be met such as subject's medical history and time of recording. Although it is not required for a research based EEG recording to comply with such a standard, an attempt was made to satisfy some of the conditions in order to obtain better quality EEG. According to the subjects' self-report, they had normal vision and hearing, and had no history of neurological disorders. All recordings took place during the daytime, within the same season of year. The experiment has been approved by the Research Ethics Committee; the letter of approval is in Appendix D. The subject consent form used is in Appendix E.

4.1.2 Choice of tasks

To explore the possible mental tasks that can be detectable from scalp EEG, seven tasks were set up for the experiment, as shown in table 4.1.

"Eyes closed" EEG were recorded for the purpose of validating the experiment and the detection system, as it is well documented in the literature that eyes closed EEG have the characteristic of an increase in alpha amplitude at the occipital channels [30]. Mental arithmetic and imagined hand movement EEG were experimented with, as they have been shown to work well in existing BCI systems [8, 11]. To our knowledge there have been no mental task based BCI systems using imagined music tasks, however, researchers have shown that listening to music causes EEG changes in the various frequency bands and channel locations [68]. Therefore, music tasks were included in the experiment to investigate whether it is useful for BCI implementation.

In music and hand movement tasks, both real and imagined EEG were recorded, to compare whether imagined tasks would give similar results to real tasks.

4.1.3 Description of tasks

All tasks were done at rest (stationary) or clenching a soft ball, and were presented to the subject on a computer screen, with white text on black background. See figure 4.1 for an example of a computer screen which the user looks at during the experiment.

For resting tasks 1 and 2, the subjects were asked to rest on a chair, relax and try to keep their minds as blank (inactive) as possible.

Table 4.1: Testing activities for the experiment

Tasks	Activity	Implementation	Description	Duration
1	rest with eyes open	None	rest on a chair with eyes open	5 mins
2	rest with eyes closed	None	rest on a chair with eyes closed	5 mins
3	listen to / imagine relaxing music	Watermark [69]	alternate between listening and imagined listening to relaxing music in 30s intervals	30s x 10 = 5 mins
4	listen to / imagine rock music	The kids aren't alright [70]	alternate between listening and imagined listening to rock music in 30s intervals	30s x 10 = 5 mins
5	Successive additions	Fibonacci series	mentally calculating successive additions with the numbers presented on the screen	5 mins
6	move / imagine right hand movement	clenching a soft ball with force	alternate between clenching and imagine clenching the ball with right hand in 10s intervals	10s x 30 = 5 mins
7	move / imagine left hand movement	clenching a soft ball with force	alternate between clenching and imagine clenching the ball with left hand in 10s intervals	10s x 30 = 5 mins

For music tasks 3 and 4, the recording times were divided into 10 trials of 30 seconds each, where the execution and imagined tasks alternated. The music played and stopped in 30-second time intervals. For the period when the music was not playing, the subjects were instructed to imagine that the music was still playing, and to sing it in their heads.

For arithmetic task 5, numbers appeared on the screen in 5 second intervals, and subjects were instructed to perform addition on the numbers.

For hand movement tasks 6 and 7, the recording time was divided up into 30 trials of 10 seconds each, where the activity alternated between movement and imagined movement of the right or left hand. A short alert sound was played in 10 second intervals to indicate a change from "execution" to "imagine" and vice versa. The hand movement activity was to clench a soft ball with some force.

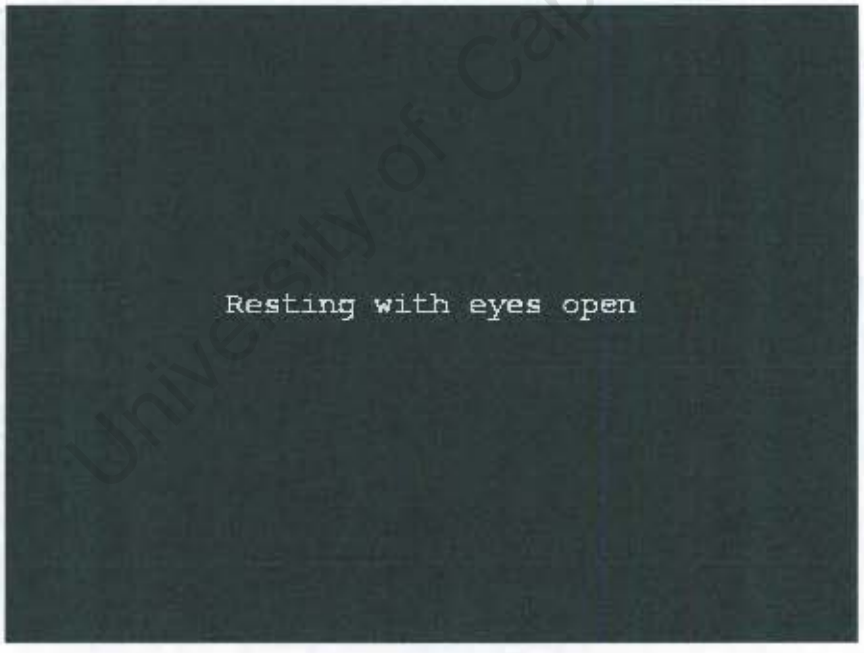

Figure 4.1: Example of the computer screen which the user looks at during the experiment

4.1.4 Equipments and trial procedure

Geodesic Sensor Net recording system

EEG was recorded with the 128-channel Geodesic sensor net system (sample rate = 200Hz, resolution = 16 bits, nominal gain = 1000). E-prime [71] was used to present the tasks to the subject, and send event signals to Net-Station [72], which stored and recorded the captured EEG signals. Figure 4.2 shows the GSN device, and figure 4.3 is an example of the data acquisition configuration. ModularEEG hardware with BrainBay software [73] was used to monitor the EMG activities during the experiment, to ensure that subjects were not moving their muscles when they were instructed to imagine the tasks.

Prior to the recording, the subjects were asked to wash their hair with shampoo to ensure good conductivity during the recording process. The subjects were then fitted with the 128-channel GSN system. Disposable adhesive electrodes were attached to the skin nearest to the motor point of the flexor carpi ulnaris muscle on the subject's left and right arm for EMG monitoring, shown in figure 4.4. See Appendix C.3 for a description of the flexor carpi ulnaris muscle. The setup of the experimental system is shown in figure 4.5.

Figure 4.2: The Geodesic Sensor Net (GSN) device [13].

Figure 4.3: Example of data acquisition configuration [13].

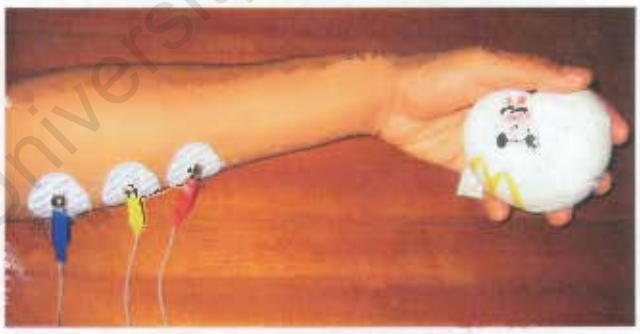

Figure 4.4: EMG monitoring using disposable adhesive electrodes

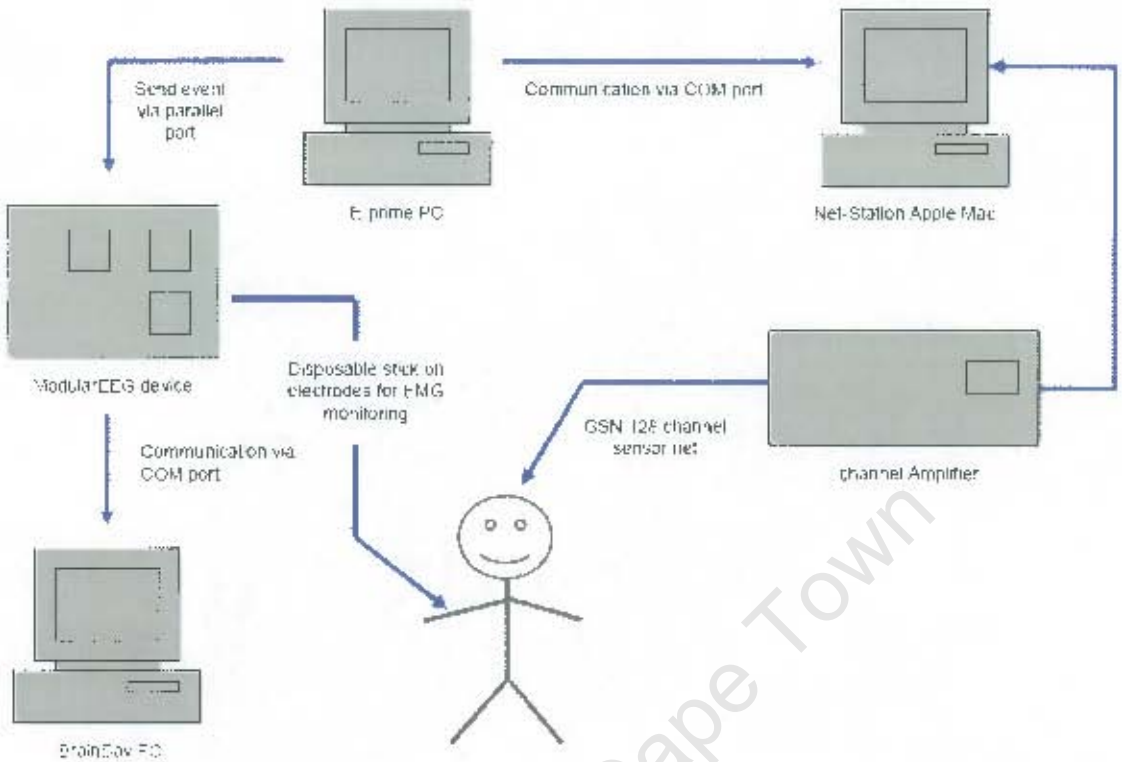

Figure 4.5: Diagram showing the Geodesic Sensor Net recording system setup

The 7 testing tasks were presented to the subject in random order. Five minutes of EEG data were recorded for each activity, with the real and imagined tasks interchanging. The subjects were asked to pay close attention to the testing tasks and to refrain from unnecessary movements. All subjects were familiarized with the trial procedure and the equipments before the commencement of the trial. At the end of the experiment, the subjects were asked to rate the level of fatigue caused by each mental tasks in a 5-step Likert scale [74], with 1 = least fatigue and 5 = most fatigue.

ModularEEG recording system

In this system, single-channel EEG was recorded with ModularEEG hardware (sample rate = 256Hz, resolution = 10 bits, gain = 640), with disposable adhesive ECG electrodes placed at pre-frontal scalp. The device was built from the ModularEEG hardware design from the OpenEEG website [12], which communicates with the PC via RS232 serial port. Figure 4.6 shows the completed hardware. BrainBay [73], an open-source software application that interfaces the ModularEEG device to the computer, was used to record the data into text files. E-prime was used to present the activity to the subject, and to send event signals to a

separate channel on ModularEEG hardware, so that event signals were recorded in parallel with EEG. The setup of the experimental system is shown in figure 4.7.

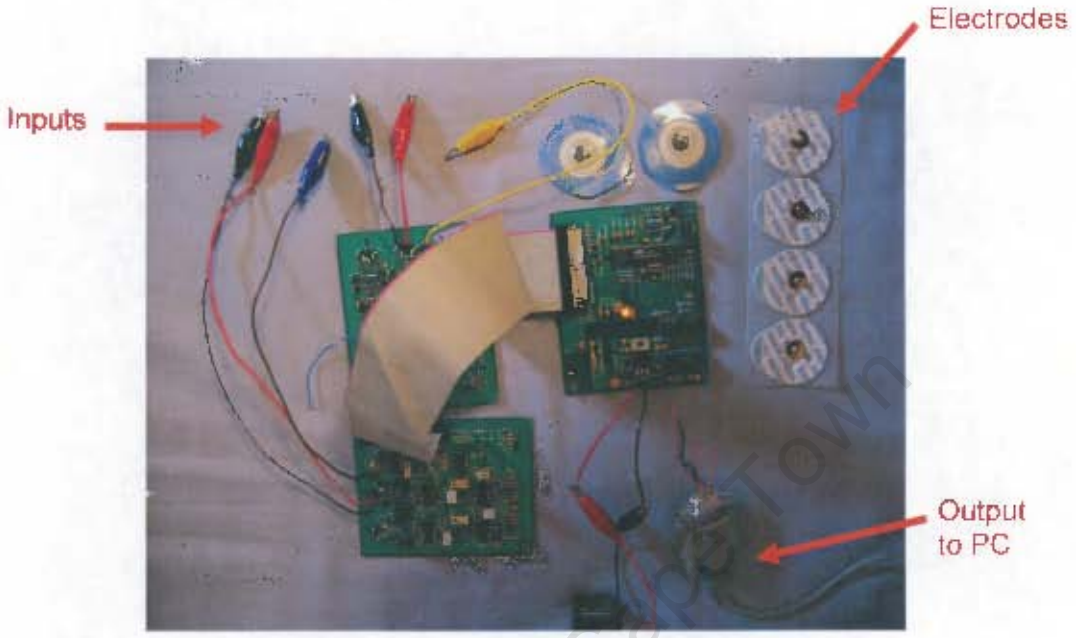

Figure 4.6: ModularEEG device with disposable adhesive ECG electrodes

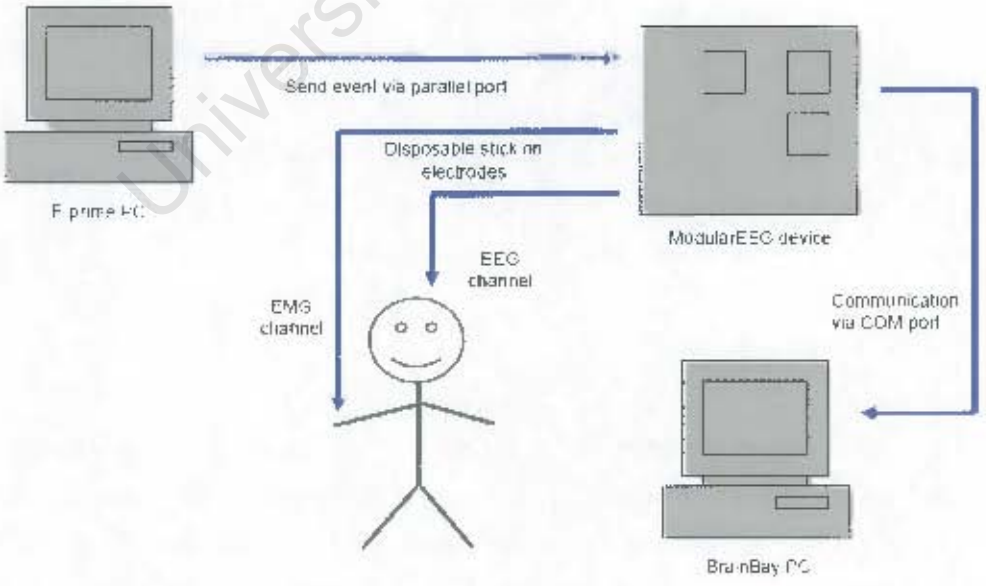

Figure 4.7: Diagram showing ModularEEG recording system setup

Prior to the recording, the subject's forehead was cleaned with methanol and sand paper, to ensure good conductivity. Disposable electrodes were then placed on the subject's forehead at positions close to Fp1 and Fp2 above the eye, here after referred to as Fp1-Fp2, shown in figure 4.8. Disposable adhesive electrodes were also placed on the flexor carpi ulnaris muscle on the subject's right and left arm for EMG monitoring, as in the GSN recording (see figure 4.4). Tasks were presented in random order. Five minutes of EEG data were recorded for each activity. The subjects were instructed to refrain from unnecessary movement, and to relax. All subjects were familiarized with the trial procedures and equipments before commencement of the trial. At the end of the experiment, the subjects were asked to rate the level of fatigue caused by each mental tasks in a 5-step Likert scale, with 1 = least fatigue and 5 = most fatigue.

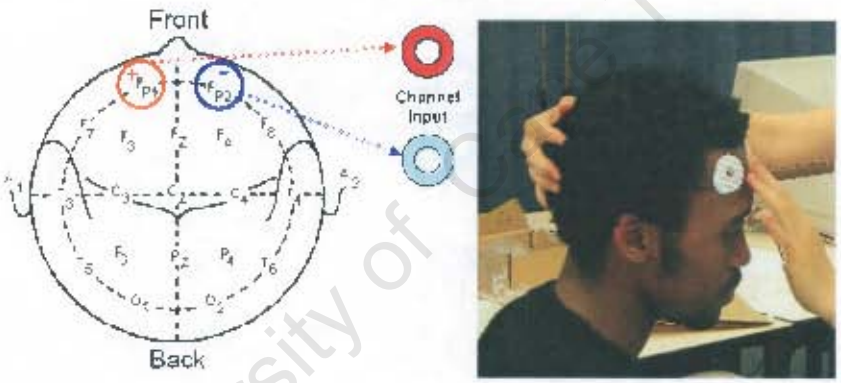

Figure 4.8: Electrode placements illustrated from the perspective of the top of the head

4.2 Data analysis

The recorded data was pre-processed to remove artifacts, and was segmented into 1-second epochs before analysis. Each extracted epoch was Fast Fourier Transformed into its frequency spectrum, with a resolution of 1Hz. Only EEG frequency bands between 4 and 40 Hz were pre-selected due to the movement and drift related noise contamination below 4Hz, as well as mains hum noise in the 50Hz region. From the 4-40Hz band, the 8-30 Hz frequency band was further selected using Thornton's Separability Index [75], which selects the frequency bands that give best separability results. The selected frequency bands were then used as inputs into the SVM. The data was randomly split into 2 groups, half for training and half for testing. The SVM was trained to discriminate between two mental tasks, and output a "1" or "-1" for different tasks. The classification accuracy was calculated from

the percentage of correct prediction on the testing set. Figure 4.9 illustrates the analysis procedure.

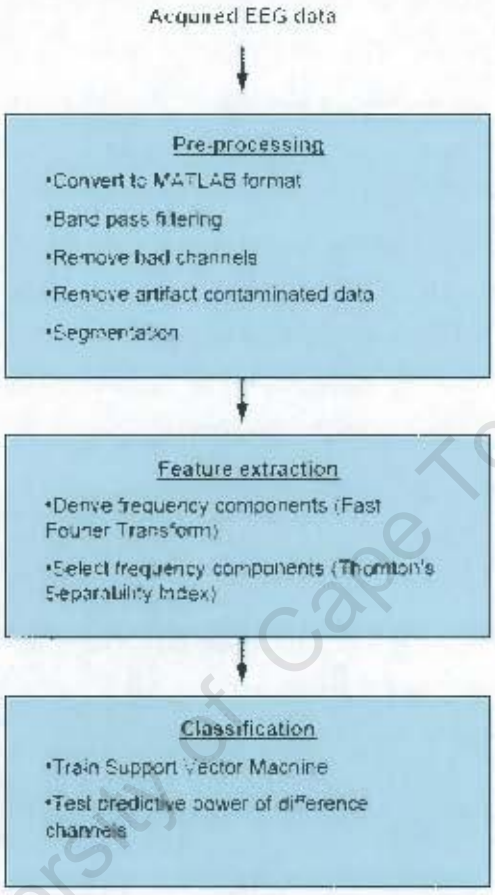

Figure 4.9: Diagram showing the data analysis procedure

4.2.1 Pre-processing

Geodesic Sensor Net recording data

The GSN systems samples EEG signals at 200 Hz. The data were then converted to raw format using Net-Station software, and loaded into MATLAB. The system uses the vertex (electrode 129) as reference electrode; hence, each channel records the potential between the recording electrode and the vertex. The outer ring of electrodes (see figure 4.10) were discarded, leaving 110 channels out of 128 for the analysis. This is because the outer ring of electrodes were not in the region of interest, and were in contact with face and neck muscles which can give rise to noisy data.

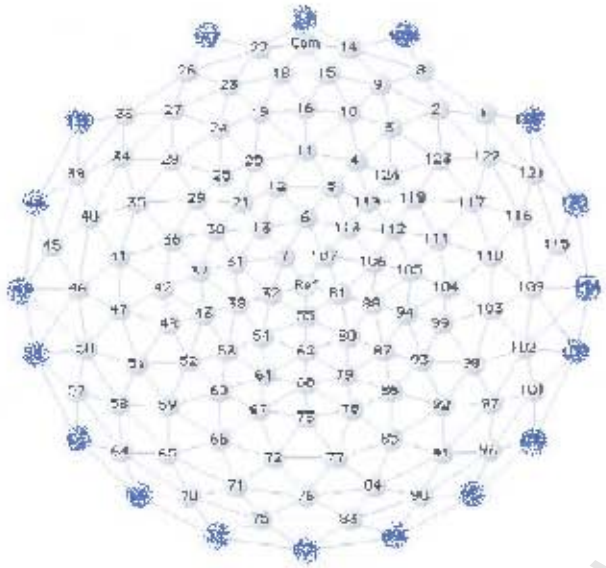

Figure 4.10: Electrode locations for 128 channel Geodesic Sensor Net system. The outer ring of electrodes are shown in blue; they were discarded.

The remaining channels were cleaned offline using the EEGLAB toolbox [76] in MATLAB to remove, by visual inspection, eye blinks and muscle movement artifacts in all channels. The EMG data was screened in parallel with the EEG data for imagined hand movement tasks. If the EMG data indicated that there were movements or muscle tension during the imagined tasks, the corresponding EEG data were rejected. This ensured that all EEG recorded for imagined tasks were not contaminated with movement EEG. The cleaned data was then segmented into 1-second length epochs in each channel. See Appendix G for examples of eye blink and muscle artifacts removed from the recorded data. Alternative techniques such as ICA removal of EOG artifact, or subtraction of EOG channels from EEG, could also be used, but were not implemented here.

ModularEEG recording data

EEG signals were sampled at 256 Hz. EEG voltage data was cleaned offline using the EEGLAB toolbox in MATLAB to remove, by visual inspection, eye blinks and muscle movement artifacts. EMG data was screened in parallel with the EEG data for imagined hand movement tasks. If the EMG data indicated that there were movement or muscle tension during the imagined tasks, the corresponding EEG data were rejected. This ensured

that all EEG recorded for imagined tasks were not contaminated with movement EEG. The cleaned data was then segmented into 1-second length epochs

4.2.2 Fast Fourier Transform

A Fast Fourier Transform is an efficient algorithm for computing the discrete Fourier transform (DFT) and its inverse. It does so by reducing the number of points for computation from $2N^2$ to $2N\log_2 N$. The FFT is performed in MATLAB, using the MATLAB *fft()* function, which is defined as:

Let $x_1, \ldots\ldots, x_N$ be a vector of number length N. The transform X is given by:

$$X(k) = \sum_{j=1}^{N} x(j)\omega_N^{(j-1)(k-1)} \quad \text{where} \quad \omega_N = e^{(-2\pi i)/N} \text{ is an } N^{th} \text{ root of unity.}$$

This will return the DFT vector of x, length N. The frequency band of interest is then selected from the DFT vector.

4.2.3 Thornton's separability index

Thornton's (Geometric) Separability Index (GSI) for a given task f is the fraction of data points whose input nearest neighbour shares the same output class [75].

$$GSI(f) = \frac{\sum_{i=1}^{n} f(x_i) + f(x_i') + 1 \bmod 2}{n} \qquad \text{with} \qquad \begin{aligned} f &= target\ function \\ x &= data\ set \\ x_i' &= nearest\ neighbour\ of\ x_i \\ n &= total\ number\ of\ data \end{aligned}$$

The GSI has a value between 0~1, with 1 indicating a complete geometric separability between the two class of data points, and 0.5 for random distribution of points. The case of 0 GSI is very rare, as it only happens when the data points are arranged like a chessboard, where each point's nearest neighbour belongs to its opposite class.

The GSI was computed for each pair of data sets, for all combinations of frequency component pairs, and results were compared. The frequency components that show higher GSI more frequently were selected as features inputs to the SVM for classification.

4.2.4 Support Vector Machine classifier

A SVM toolbox [64] was used to classify the EEG data in MATLAB, using a linear kernel and C = 0.1. The linear kernel was chosen due to the high dimensionality of the input feature space; non-linear classifiers were therefore not necessary. Both broadband (4-30Hz, 8-32Hz) and narrow band (4-8Hz, 9-13Hz, and 14-30Hz) were used as inputs to the classifier and results compared. The inputs to the SVM were not normalized, as normalization did not improve the classification results. The SVM toolbox was validated with artificial data, described in 4.4.

4.3 Multi-channel analysis

The analysis method for a single channel of data was described in the above section. For a multi-channel analysis, single channel analysis was performed on all the channels, and classification accuracy compared between the channels. Two types of montage were used: average reference, and bi-polar montage.

4.3.1 Average reference montage

The GSN system uses a uni-polar reference montage with the vertex as reference. To obtain an average reference montage, all channels were averaged to obtain the value for the reference electrode, which was then subtracted from each of the channels. This was done in MATLAB using the EEGLAB software.

Support Vector Machine classification result were computed for each channel as well as the broad and narrow bands. The classification accuracy (averaged from 10 cross validations [77]) for each channel were plotted in a head plot. The colours of the head plot indicate the level of classification accuracy, with red showing the highest (above 80%) and green the lowest (50%); see figure 4.11 for an example of the head plot. Head plots were plotted for each mental task versus the resting with eyes open task, as well as each real task versus the corresponding imagined tasks for discrimination.

The GSN electrode numbers corresponding to the brain regions and the terms used to describe these regions are shown in figure 4.12.

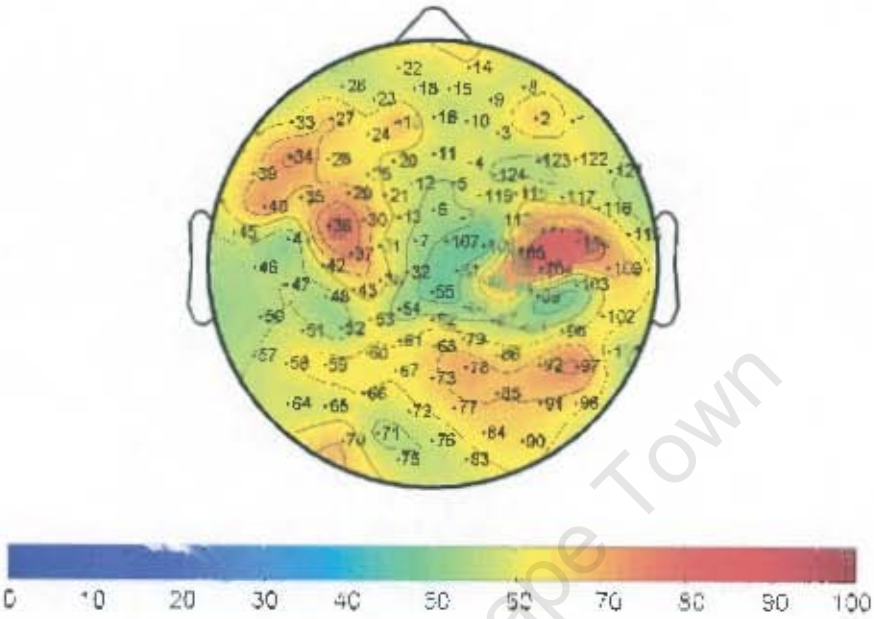

Figure 4.11: An example of a head plot. The colours indicate the SVM classification accuracy between two tasks, with red the highest and green the lowest.

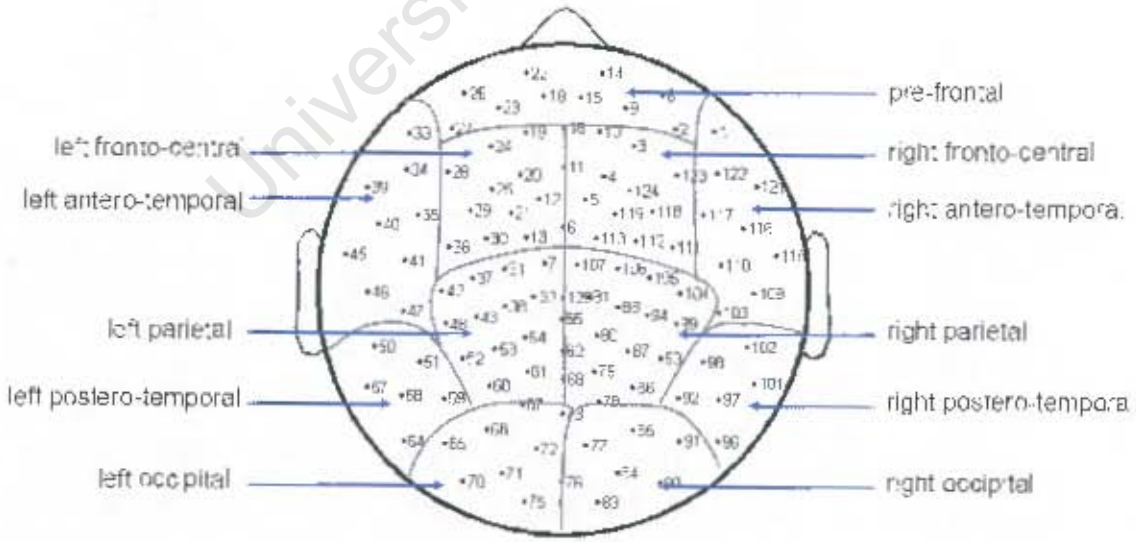

Figure 4.12: A head plot showing the channels grouped into regions corresponding to the terms used for describing these brain regions.

4.3.2 Bi-polar montage

Out of the 110 electrodes in the GSN system, the 19 electrodes corresponding to the 10-20 electrode system coordinates were selected (see figure 4.13), and bi-polar channels were computed from all the possible combinations of the electrodes, by subtracting the channels from one another, resulting in 171 bi-polar channels.

Support Vector Machine classification results were computed for each bi-polar channel for the different pair of mental tasks. Results were plotted in a bi-polar topographical head plot. The colour of the line joining the electrode locations shows the classification accuracy for that channel. Red indicates a classification accuracy of above 90% and blue indicates classification accuracy of above 80%. An example of the bi-polar topographical head plot is shown in figure 4.14.

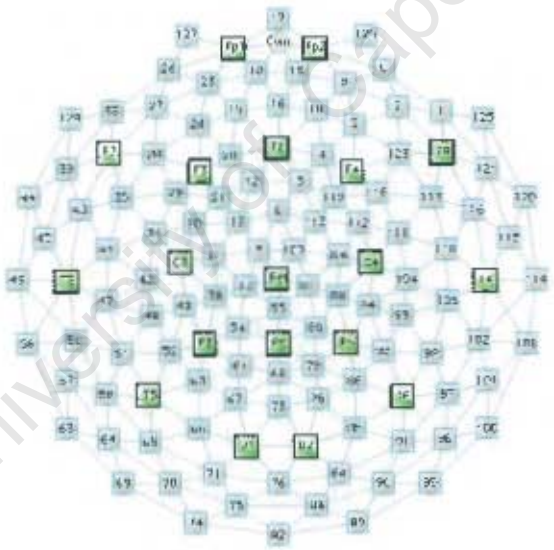

Figure 4.13: 10-20 system electrode location on the 128 channel Geodesic sensor net

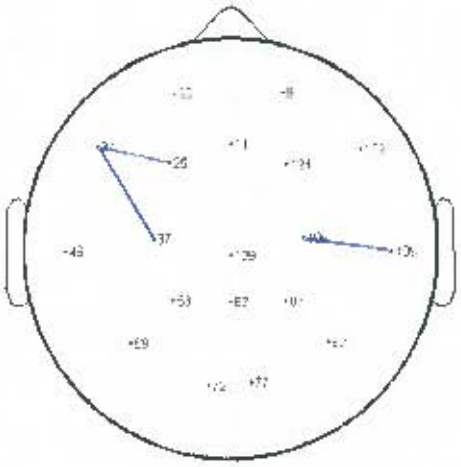

Figure 4.14: An example of a bi-polar topographical head plot. The line colour indicates the SVM classification accuracy between two tasks. Red line: above 90%, blue line: 80%~90%.

4.4 SVM validation

Prior to the analysis of EEG data, the SVM toolbox was tested with artificial data. In MATLAB, sine waves with varying frequencies (in the range from 10-40 Hz) and amplitudes were generated. The sine waves were Fast Fourier Transformed into their frequency spectra, and frequency components from 8-30 Hz were fed into the SVM classification module for classification, to test whether SVM toolbox was able to discriminate known waves accurately. This was used to validate the SVM toolbox, results in Appendix H.

Chapter 5 Experimental results

This chapter is divided into three sections: section 5.1 presents the results of multi-channel EEG recordings from the Geodesic Sensor Net device, and section 5.2 presents the results from single-channel (Fp1-Fp2) EEG recordings using the GSN and ModularEEG device. The reason for further investigating the ModularEEG recording was to determine whether disposable adhesive electrodes and ModularEEG hardware was suitable for brain computer interface implementation. Section 5.3 shows the comparison between the Fp1-Fp2 channel results from the GSN and the modularEEG device.

It was found that the EEG data recorded were very different for each subject. EEG responses to mental tasks were very subject dependent, as there were no common patterns found for each task. No data was combined or averaged across subjects.

5.1 Analysis results for the multi-channel GSN system

Two montages were used to represent the multi-channel GSN recordings: the average reference montage, and the bi-polar montage.

5.1.1 Results from average reference montage

For each subject, the classification accuracy for each mental task versus the "resting with eyes open" task were plotted on a topographical plot, with green indicating no (50%) predictive power, and red indicating high (80% and above) predictive power. Topographical plots were plotted for SVM classification results using alpha (8-13Hz), beta (14-30Hz) and both alpha and beta (8-30Hz) bands, for each subject and each task, shown in figures 5.1-5.7. Topographical plots for real tasks are shown in Appendix F. The high classification channels for each task versus the "resting with eyes open" task are summarized in the tables 5.1-5.12.

Overall, there were more differences than similarities between the results from different subjects, but certain common characteristics of the results were also found:

- The alpha and beta component topographical plots appeared as a linear combination between the alpha and beta topographical plot.
- The topographical plots for real and imagined tasks were similar in both the regions and predictive accuracy.
- The topographical plots for real vs. imagined tasks showed no predictive accuracy for all channels.
- Results from all subjects show low classification in the midline channels (Fz, Cz, Pz).
- Results from all subjects show high classification in the temporal channels.
- Central channels gave lower classification accuracy for "eyes open" vs. "eyes closed" task.
- The alpha component was the main discriminating band for "eyes open" vs. "eyes closed" in the parietal-occipital channels,.
- The beta component was the main discriminating band for "eyes open" vs. music, mental arithmetic, and hand movement tasks.

Eyes open vs. eyes closed

There is generally high classification accuracy over the entire scalp except the central channels (C3, C4, and Cz). The high classification accuracy in the parietal and occipital channels is attributed to the alpha component. Overall, the beta component has low classification accuracy; only subject 1 and 5 showed a high classification. The best predictive channels were mainly in the temporal-occipital scalp. Figure 5.1 shows topographical plots of the classification accuracy for each frequency component. Table 5.1 summarizes the high (above 80%) classification channels, and table 5.2 shows the best predictive channels for each frequency band. The closest 10-20 electrode locations to the channel number are shown in brackets.

Table 5.1: List of channels having classification accuracy of above 80% in each frequency band for tasks "eyes open" vs. "eyes closed".

Eyes open vs. Eyes close	Alpha	beta	alpha+beta
sub 1	None	Fp1, T3, O1, O2	Fp1, T3, O1, O2, P3, P4, Pz
sub 2	T5, T6, O1, O2	none	T5, T6, O1, O2
sub 3	none	none	T5, Pz, P4
sub 4	F3, Fz, F4, Cz, P3, P4, Pz, O1, O2, T5, T6,	T3	F3, Fz, F4, Cz, P3, P4, Pz, O1, O2, T5, T6,
sub 5	P3, P4, O1, O2	few channels near T3, T6, O1	T3, T5, T6, P3, P4, Pz, O1, O2,

Table 5.2: List of best predictive channels in each frequency band for tasks "eyes open" vs. "eyes closed".

eyes open vs. eyes closed	alpha		beta		alpha+beta	
	%	Channel	%	Channel	%	Channel
sub 1	76.98	68 (Pz)	85.28	83 (O2)	86.07	50 (T3)
sub 2	82.85	70 (T5-O1)	69.61	50 (T3)	82.85	70 (T5-O1)
sub 3	77.10	58 (T5)	78.39	40 (F7-T3)	80.20	68 (Pz)
sub 4	86.95	92 (T6)	82.76	46 (T3)	87.24	85 (T6-O2)
sub 5	85.97	85 (T6-O2)	80.80	101 (T6)	87.88	67 (O1)

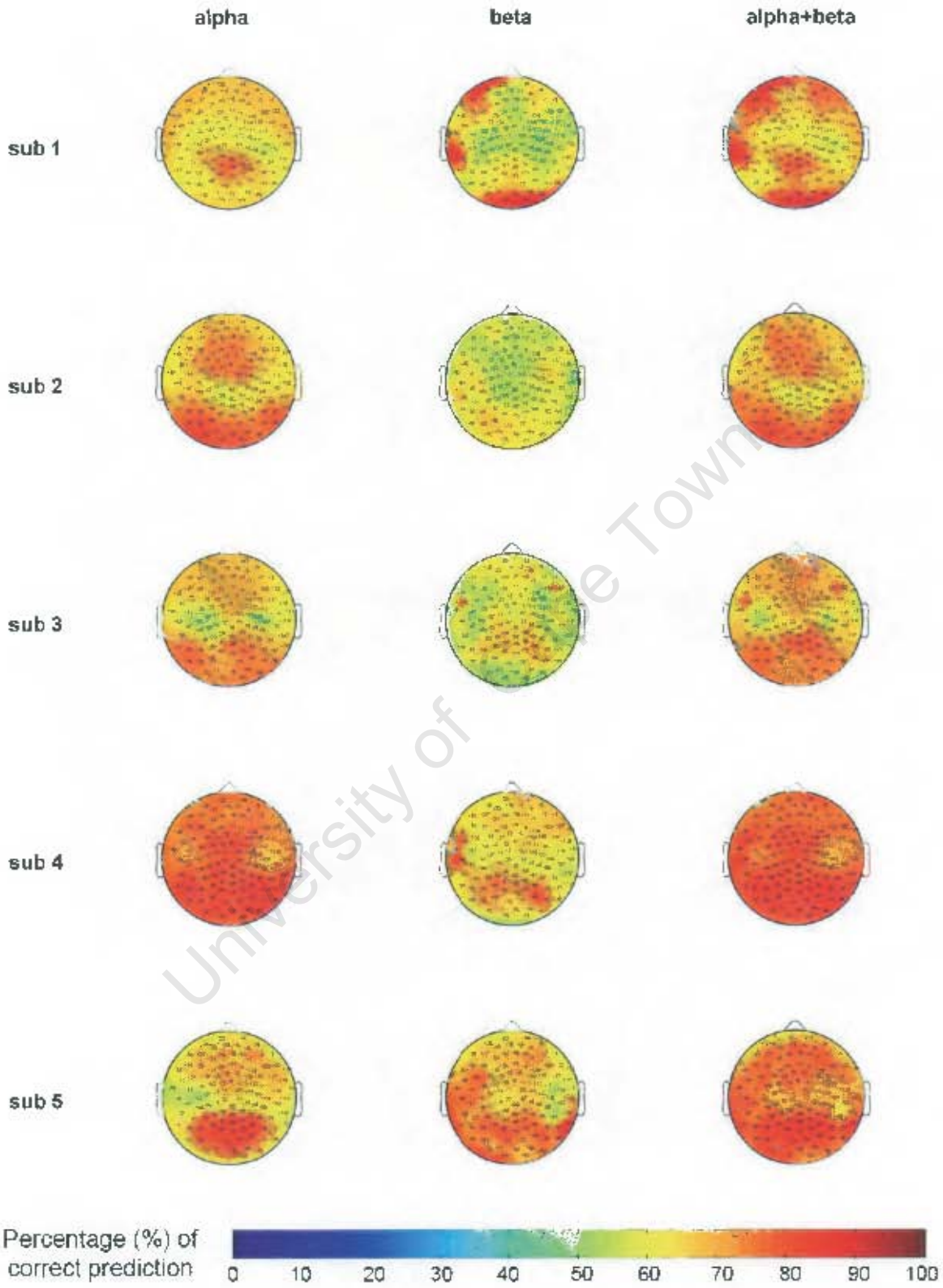

Figure 5.1: Topographical plots showing SVM classification accuracy for task "eyes open" versus "eyes closed", for components alpha, beta, and alpha plus beta.

Eyes open vs. relaxing music

For all subjects, the high classification channels were similar for both the real and imagined listening to the relaxing music – see also figure F.1 in Appendix F. Overall, alpha components had low classification, and beta components were the discriminating band. Subjects 1, 2, 3 and 4 showed similarity in having high classification at temporal channels (T3 or T4, or both), and subject 5 at occipital channels (O1, O2). Figure 5.2 shows topographical plots of the classification accuracy for each frequency component. Table 5.2 summarizes the high (above 80%) classification channels, and table 5.3 shows the best predictive channels for each frequency band. The closest 10-20 electrode locations to the channel number are shown in brackets.

Table 5.3: List of channels having classification accuracy of above 80% in each frequency band for tasks "eyes open" vs. "relaxing music".

eyes open vs. relaxing music	alpha		beta		alpha+beta	
	real	imagine	real	imagine	real	imagine
sub 1	none	none	T3	T3	T3	T3
sub 2	none	none	T3	T3	T3	T3
sub 3	none	none	T4	T4	T4	T4
sub 4	none	none	T3, T4	T3, T4	T3, T4	T3, T4
sub 5	none	none	O1, O2	O1, O2	O1, O2	O1, O2

Table 5.4: List of best predictive channels in each frequency band for tasks "eyes open" vs. "imagine listening to relaxing music".

eyes open vs. relaxing music	alpha		Beta		alpha+beta	
	%	channel	%	Channel	%	channel
sub 1	68.21	85 (T6-O2)	87.86	46 (T3)	87.07	46 (T3)
sub 2	68.92	113 (F4-C4)	85.31	40 (F7-T3)	84.31	40 (F7-T3)
sub 3	58.31	119 (F4)	84.41	109 (T4)	87.37	109 (T4)
sub 4	64.24	73 (O1-O2)	98.56	46 (T3)	98.05	103 (T4)
sub 5	69.03	83 (O2)	92.10	75 (O1)	93.47	83 (O2)

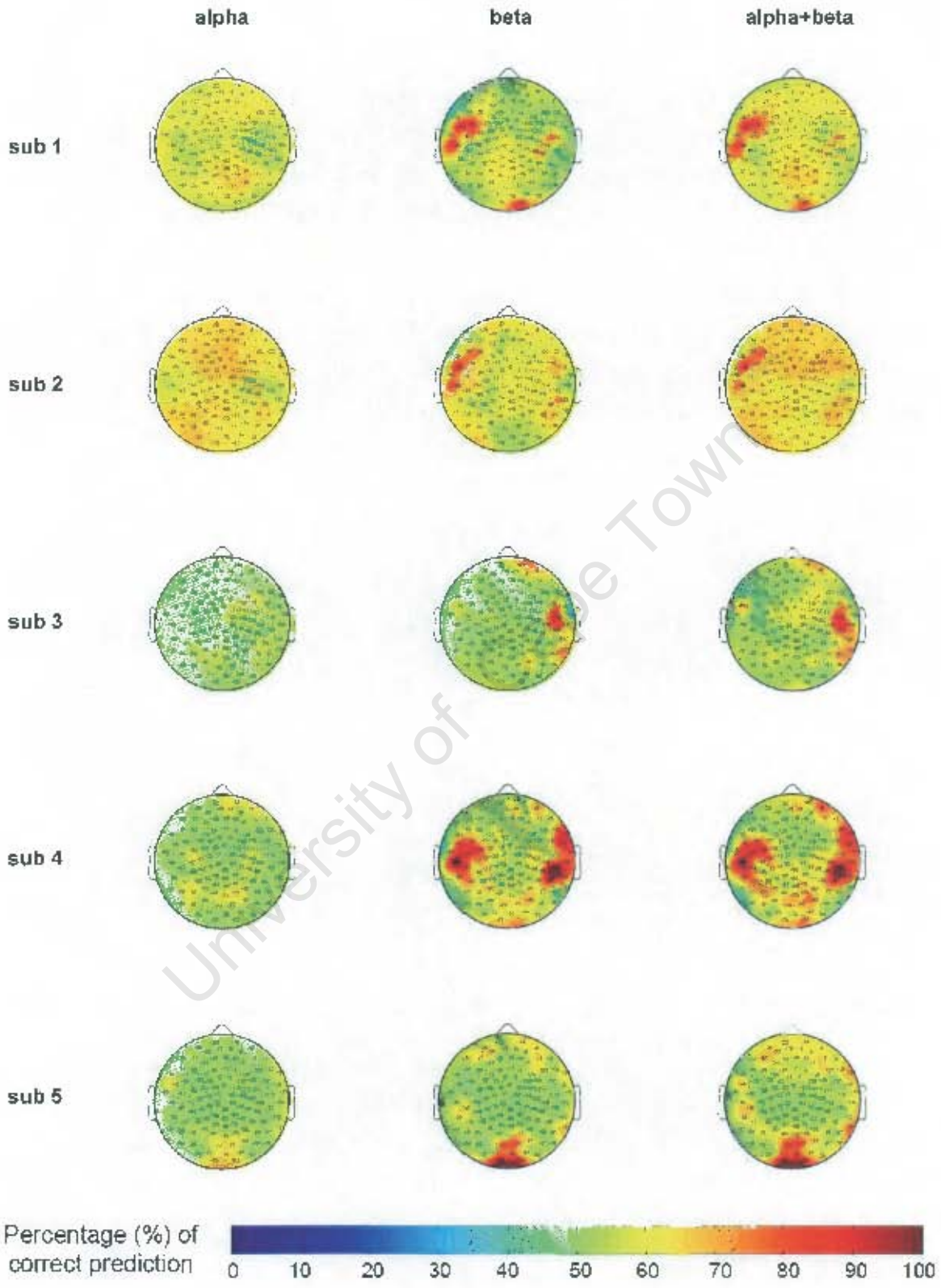

Figure 5.2: Topographical plots showing SVM classification accuracy for tasks "eyes open" versus "imagined listening to relaxing music".

Eyes open vs. rock music

For all subjects, the high classification channels were the same for both real and imagined listening to rock music – see also figure F.1 in Appendix F. Alpha components have low classification, and the beta components are the discriminating band. Classification results were high at the frontal and temporal channels. Figure 5.3 shows topographical plots of the classification accuracy for each frequency component. Table 5.5 summarizes the high (above 80%) classification channels and table 5.6 shows the best predictive channels for each frequency band. The closest 10-20 electrode locations to the channel number are shown in brackets.

Table 5.5: List of channels having classification accuracy of above 80% in each frequency band for tasks "eyes open" vs. "rock music".

eyes open vs. rock music	alpha		Beta		alpha+beta	
	real	imagine	real	imagine	real	imagine
sub 1	none	none	T3, F3, F7, Fp1, T6	T3, F3, F7, Fp1, T6	T3, F3, F7, Fp1, T6	T3, F3, F7, Fp1, T6
sub 2	none	none	T4, F4	T4, F4	T4, F4	T4, F4
sub 3	none	none	none	none	none	None
sub 4	none	none	T3, T4, Fp2	T3, T4, Fp2	T3, T4, Fp2	T3, T4, Fp2
sub 5	none	none	Fp2	Fp2	Fp2	Fp2

Table 5.6: List of best predictive channels in each frequency band for tasks "eyes open" vs. "imagine listening to rock music"

eyes open vs. rock music	alpha		beta		alpha+beta	
	%	channel	%	channel	%	channel
sub 1	71.85	26 (Fp1)	93.29	46 (T3)	92.67	46 (T3)
sub 2	70.38	4 (Fz-F4)	85.85	102 (T4)	83.68	111 (C4)
sub 3	60.80	31 (C3)	73.21	40 (F7-T3)	71.88	40 (F7-T3)
sub 4	69.83	14 (Fp2)	99.66	46 (T3)	99.58	46 (T3)
sub 5	60.49	26 (Fp1)	86.34	8 (Fp2)	89.51	8 (Fp2)

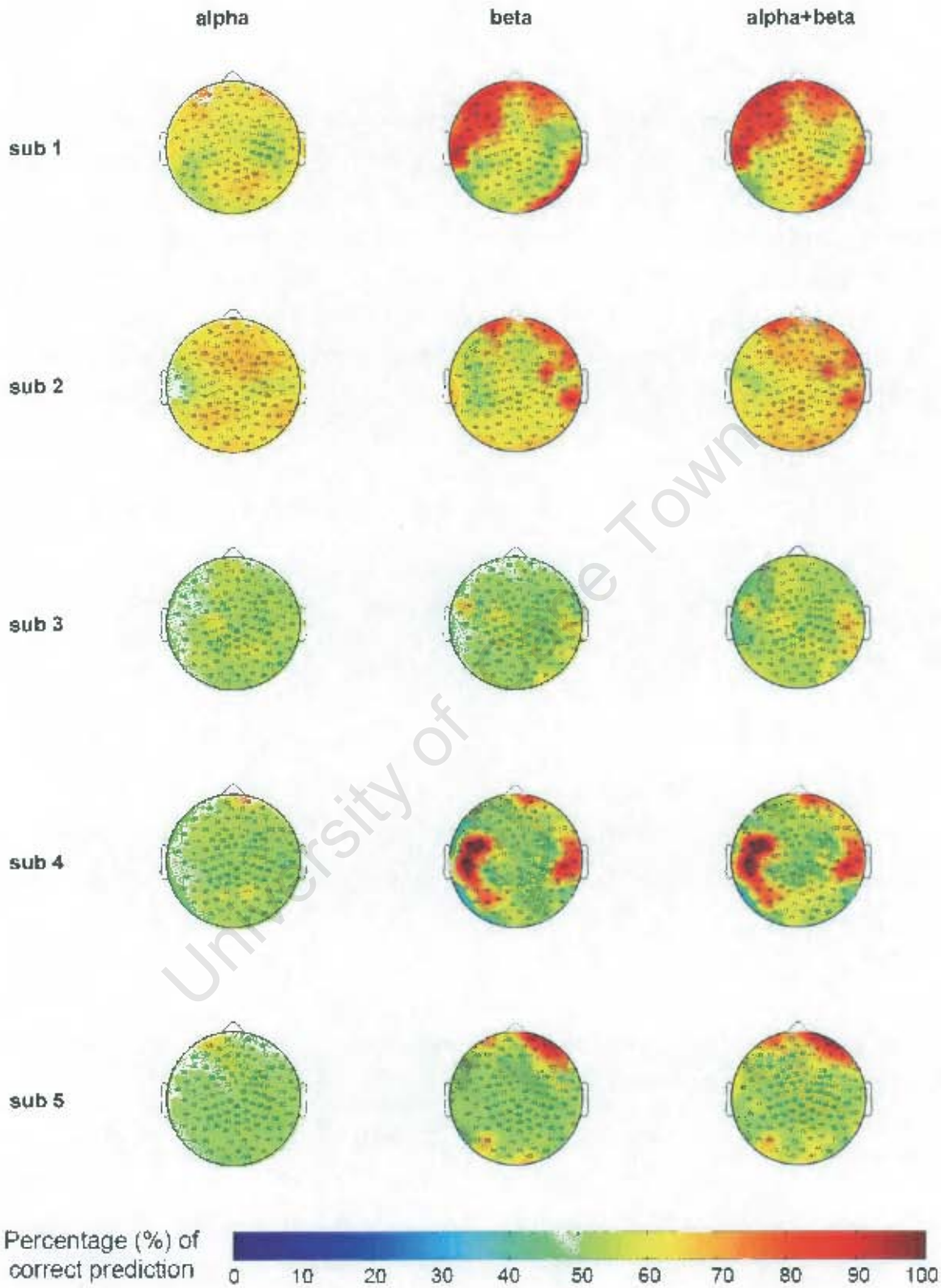

Figure 5.3: Topographical plots showing SVM classification accuracy for tasks "eyes open" versus "imagined listening to rock music".

Eyes open vs. mental arithmetic

Alpha bands have low classification, and beta bands have high classification. Subjects 2, 3, and 4 had high classification at pre-frontal channels. Subjects 1, 2, 4 and 5 had high classification at temporal channels. The best predictive channels were mainly in the pre-frontal and temporal scalp. Figure 5.4 shows topographical plots of the classification accuracy for each frequency component. Table 5.7 summarizes the high (above 80%) classification channels, and table 5.8 shows the best predictive channels for each frequency band. The closest 10-20 electrode locations to the channel number are shown in brackets.

Table 5.7: List of channels having classification accuracy of above 80% in each frequency band for tasks "eyes open" vs. "mental arithmetic".

Eyes open vs. mental arithmetic	alpha	beta	alpha+beta
sub 1	none	T6, O2	T6, O2
sub 2	none	T3, T4, T6, F4, Fp2, F8	T3, T4, T6, F4, Fp2, F8
sub 3	none	Fp1, Fp2	Fp1, Fp2
sub 4	none	T3, T4, T5, T6, F3, F4, F7, F8, Fp1, Fp2, O1, O2	T3, T4, T5, T6, F3, F4, F7, F8, Fp1, Fp2, O1, O2
sub 5	none	T5	T5

Table 5.8: List of best predictive channels in each frequency band for tasks "eyes open" vs. "mental arithmetic".

eyes open vs. mental arithmetic	alpha		beta		alpha+beta	
	%	channel	%	channel	%	channel
sub 1	68.46	96 (T6)	85.61	96 (T6)	86.23	96 (T6)
sub 2	67.10	85 (T6-O2)	93.86	118 (F4)	94.00	118 (F4)
sub 3	58.63	105 (C4)	82.75	14 (Fp2)	82.31	14 (Fp2)
sub 4	69.53	37 (C3)	99.81	103 (T4)	99.49	103 (T4)
sub 5	65.69	8 (Fp2)	80.49	57 (T5)	80.34	51 (T5)

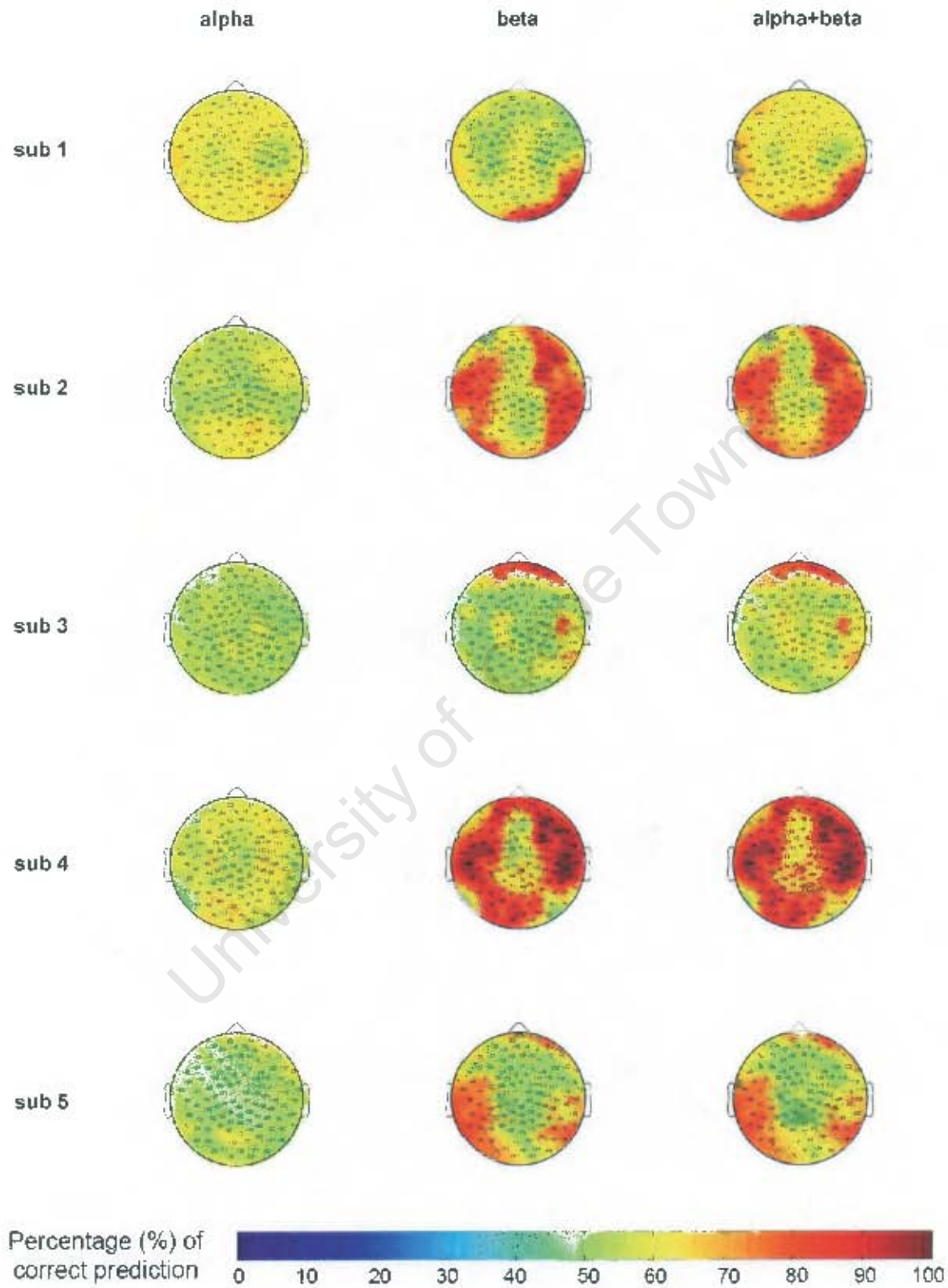

Figure 5.4: Topographical plots showing SVM classification accuracy for tasks "eyes open" versus "Math problems".

Eyes open vs. left hand movement

For all subjects, the high classification accuracy channels were similar for imagined and real hand movement tasks – see also figure F.2 in Appendix F; however, the imagined task had slightly lower classification accuracy than the real task. Subject 1 and 5 showed similarity in having high classification at pre-frontal, temporal and occipital channels, and subject 2 and 3 at central channels (C3 or C4). Subject 4 had high classification at frontal and temporal channels. The best predictive channels were varied from subject to subject. Figure 5.5 shows topographical plots of the classification accuracy for each frequency component. Table 5.9 summarizes the high (above 80%) classification channels, and table 5.10 shows the best predictive channels for each frequency band. The closest 10-20 electrode locations to the channel number are shown in brackets.

Table 5.9: List of channels having classification accuracy of above 80% in each frequency band for tasks "eyes open" vs. "left hand movement".

eyes open vs. left hand movement	alpha		beta		alpha+beta	
	real	imagine	real	imagine	real	imagine
sub 1	none	none	Fp1, Fp2, F3, F7, T3, T6, O2	Fp1, Fp2, F3, F7, T3, T6, O2	Fp1, Fp2, F3, F7, T3, T6, O2	Fp1, Fp2, F3, F7, T3, T6, O2
sub 2	none	none	C3, C4	C3, C4	C3, C4	C3, C4
sub 3	C3	none	T3, C4, P4, O2	T3, P4, O2	C3, C4, T3, P4, O2	T3, P4, O2
sub 4	none	none	T3, T4, F7, Fp2, F4, F8, T6	T3, T4, F7, Fp2, F4, F8, T6	T3, T4, F7, Fp2, F4, F8, T6	T3, T4, F7, Fp2, F4, F8, T6
sub 5	O1	O1	Fp1, Fp2, O1, O2, T6	Fp1, Fp2, O1, O2, T6	Fp1, Fp2, O1, O2, T6	Fp1, Fp2, O1, O2, T6

Table 5.10: List of best predictive channels in each frequency band for tasks "eyes open" vs. "imagine left hand movement".

eyes open vs. left hand movement	alpha		beta		alpha+beta	
	%	channel	%	channel	%	channel
sub 1	70.52	26 (Fp1)	92.54	33 (F7)	92.01	26 (Fp1)
sub 2	64.60	85 (T6-O2)	82.42	36 (C3)	81.37	36 (C3)
sub 3	71.83	31 (C3)	85.42	85 (T6-O2)	89.83	85 (T6-O2)
sub 4	70.69	14 (Fp2)	99.38	47 (T3)	99.17	47 (T3)
sub 5	82.57	75 (O1)	98.82	75 (O1)	99.44	75 (O1)

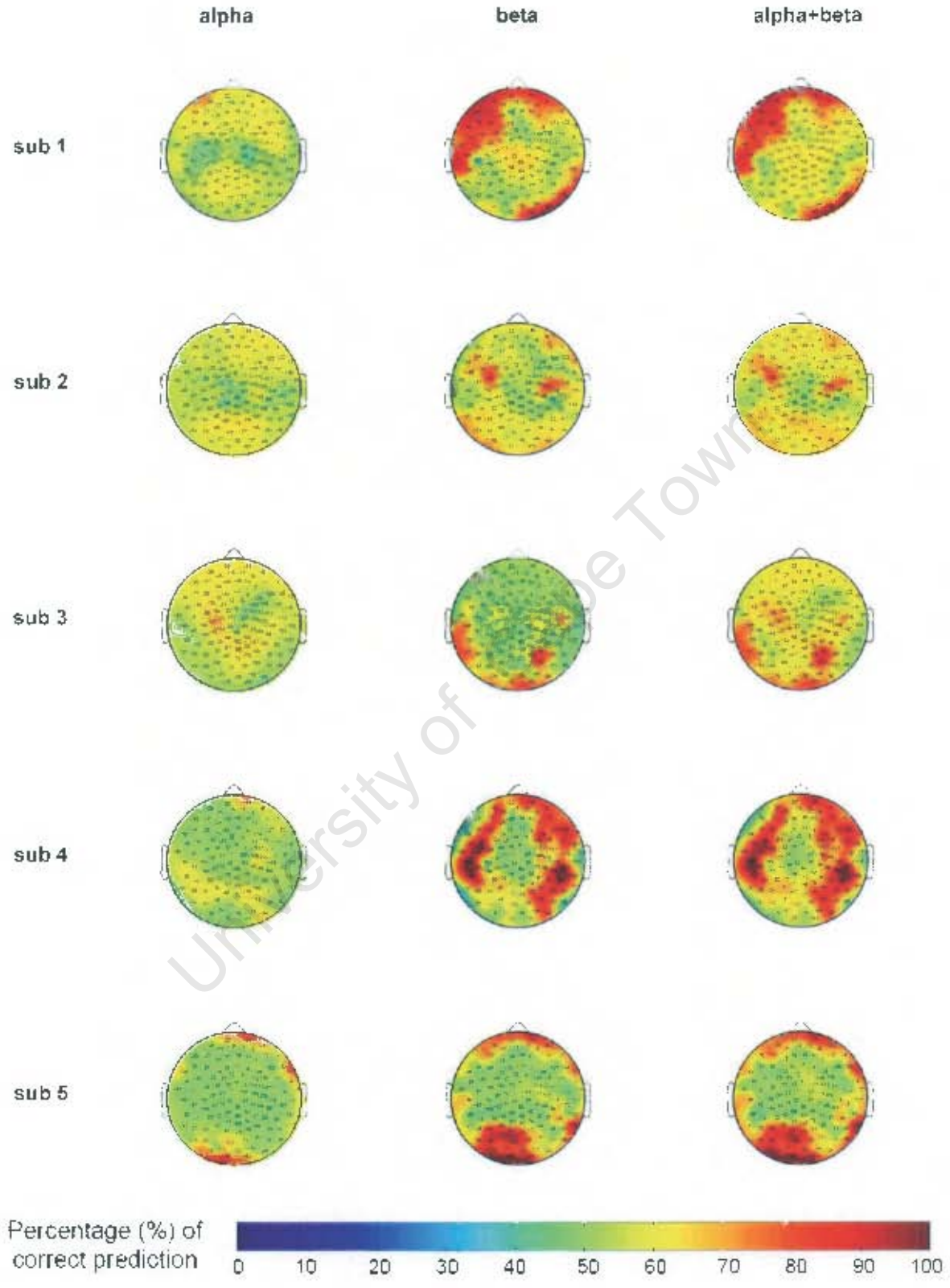

Figure 5.5: Topographical plots showing SVM classification accuracy for tasks "eyes open" versus "imagined left hand movement'

Eyes open vs. right hand movement

For all subjects, the high classification accuracy channels were similar for imagined and real hand movement tasks – see also figure F.2 in Appendix F; however, as for the left hand movement task, imagined tasks had slightly lower classification accuracy than the real tasks. Subject 1 and 3 showed similarity in having high classification channels at T6, and subject 4 and 5 at temporal and occipital channels. Subject 2 was the only one having high classification channels at central channels (C3 and C4). The best predictive channels were mainly in the temporal and occipital scalp. Figure 5.6 shows topographical plots of the classification accuracy for each frequency component. Table 5.11 summarizes the high (above 80%) classification channels, and table 5.12 shows the best predictive channels for each frequency band. The closest 10-20 electrode locations to the channel number are shown in brackets.

Table 5.11: List of channels having classification accuracy of above 80% in each frequency band for tasks "eyes open" vs. "right hand movement".

eyes open vs. right hand movement	alpha		beta		alpha+beta	
	real	imagine	real	imagine	real	imagine
sub 1	none	none	T6	T6	T6	T6
sub 2	none	none	C3, C4, T4	C3, C4, T4	C3, C4, T4	C3, C4, T4
sub 3	C3	none	T6	T6	C3, C4, T6	T6
sub 4	none	none	T3, T4, F4, F8, Fp2, O1, O2	T3, T4, F4, F8, Fp2, O1, O2	T3, T4, F4, F8, Fp2, O1, O2	T3, T4, F4, F8, Fp2, O1, O2
sub 5	none	none	O1, O2, T3, T6	O1, O2, T3, T6	O1, O2, T3, T6	O1, O2, T3, T6

Table 5.12: List of best predictive channels in each frequency band for tasks "eyes open' vs "imagine right hand movement'

eyes open vs. right hand movement	alpha		beta		alpha+beta	
	%	channel	%	channel	%	channel
sub 1	63.55	67 (O1)	81.38	101 (T6)	83.33	101 (T6)
sub 2	67.93	68 (Pz)	83.71	110 (T4)	83.97	110 (T4)
sub 3	75.00	31 (C3)	92.25	97 (T6)	91.25	97 (T6)
sub 4	68.85	103 (T4)	99.85	102 (T4)	99.85	102 (T4)
sub 5	80.40	75 (O1)	98.17	83 (O2)	98.73	75 (O1)

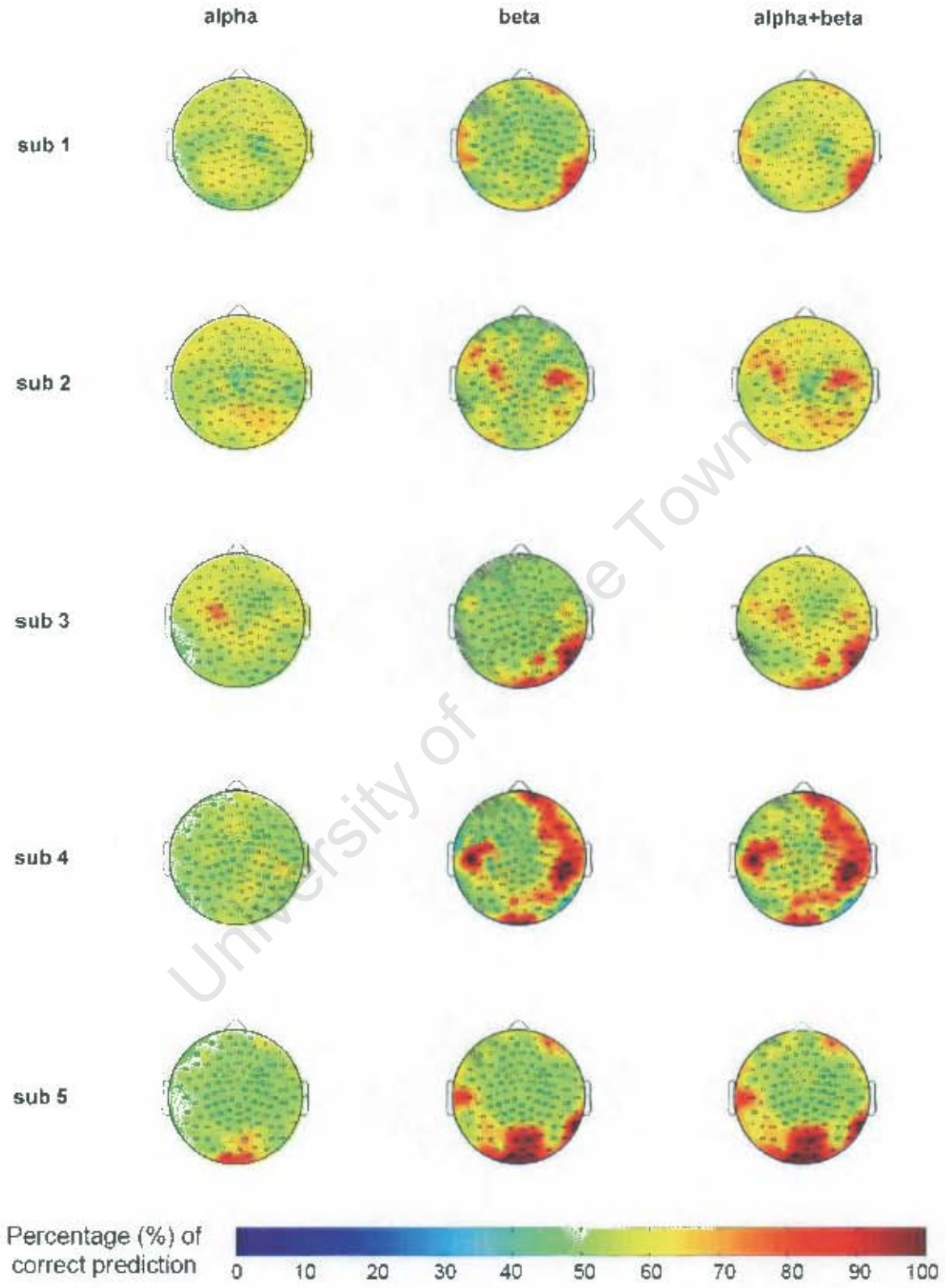

Figure 5.6: Topographical plots showing SVM classification accuracy for tasks "eyes open" versus "imagined right hand movement".

5.1.2 Results for bi-polar montage

The bipolar channel results were plotted in bi-polar topographical plots. The colour of the line joining the electrode locations shows the classification accuracy for that bi-polar channel. Red indicates a classification accuracy of above 90% and blue indicates classification accuracy of between 80~90%. Figures 5.7 and 5.8 show bi-polar topographical plots for tasks "eyes open" versus "eyes closed", "imagine listening to relaxing/rock music", "mental arithmetic" and "imagine left/right hand movement". The rest of the plots for real tasks can be found in Appendix F.

It was found that at least one of the high classification bi-polar channels had similar electrode locations as the high classification channels in average reference montage. The classification accuracies were also similar for the two montages.

The bipolar channels that gave the highest classification results are shown in Tables 5.13-5.17, with the 10-20 electrode locations corresponding to the channel number shown in bracket.

Table 5.13: List of best predictive bipolar channel in alpha and beta frequency band for tasks "eyes open" vs. "eyes closed".

	alpha + beta		
eyes open vs. eyes closed	**%**	**+ channel**	**- channel**
sub 1	85.99	34 (F7)	46 (T3)
sub 2	80.83	53 (P3)	59 (T5)
sub 3	81.13	109 (T4)	122 (F8)
sub 4	89.35	34 (F7)	46 (T3)
sub 5	89.29	72 (O1)	92 (T6)

Table 5.14: List of best predictive bipolar channel in alpha and beta frequency band for tasks "eyes open" vs. "imagine listening to relaxing music".

eyes open vs. relaxing music	alpha + beta		
	%	+ channel	- channel
sub 1	92.71	34 (F7)	46 (T3)
sub 2	82.92	23 (Fp1)	34 (F7)
sub 3	86.02	105 (C4)	109 (T4)
sub 4	99.32	34 (F7)	46 (T3)
sub 5	86.05	77 (O2)	92 (T6)

Table 5.15: List of best predictive bipolar channel in alpha and beta frequency band for tasks "eyes open" vs. "imagine listening to rock music".

eyes open vs. rock music	alpha + beta		
	%	+ channel	- channel
sub 1	97.60	34 (F7)	46 (T3)
sub 2	80.66	23 (Fp1)	25 (F3)
sub 3	75.89	105 (C4)	109 (T4)
sub 4	99.75	25 (F3)	46 (T3)
sub 5	83.78	9 (Fp2)	124 (F4)

Table 5.16: List of best predictive bipolar channel in alpha and beta frequency band for tasks "eyes open" vs. "mental arithmetic".

eyes open vs. mental arithmetic	alpha + beta		
	%	+ channel	- channel
sub 1	68.82	92 (T6)	105 (C4)
sub 2	97.52	122 (F8)	124 (F4)
sub 3	80.13	11 (Fz)	23 (Fp1)
sub 4	99.99	109 (T4)	122 (F8)
sub 5	80.05	34 (F7)	46 (T3)

Table 5.17: List of best predictive bipolar channel in alpha and beta frequency band for tasks "eyes open" vs "imagine left hand movement"

eyes open vs. left hand movement	alpha + beta		
	%	+ channel	- channel
sub 1	63.75	62 (Pz)	129 (Cz)
sub 2	85.16	25 (F3)	34 (F7)
sub 3	81.75	46 (T3)	92 (T6)
sub 4	98.75	34 (F7)	46 (T3)
sub 5	97.15	72 (O1)	77 (O2)

Table 5.18: List of best predictive bipolar channel in alpha and beta frequency band for tasks "eyes open" vs. "imagine right hand movement".

eyes open vs. right hand movement	alpha + beta		
	%	+ channel	- channel
sub 1	66.30	62 (Pz)	129 (Cz)
sub 2	84.40	34 (F7)	37 (C3)
sub 3	84.42	77 (O2)	92 (T6)
sub 4	99.69	34 (F7)	46 (T3)
sub 5	97.86	77 (O2)	92 (T6)

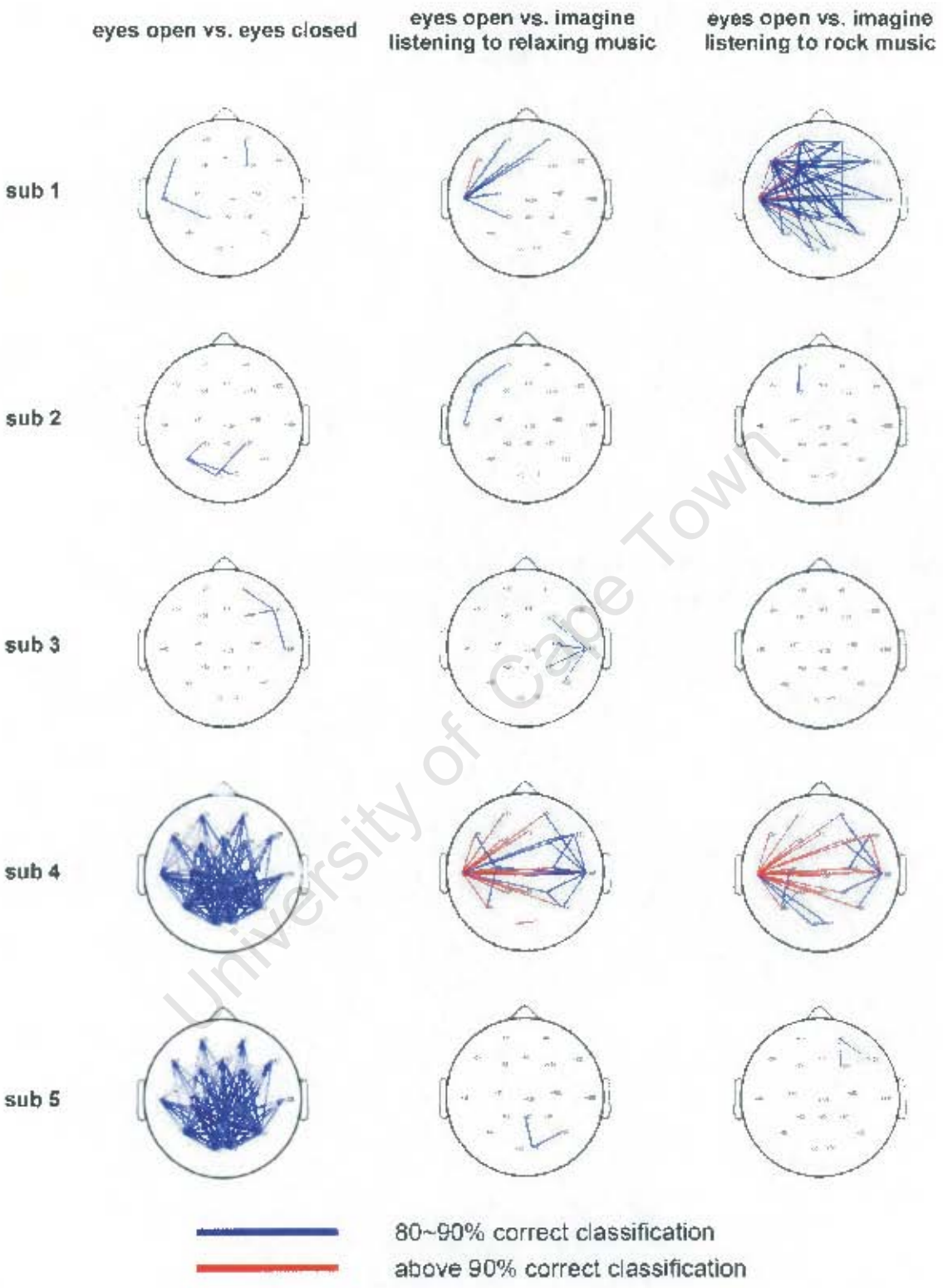

Figure 5.7: Bi-polar topographical plots showing 10-20 channels having classification accuracy of 80% and above for tasks "eyes open" versus "eyes closed" and "imagine listening to relaxing/rock music".

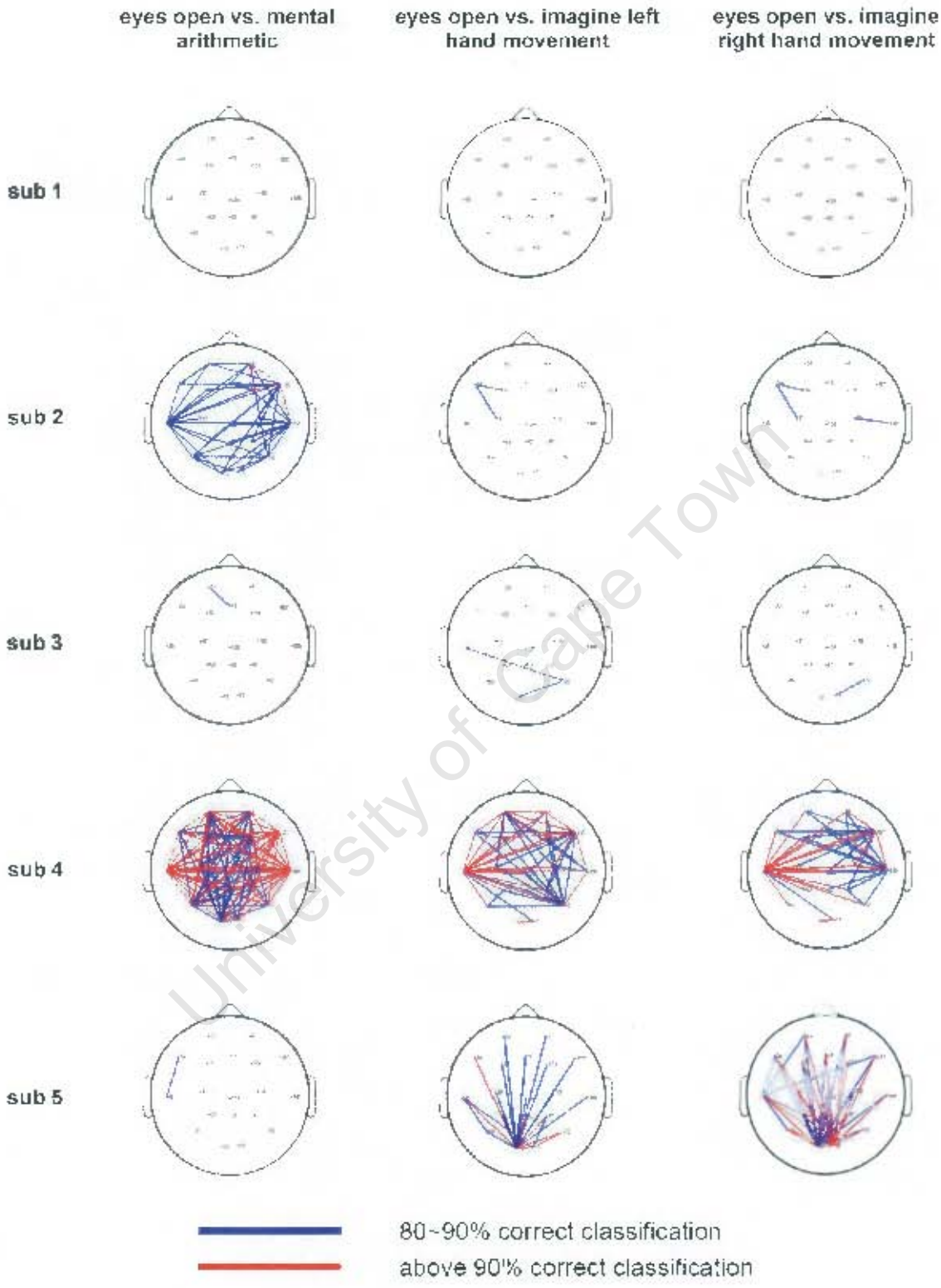

Figure 5.8: Bi-polar topographical plots showing 10-20 channels having classification accuracy of 80% and above for tasks "eyes open" versus "mental arithmetic" and "imagine left/right hand movement".

5.2 Analysis results for the single-channel (Fp1-Fp2) GSN and ModularEEG system

GSN system

The correct classification accuracies for Fp1-Fp2 channel for the "eyes open" task versus all other tasks are shown in table 5.19. and plotted in figure 5.9 for the GSN system. From the graph, we can see that the SVM was able to discriminate pre-frontal EEG (Fp1-Fp2) between the "eyes open" resting task vs. "mental arithmetic" in subjects 2 and 4 with above 82% accuracy, and "eyes open" vs. "imagine left hand movement" in subject 4 with 90% accuracy, and "imagine listening to rock music" in subject 1 with 81% accuracy. SVM was unable to detect changes in subject 3 and 5 with above 80% classification accuracy.

Table 5.19: Percentage of correct classification for all tasks versus eyes open task for the GSN recording.

GSN	eyes close	relax listen	relax imagine	rock listen	rock imagine	mental arithmetic	LH move	LH imagine	RH move	RH imagine
sub1	73.73	54.11	59.29	79.54	81.64	61.58	93.53	63.31	68.09	66.09
sub2	69.21	66.00	72.08	77.00	79.62	82.86	61.48	56.77	58.80	53.62
sub3	59.15	54.53	58.73	50.38	50.36	66.38	52.28	52.00	58.85	67.83
sub4	50.81	51.15	50.51	50.00	50.17	97.43	91.72	90.90	59.58	68.92
sub5	54.56	70.74	75.89	74.64	79.15	62.99	75.00	76.18	70.75	70.63

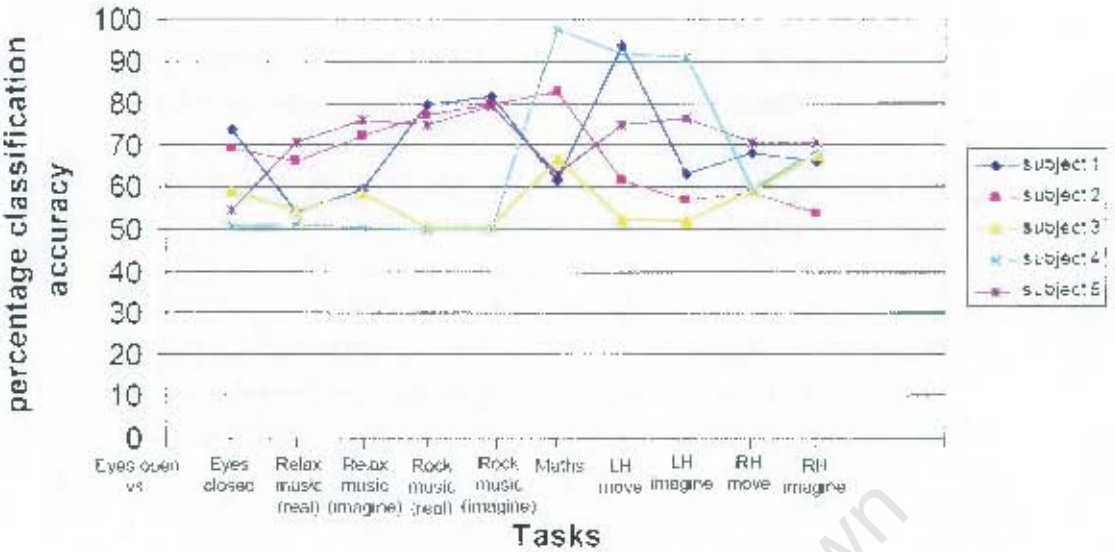

Figure 5.9: Graph showing percentage of correct classification for all tasks versus eyes open task for the GSN recording

ModularEEG system

The SVM classification results were best using a 1 second FFT epoch size, and broadband EEG (8~30 Hz). In subjects 1, 2 and 4, the SVM was able to discriminate the "imagined hand movement" tasks vs. "eyes open" task with above 85% accuracy, as well as the "mental arithmetic" task vs. "eyes open" task with above 83% accuracy. For subjects 3 and 5 it was unable to classify any of the imagined tasks. Table 5.20 shows the classification accuracy for the "eyes open" task versus all other tasks for each subject, averaged over 10 cross validations, also plotted in figure 5.10.

Table 5.20: Percentage of correct classification for all tasks versus "eyes open" task for the ModularEEG recording.

ModEEG	eyes close	relax listen	relax imagine	rock listen	rock imagine	mental arithmetic	LH move	LH imagine	RH move	RH imagine
sub1	53.23	68.73	75	61.57	67.15	83.74	83.75	88.93	92.78	92.94
sub2	55.14	69.84	74.19	75.45	80.36	90.86	85.32	85.77	93.59	93.51
sub3	59.3	51.57	50.29	50.09	52.34	58.1	54.15	56.52	57.47	50.87
sub4	88.58	69.39	69.58	78.79	78.04	91.48	60.76	63.92	90.33	86.23
sub5	54.08	54.84	55.23	61.48	63.86	56.46	55.77	54.73	70	63.2

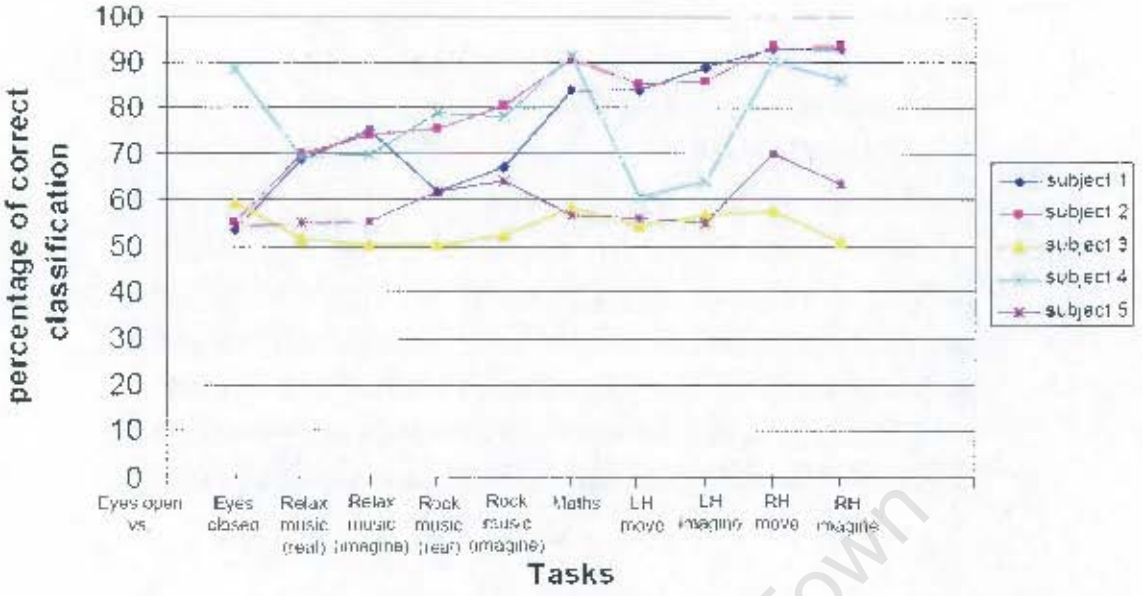

Figure 5.10: Graph showing percentage of correct classification for all tasks versus "eyes open" task for the ModularEEG recording

5.3 Comparisons between modularEEG recording and GSN recording in Fp1-Fp2 channel.

The Fp1-Fp2 channel classification results were similar for ModularEEG and GSN recording. Subject who showed low classification (e.g. subject 3 and 5) for ModularEEG also showed a low classification for GSN, and vice versa. However, there were slight variations in the tasks that had high classification accuracy (i.e. the proportion of high classification tasks remained the same, but the high classification tasks were different). Overall, ModularEEG recordings gave more high (above 80%) classification accuracy than the GSN recording.

5.3.1 Results for the subjective level of fatigue rating for GSN and ModularEEG system

The subjective rating of the level of fatigue during each task, for both recording systems is shown in table 5.13 below. It was found that 3 out of 5 subjects felt less fatigue using the ModularEEG recording system as compare to the GSN system. One subject felt the same for both systems, and one felt more fatigue with the ModularEEG system.

Table 5.21: Subjective rating for the level of fatigue in different tasks, on a Likert scale, with 1 = least fatigue, and 5 = most fatigue. GSN = Geodesic Sensor Net system; Mod = ModularEEG recording system.

subject	1		2		3		4		5	
system	GSN	Mod	GSN	Mod	GSN	Mod	GSN	Mod	GSN	Mod
eye open	5	4	1	1	4	4	3	2	1	1
eye close	1	1	1	1	1	1	1	1	1	1
relax listen/imagine	4	3	1	1	2	2	1	1	3	1
rock listen/imagine	4	3	1	1	2	3	1	1	5	2
mental arithmetic	2	2	1	1	4	3	2	3	3	2
left hand move/imagine	3	2	1	1	3	5	4	2	4	1
right hand move/imagine	3	2	1	1	3	5	4	2	4	1
Combined score	**22**	**17**	**7**	**7**	**19**	**23**	**16**	**12**	**21**	**9**

5.4 Results from SVM validation

The SVM was able to classify the frequency spectrum of sine waves with varying amplitude and frequency fed into the system. This shows the SVM classifier implementation is sensitive to both change in amplitude and frequency. See Appendix H for results.

5.5 Summary of results

The main findings are summarized below. Some relevant implications of these findings will be discussed in the next chapter.

- The alpha plus beta component topographical plots appeared as a linear combination of the alpha and beta topographical plots.
- The topographical plots for real and imagined tasks were similar in both the regions and predictive accuracy.
- The topographical plots for real vs. imagined tasks showed no predictive accuracy for all channels.
- Results from all subjects show low classification in the midline channels (Fz, Cz, Pz).

- Results from all subjects show high classification in the temporal channels.
- All subjects have at least 1 channel for each task that has classification accuracy of 80% and above, except for "imagine listening to rock music" task in subject 3.
- Central channels gave low classification accuracy for "eyes open" vs. "eyes closed" task.
- The alpha component was the main discriminating band for "eyes open" vs. "eyes closed" in the parietal-occipital channels.
- The beta component was the main discriminating band for "eyes open" vs. "imagined listening to relaxing/rock music", "mental arithmetic", and "imagined left/right hand movement".
- Temporal and occipital channels were the main discriminating channels for "eyes open" vs. "imagine listening to relaxing music".
- Temporal and frontal channels were the main discriminating channels for "eyes open" vs. "imagine listening to rock music".
- Temporal and frontal channels were the main discriminating channels for "eyes open" vs. "mental arithmetic".
- Channels having high classification results were similar for both the average reference and bi-polar montages, with bipolar results being slightly higher.

Chapter 6 Discussion

This chapter documents the more detailed discussion on the topics of SVM-FFT classifier implementation; the results found; the choice of mental task; the feasibility of single channel EEG for mental task based BCI implementation; and lastly, the possibility of further improvement of classification results.

6.1 Validation of the FFT-SVM classifier implementation

The FFT-SVM classification results were as expected when different frequencies of artificial sine waves were fed into the system. This shows that the FFT-SVM was operating correctly, and it should therefore be able to classify unknown EEG waveforms varying in spectral components.

Much research has been done in EEG recorded with eyes closed, which documented that alpha amplitude increases in the posterior channels when eyes are closed [30]. The experimental result from "eyes open" vs. "eyes closed" tasks in this research corresponds to the literature. Classification accuracies from all subjects were above 80% in the temporal, parietal or occipital channels for tasks "eyes open" versus "eyes closed", with the alpha component as the discriminating band. The agreement between the finds of this research and the past studies further validated the merit FFT-SVM implementation.

6.2 Performance of the FFT-SVM classifier implementation

In the average reference multi-channel analysis, the results of individual channel predictors were presented on a topographical map, and the use of multiple channel predictors was not investigated. The percentage of correct classification was above 80% for at least one channel in all subjects for all tasks, except for "rock music" task in subject 3. Classification accuracies were above 90% for "imagine left and right-hand movement" task in 3 out of 5 subjects, and for "imagine listening to relaxing/rock music" and "mental arithmetic" tasks in 2 out of 5 subjects. The highest classification results were achieved from subject 4, who has

classification accuracy of 98.0~99.8% for imagined music, mental arithmetic and imagined movement tasks.

In bi-polar channel analysis, the percentage of correct classification was above 80% for at least one bi-polar channel in most of the tasks. Classification accuracies were above 90% for "imagine listening to relaxing/rock music", "mental arithmetic" and "imagine left and right-hand movement" tasks in 2 out of 5 subjects. The highest classification results were achieved from subject 4, who had classification accuracies of 98.7~99.9% for imagined music, mental arithmetic and imagined movement tasks.

Table 6.1: Summary of various studies on classification of EEG for BCI implementation

reference	tasks	number of subjects	signal processing method	number of electrodes	% correct classification
Neuper et al. [78]	motor imagery	14	distinction sensitive vector quantization (DSLVQ)		56%
Babiloni et al. [47]	imagine hand movement of left and right middle finger	5	Single space projection (SSP) and low resolution SL	9 (Fz, F4, C3, Cz, C4, P3, Pz, P4)	81%
Costa et al. [58]	imagine left or right hand movement	10	adaptive gaussian representation (AGR), Multi-layer perceptron (MLP) with back propagation	2 (C3, C4)	87% +/- 5.0%
Kostov et al. [56]	voluntary EEG modulation	2	sutoregressive (AR) feature extraction, Adaptive logic network (ALN)	2-4 electrode (out of 28 electrodes inn 10-20 locations)	100% (after training)
Wang et al. [57]	motor imagery of hand and foot movement	2	common spacial pattern (CSP), Fisher discriminant (FD)	4 channels	93.45% and 91.88%
Pfurtscheller et al. [45]	imagine left or right hand movement	3	DSLVQ, neural network	6 electrode, 3 bipolar channels, (C3-C4, P3-P4)	80%
Adaptive brain Interface [11]	imagination of left and right hand movement, cube rotation, subtraction, word association	15	Neural network	F3, F4, C3, Cz, C4, P3, Pz, P4	N/A

Comparing the FFT-SVM classification results with other 2-choice mental task classification systems, shown in table 6.1, it performs equally well, in some cases better, than other signal processing implementations.

This suggests FFT-SVM implementation is a good method for BCI implementation. Results also suggested that imagining music, mental arithmetic and movement mental tasks are possible mental tasks for BCI implementation. However, the cross validation of the classifier was done using random selection of 1-second segments, with each of the different tasks having duration of at least 30s, and thus the 1-second data segments within the longer segment cannot be considered independent. In order to estimate the prediction power of the SVM-FFT implementation more accurately, continuous data in original time sequence would have to be used.

Since the classification result were based on EEG data recorded continuously for 5 minutes for each task. Further experiments recording shorter trials (5-10s) of EEG with interchanging mental tasks should be done to investigate the minimum time required for EEG responses to mental tasks to be detected. The performance of a BCI system is measured by its information transfer rate in bits/mins or commands/mins [55]. BCI systems should therefore use mental tasks that are able to give high information transfer rate, in order to operate more efficiently.

6.3 Discussion of multi-channel analysis results

Temporal channels gave high classification accuracy

Overall, the temporal channels show high classification accuracy. This suggests that temporal channels were more responsive to the tasks tested, or perhaps EEG changes in the temporal channels are picked up by the SVM classifier more easily. However, this may also be caused by undetected artifacts contaminated EEG correlating to the task, as EEG measured on the temporal electrodes are relatively closer to facial and neck muscles.

Eyes open vs. relaxing/rock music

The beta bands in the temporal and occipital channels were the main discriminating channels for imagine listening to relaxing music task, and the beta band in the fronto-temporal channels were the main discriminating channels for imagine listening to rock music

task. Subject 5 was different to the others in having the beta band in the occipital channels as the discriminating band for imagine listening to relaxing music.

This corresponds to previous studies which showed that, when listening to music, EEG activations were found in the fronto-temporal channels [34], and that an increase in beta power in the posterior scalp occurs [33]. Studies looking at effect of different types of music also found beta and gamma band changes in the right temporal channels when listening to classical music; and in the right temporal, central and parietal changes when listening to rock music [37]. However, previous studies have also shown alpha and theta changes when listening to music [35, 36], which were not found in the present results. The different findings may be due to the different style of music used, or that the music was played at a different volume, as found in [37], or perhaps the music induced a different emotion to the subject, and emotion were found to have more influence to the EEG than the actual music itself. Other possibility would be that different classifiers were used, and that alpha changes were insufficient for the FFT-SVM to detect. The EEG response to music may also be affected by eyes open and eyes closed state.

Topographical plots for eyes open vs. real and imagined music were very similar for both relaxing and rock music. There are two possible causes to this phenomenon. One, that brain behaves in a similar manner when actually listening to music and when imagined listening to music. Two, spectral changes in EEG have persisted after the music has stopped, as shown in [37] for rock music.

However, definite conclusion cannot be reached without further experiments. In the music experiment presented in this thesis, the subjects were specifically instructed to imagine the same musical composition. In the experiment by [37], subjects were not explicitly instructed to do anything else – meaning it is possible that the subjects were in fact reciting or remembering the music silently during this period. Therefore, it is debatable whether their results indicate EEG persistence or an imagined music effect. An experiment that introduces some effective distracter before subjects are instructed to imagine music may provide a definite conclusion. This should be investigated further.

Eyes open vs. mental arithmetic

The beta components in the temporal and pre-frontal/frontal channels were the discriminating band for "mental arithmetic" task. The temporal and frontal discrimination

corresponds to previous studies, which documented that beta increases in the parietal-temporal channels during mental arithmetic (with eyes closed) [40], and beta differences in the frontal channels during mental arithmetic (with eyes open) [41]. However, previous findings also documented alpha changes during mental arithmetic (with eyes closed) [38, 39], which were not found in this experiment.

There are two possible explanations to the disagreement between the results and previous findings. One, previous mental arithmetic tasks were done with eyes closed, whereas in this research, mental arithmetic tasks were done with eyes open. Two, previous studies uses simple addition, subtraction and multiplication problems, whereas in this research, Fibonacci series were used for the experiment. The level of task difficulty may therefore be different and affecting the EEG results, as shown in [79]. It is possible that a task as complex as the Fibonacci sequence could selectively modulate beta. This should be investigated through additional experiments as mentally computing the Fibonacci sequence may be more complex than the relatively simple arithmetic tasks used in previously published studies.

Eyes open vs. left or right hand movement

In subjects 2 and 3, the classification accuracies were around 75 – 83% in the sensory motor (C3 and C4) channels, for tasks "eyes open" versus "left hand movement". This corresponds to previous studies, which documented that beta changes in left and right central (sensorimotor) channels during motor movements or motor imagery [43-45].

However, in subjects 1, 4 and 5, discriminating channels were found to be in the frontal, temporal and occipital regions, which were not reported in previous studies.

There are two possible explanations to this difference. One, in this experiment, the subjects were instructed to mentally clench a "soft ball" – it is possible that the mental effort involved in this process were stronger/weaker than the imagined tasks used in other studies, and resulted in different EEG responses, as shown in [80].

In addition, predictive power of the mu or beta rhythm varies between subjects in other studies. For example Pfurtscheller et al. [45] analyzed predictions between left and right hand imagined-movement in 3 subjects. The best predictors were reported as beta for subject 3, mu for subject 2, and both mu and beta for subject 1. Pfurtscheller et al.'s results

suggest that subject-specific variation could also be a reason that the FFT-SVM has better classification results for beta than alpha for the 5 subjects tested.

No changes were detected by the FFT-SVM for real vs. imagined tasks

The topographical plots were similar for real and imagined tasks, and topographical plots for real vs. imagined tasks showed no/low predictive accuracy for all channels. The result suggests that the EEG responses (in frequencies and channels) to imagined and real tasks were very similar, or perhaps the changes (such as amplitude and phase) were undetectable with the FFT-SVM classification system.

Average reference montage and bi-polar montage yield similar classification results

The classification accuracies were similar for both the average reference and bi-polar montage, and both montages have classification accuracy of above 80% in most of the tasks. This suggests EEG changes due to mental tasks, with the FFT-SVM detection system is insensitive to the recording montage used, and that one channel (two electrodes) is sufficient to capture EEG information for detection of mental tasks – provided that the electrodes are optimally located.

6.4 Discussion of single channel analysis

ModularEEG system is a possible candidate for BCI implementation

In the ModularEEG system, classification results from subjects 3 and 5's data were below 80% for all tasks. In subjects 1, 2, and 4, the SVM was able to discriminate between "eyes open" tasks vs. "mental arithmetic", and "imagined hand movement" tasks, with 83% and above classification accuracy. The difference may be due to inter-subject variability of EEG, or difference in subject's skull thickness – EEG may not fully propagate to the pre-frontal scalp in some subjects, therefore EEG changes are harder to detect. For example, Benbadis and Rielo [81] described the effect of skull thickness abnormalities on EEG asymmetry.

The classification results are similar for ModularEEG and Fp1-Fp2 GSN recording, however, there were slight variations in the tasks that had high classification accuracy. This may be due to intra subject variability in EEG, as the recordings were taken on a different day.

Overall, ModularEEG recordings gave higher classification results than the GSN recording. This may be due to the fact that ModularEEG recording systems are more comfortable for the users, and therefore users are able to relax and concentrate more on the tasks.

The overall subjective rating for the level of fatigue for the GSN and ModularEEG recording systems shows that ModularEEG recording system causes less fatigue. This was expected, as the preparation procedure for ModularEEG system is much simpler and shorter than the GSN system. The GSN system requires the subjects' hair to be washed with shampoo prior to recording; and wetted with salt solution throughout the recording. The ModularEEG system does not require these procedures – only the scalp locations where electrodes were placed require cleaning with light sand paper and diluted methanol.

The results suggest that ModularEEG is a good candidate for BCI implementation, as it is simple to use, causes less fatigue to the user, and yield good classification accuracy (above 80% in 3 out of 5 subjects)

6.5 Individual differences

There were more differences than similarities found in the classification results among the subjects. This is compatible with the literature where individual differences were found. For example in Pfurtscheller's experiment, 3 different predictors were reported for 3 subjects [45]. The number of subjects used in this experiment is also in line with typical BCI subject numbers, see table 6.1. The large individual differences also indicate that subjects should be individually tested and will require a customized BCI.

6.6 Widespread vs. localized EEG changes

The topographical plots of the individual channel classification results show both widespread and localized high classification channels (widespread and localized changes in EEG), see figure 6.1 for an example.

When implementing a BCI system, the widespread changes indicate that there is a large choice of scalp areas for electrode placement, and hence the experimenter does not have to be very precise with electrode placement and may use a low-resolution system for detection of mental tasks. The localized changes imply that the experimenter either has to be very

precise with the electrode placement in order to capture the changes, or has to use a high-resolution EEG system for mental task detection.

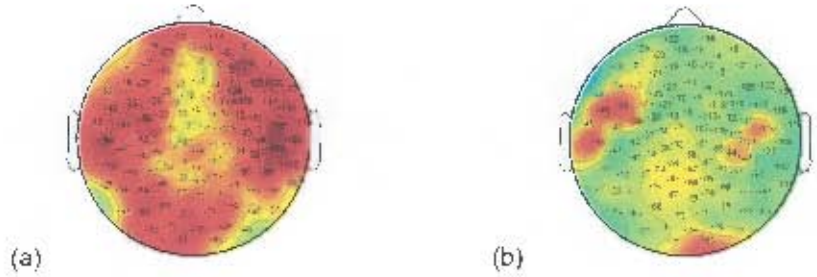

Figure 6.1: (a) Topographical plots showing widespread changes.
(b) Topographical plots showing localized changes.

6.7 Pre-processing method

The artifact correction approach used in this project is removal by visual inspection. However, variable length artifacts were removed prior to segmentation of data into fixed length time-windows for FFT-SVM classification. This has potential for discontinuous data windows. The effect of discontinuity of data was not looked at, but segmenting data first and removes contaminated windows can ensure that discontinuities of data are avoided. which would be a more suitable method. However, this would results in an increase in loss of data.

6.8 Possibility of further improvement

Subject training improves classification results

Previous studies have shown that subject training improves classification results [65, 66]. Some BCI systems require days or weeks of training time, before the BCI system can be optimally operated. See table 2 2 for examples of these BCI systems. The subjects used for this experiment have not participated in other EEG experiments before, and no training was done prior to the recording. Therefore, with addition of subject training prior to experiment, the results are expected to improve.

Both real and imagined tasks were experimented in order to investigate whether the system could detect EEG changes during real tasks, and whether imagined tasks would give similar

results. In the case (such as left and right hand movement) where real tasks gave higher classification results than the imagined tasks, subject training may be able to help the subject on imagining these tasks, and hence improve classification results for imagined tasks.

Active electrodes outperform disposable adhesive electrodes for ModularEEG system

Active electrodes are electrodes with a unity gain amplifier right next to the electrode up on the scalp, initially designed by Foltynski (see [12] for design and prototype). This greatly improves the signal quality received by an EEG system. However, active electrodes are heavier and required additional power lines for powering the amplifiers, which becomes complicated when recording with large number of electrodes. With a single channel ModularEEG system, active electrodes will be a good choice for further improvement of EEG signal quality, therefore making mental tasks easier to discriminate.

Chapter 7 Conclusions

Based on the findings of this research, the following conclusions are drawn:

1. ***Imagined music, mental arithmetic and imagined hand movement are feasible mental tasks for BCI implementation***

   The experimental results and literature search have both found EEG changes between the resting conditions versus imagined music, mental arithmetic and imagined hand movement. In addition, working BCI systems using mental arithmetic and imagined movement tasks have already been successfully implemented (e.g. Adaptive Brain Interface, ERS/ERD cursor control). This indicates that with appropriate signal processing techniques, these tasks are feasible for BCI implementation.

2. ***Temporal channels are good predictive channels for mental task discrimination***

   Most of the high classification accuracies between resting with eyes open conditions versus imagined listening to relaxing/rock music, mental arithmetic, and imagined left/right hand movement were found in the temporal channels. This is an indication that temporal channels are good predictive channels for a mental task based BCI implementation.

3. ***FFT-SVM classifier is feasible for mental task based BCI implementation***

   The bi-polar classification results for different mental tasks using the FFT-SVM classifier were above 80% in most of the tasks, and above 90% in 2 out of 5 untrained subjects for imagined music, metal arithmetic and imagined movement tasks. This performance is similar to the existing classifiers (e.g. adaptive Gaussian representation with neural networks, and common spatial pattern with Fisher discriminant) used for mental task BCI systems. This suggests that FFT-SVM classifier is feasible for BCI implementation.

4. ***ModularEEG system is a good candidate for BCI implementation***

The ModularEEG results were similar to the Fp1-Fp2 GSN results and yield good classification accuracy (above 80% in 3 out of 5 subjects). The ModularEEG was also rated to be less fatiguing to use when compared to the GSN system. This suggests that ModularEEG is a good candidate for BCI implementation.

Chapter 8 Recommendations for further research

Based on the findings and conclusions of this research, the following recommendations for further developments are made:

1. ***Investigate whether EEG responses to mental tasks can be detected spontaneously by recording shorter trials of EEG with interchanging mental tasks.***

   Further experiments recording shorter trials (5-10s trials as compare to 30s to 5 mins recording in the current experiment) of EEG with interchanging mental tasks should be done to investigate whether EEG responses to mental tasks can be detected more spontaneously. BCI systems should use mental tasks that are able to give high information output (more commands per minute), in order to operate more efficiently.

2. ***Use active electrodes for ModularEEG based BCI implementations***

   Active electrodes should be used instead of adhesive electrodes with a ModularEEG system, to improve signal quality for better discrimination of mental tasks.

3. ***Investigate wavelet spectral estimates-SVM classifier for mental task detection***

   Wavelet transforms have been shown to perform better than Fast Fourier Transforms, and require shorter EEG epochs. A wavelet-SVM classifier may perform better than FFT-SVM classifier.

4. ***Investigate task vs. task classification accuracy.***

   In this thesis, only the "resting with eyes open" task was compared with all other tasks. Further work should also be done on investigating all combinations of task vs. task classification accuracy (such as imagined rock music vs. mental arithmetic). See figure F.3 - F.7 in Appendix F.

5. ***Implement a 3-choice FFT-SVM classifier***

   The 2-choice FFT-SVM classifier can be developed into a 3-choice FFT-SVM classifier. This could allow the user to perform the least uncomfortable mental task (such as "resting with eyes open") to denote an "Idle" state for the system, and have the two tasks (such as mental arithmetic and imagined hand movement) as commands.

6. ***Investigate the effect of training on imagined listening to music***

   Subject training has shown to improve classification accuracy in mental tasks such as imagined movement. Further experiment should be done on giving subjects regular training sessions for a period of several months on music tasks, to investigating the effect of training on imagined listening to music tasks.

7. ***Investigate the use of multi-channel EEG features as inputs to the SVM***

   In this thesis, only single channel EEG features was used as inputs to the SVM for mental task detection. Multi-channel EEG features may provide better classification results and should be investigated further.

Bibliography

[1] E. A. Curran and M. J. Stokes, "Learning to control brain activity: a review of the production and control of EEG components for driving brain-computer interface (BCI) systems," *Brain Cogn,* vol. 51, pp. 326-36, Apr 2003.

[2] J. R. Wolpaw, N. Birbaumer, D. J. McFarland, G. Pfurtscheller, and T. M. Vaughan, "Brain-computer interfaces for communication and control," *Clin Neurophysiol,* vol. 113, pp. 767-91, Jun 2002.

[3] N. Weiskopf, R. Veit, M. Erb, K. Mathiak, W. Grodd, R. Goebel, and N. Birbaumer, "Physiological self-regulation of regional brain activity using real-time functional magnetic resonance imaging (fMRI): methodology and exemplary data," *Neuroimage,* vol. 19, pp. 577-86, Jul 2003.

[4] L. Parra, C. Alvino, A. Tang, B. Pearlmutter, N. Yeung, A. Osman, and P. Sajda, "Single-trial detection in EEG and MEG: Keeping it linear," *Neurocomputing,* vol. 52-54, pp. 177-183, Jun 2003.

[5] N. Birbaumer, C. Weber, C. Neuper, E. Buch, K. Haapen, and L. Cohen, "Physiological regulation of thinking: brain-computer interface (BCI) research," *Prog Brain Res,* vol. 159, pp. 369-91, 2006.

[6] J. R. Wolpaw and D. J. McFarland, "Control of a two-dimensional movement signal by a noninvasive brain-computer interface in humans," *Proc Natl Acad Sci U S A,* vol. 101, pp. 17849-54, Dec 21 2004.

[7] N. Birbaumer, A. Kubler, N. Ghanayim, T. Hinterberger, J. Perelmouter, J. Kaiser, I. Iversen, B. Kotchoubey, N. Neumann, and H. Flor, "The thought translation device (TTD) for completely paralyzed patients," *IEEE Trans Rehabil Eng,* vol. 8, pp. 190-3, Jun 2000.

[8] G. Pfurtscheller, C. Neuper, C. Guger, W. Harkam, H. Ramoser, A. Schlogl, B. Obermaier, and M. Pregenzer, "Current trends in Graz Brain-Computer Interface (BCI) research," *IEEE Trans Rehabil Eng,* vol. 8, pp. 216-9, Jun 2000.

[9] L. A. Farwell and E. Donchin, "Talking off the top of your head: toward a mental prosthesis utilizing event-related brain potentials," *Electroencephalogr Clin Neurophysiol,* vol. 70, pp. 510-23, Dec 1988.

[10] J. D. Bayliss, "Use of the evoked potential P3 component for control in a virtual apartment," *IEEE Trans Neural Syst Rehabil Eng,* vol. 11, pp. 113-6, Jun 2003.

[11] R. Millan Jdel and J. Mourino, "Asynchronous BCI and local neural classifiers: an overview of the Adaptive Brain Interface project," *IEEE Trans Neural Syst Rehabil Eng,* vol. 11, pp. 159-61, Jun 2003.

[12] "The OpenEEG project," http://openeeg.sourceforge.net (last viewed: Oct 2006).

[13] Electrical Geodesics, Inc. "EGI system 200," *technical manual,* 2001.

[14] H. Berger, "Uber das elektrephalogramm des menschen," *Arch. Psychiatr. Nervenkr,* vol. 87, pp. 527-570, 1929.

[15] P. Olejniczak, "Neurophysiologic basis of EEG," *J Clin Neurophysiol,* vol. 23, pp. 186-9, Jun 2006.

[16] J. G. Webster, *Medical instrumentation*, 3 ed.: John Wiley & Sons, inc., pp. 10, 165-175, 183-285, 1998.

[17] M. Teplan, "Fundamentals of EEG measurement," *Measurement science review,* vol. 2, 2002.

[18] N. Mohamed, "Detection of epileptic activity in the EEG using Artificial Neural Networks," in *Engineering.* vol. M.Sc. Johannesberg Univeristy of the Witwatersrand, pp. 12-13, 19, 2004.

[19] M. Fatourechi, A. Bashashati, R. K. Ward, and G. E. Birch, "EMG and EOG artifacts in brain computer interface systems: A survey," *Clin Neurophysiol,* vol. 118, pp. 480-94, Mar 2007.

[20] Delsys Incorporated, "Surface Electromyography: Detection and Recording," www.delsys.com/Attachments_pdf/WP_SEMGintro.pdf (last viewed: March 2007).

[21] H. H. Jasper, "The ten-twenty electrode system of the International Federation," *Electroencephalogr Clin Neurophysiol,* vol. 10, pp. 371-375, 1985.

[22] G. Chatrian, E. Lettich, and P. Nelson, "Ten percent electrode system for topographic studies of spontaneous and evoked EEG activity," *Am J EEG Technol,* vol. 25, pp. 83-92, 1985.

[23] R. Oostenveld and P. Praamstra, "The five percent electrode system for high-resolution EEG and ERP measurements," *Clin Neurophysiol,* vol. 112, pp. 713-9, Apr 2001.

[24] R. Oostenveld, "Improving EEG source analysis using prior knowledge." Ph.D thesis, University of Nijmegen, p. 44, 2003.

[25] "The '10-20 system' of electrode placement," in *Neuroscience for kids*: http://faculty.washington.edu/chudler/1020.html (last viewed: Feb 2007).

[26] G. Garcia Molina, "Direct brain-computer communication through scalp recorded EEG signals," in *Electrical Engineering.* Ph.D thesis, Swiss Federal Institiute of Technology EPFL, pp. 21-23, 2004.

[27] G. Garcia Molina, U. Hoffmann, T. Ebrahimi, and J. M. Vesin, "Direct Brain-Computer Communication through EEG Signals," *To appear in IEEE EMBS Book Series on Neural Engineering,* 2004.

[28] G. E. Birch, S. G. Mason, and J. F. Borisoff, "Current trends in brain-computer interface research at the Neil Squire Foundation," *IEEE Trans Neural Syst Rehabil Eng,* vol. 11, pp. 123-6, Jun 2003.

[29] S. G. Mason and G. E. Birch, "A brain-controlled switch for asynchronous control applications," *IEEE Trans Biomed Eng,* vol. 47, pp. 1297-307, Oct 2000.

[30] R. Srinivasan, "Spatial structure of the human alpha rhythm: global correlation in adults and local correlation in children," *Clin Neurophysiol,* vol. 110, pp. 1351-62, Aug 1999.

[31] J. Maltez, L. Hyllienmark, V. V. Nikulin, and T. Brismar, "Time course and variability of power in different frequency bands of EEG during resting conditions," *Neurophysiol Clin,* vol. 34, pp. 195-202, Dec 2004.

[32] J. Ramos and M. Corsi-Cabrera, "Does brain electrical activity react to music?," *Int J Neurosci,* vol. 47, pp. 351-7, Aug 1989.

[33] S. Nakamura, N. Sadato, T. Oohashi, E. Nishina, Y. Fuwamoto, and Y. Yonekura, "Analysis of music-brain interaction with simultaneous measurement of regional cerebral blood flow and electroencephalogram beta rhythm in human subjects," *Neurosci Lett,* vol. 275, pp. 222-6, Nov 1999.

[34] E. Altenmuller, K. Schurmann, V. K. Lim, and D. Parlitz, "Hits to the left, flops to the right: different emotions during listening to music are reflected in cortical lateralisation patterns," *Neuropsychologia,* vol. 40, pp. 2242-56, 2002.

[35] Q. Yuan, X. H. Liu, D. C. Li, H. L. Wang, and Y. S. Liu, "Effects of noise and music on EEG power spectrum," *Space Med Med Eng (Beijing),* vol. 13, pp. 401-4, Dec 2000.

[36] A. V. Sulimov, V. Liubimova Iu, R. A. Pavlygina, and V. I. Davydov, "Spectral analysis of the human EEG while listening to music," *Zh Vyssh Nerv Deiat Im I P Pavlova,* vol. 50, pp. 62-7, Jan-Feb 2000.

[37] R. A. Pavlygina, D. S. Sakharov, and V. I. Davydov, "Spectral analysis of the human EEG during listening to musical compositions," *Fiziol Cheloveka,* vol. 30, pp. 62-9, Jan-Feb 2004.

[38] A. Glass, "Intensity of attenuation of alpha activity by mental arithmetic in females and males " *Physiology & Behavior* vol. 3, pp. 217-220, Mar 1968.

[39] A. Glass and A. W. Kwiatkowski, "Power spectral density changes in the EEG during mental arithmetic and eye-opening," *Psychol Forsch,* vol. 33, pp. 85-99, 1970.

[40] J. Volavka, M. Matousek, and J. Roubicek, "Mental arithmetic and eye opening. An EEG frequency analysis and GSR study," *Electroencephalogr Clin Neurophysiol,* vol. 22, pp. 174-6, Feb 1967.

[41] T. Fernandez, T. Harmony, M. Rodriguez, J. Bernal, J. Silva, A. Reyes, and E. Marosi, "EEG activation patterns during the performance of tasks involving different components of mental calculation," *Electroencephalogr Clin Neurophysiol,* vol. 94, pp. 175-82, Mar 1995.

[42] C. Yamaguchi, "FFT and wavelet analysis of electroencephlograms measured during simple arithmetic calculations and e-mail keying on cell-phone keypad," *Int. J. Sci. Res,* vol. 15, 2005.

[43] D. J. McFarland, L. A. Miner, T. M. Vaughan, and J. R. Wolpaw, "Mu and beta rhythm topographies during motor imagery and actual movements," *Brain Topogr,* vol. 12, pp. 177-86, 2000.

[44] C. Neuper, M. Wortz, and G. Pfurtscheller, "ERD/ERS patterns reflecting sensorimotor activation and deactivation," *Prog Brain Res,* vol. 159, pp. 211-22, 2006.

[45] G. Pfurtscheller, C. Neuper, D. Flotzinger, and M. Pregenzer, "EEG-based discrimination between imagination of right and left hand movement," *Electroencephalogr Clin Neurophysiol,* vol. 103, pp. 642-51, Dec 1997.

[46] M. Peltoranta and G. Pfurtscheller, "Neural network based classification of non-averaged event-related EEG responses," *Med Biol Eng Comput,* vol. 32, pp. 189-96, Mar 1994.

[47] F. Babiloni, F. Cincotti, L. Bianchi, G. Pirri, R. M. J. del, J. Mourino, S. Salinari, and M. G. Marciani, "Recognition of imagined hand movements with low resolution surface Laplacian and linear classifiers," *Med Eng Phys,* vol. 23, pp. 323-8, Jun 2001.

[48] T. P. Jung, C. Humphries, T. W. Lee, S. Makeig, M. J. McKeown, V. Iragui, and T. J. Sejnowski, "Removing electroencephalographic artifacts: comparison between ICA and PCA," *Neural Networks Signal Processing,* vol. 8, pp. 63-72, 1998.

[49] T. P. Jung, C. Humphries, T. W. Lee, S. Makeig, M. J. McKeown, V. Iragui, and T. J. Sejnowski, "Extended ICA removes artifacts from electroencephalographic recordings," in *Advances in Neural Information Processing Systems* vol. 10, M. Jordan, M. Kearns, and S. Solla, Eds. Cambridge MA: MIT Press, 1998.

[50] R. Bogacz, U. Markowska-Kaczma, and A. Kozik, "Blinking artefact recognition in EEG signal using artificial neural network," in *Proc 4th Conference on Neural Networks,* Zakopane, Poland, 1999.

[51] C. Robert, J. F. Gaudy, and A. Limoge, "Electroencephalogram processing using neural networks," *Clin Neurophysiol,* vol. 113, pp. 694-701, May 2002.

[52] K. Polat and S. Güneş, "Classification of epileptiform EEG using a hybrid system based on decision tree classifier and fast Fourier transform," *Applied Mathematics and Computation,* vol. In Press, Corrected Proof, 2006.

[53] A. Subasi, "Selection of optimal AR spectral estimation method for EEG signals using Cramer-Rao bound," *Comput Biol Med,* vol. 37, pp. 183-94, Feb 2007.

[54] A. Subasi, "EEG signal classification using wavelet feature extraction and a mixture of expert model," *Expert Systems with Applications,* vol. 32, pp. 1084-1093, May 2007.

[55] D. J. McFarland, W. A. Sarnacki, and J. R. Wolpaw, "Brain-computer interface (BCI) operation: optimizing information transfer rates," *Biol Psychol,* vol. 63, pp. 237-51, Jul 2003.

[56] A. Kostov and M. Polak, "Parallel man-machine training in development of EEG-based cursor control," *IEEE Trans Rehabil Eng,* vol. 8, pp. 203-5, Jun 2000.

[57] Y. Wang, S. Gao, and G. X., "Common spatial pattern method for channel selection in motor imagery based brain-computer interface," in *Proceedings of the 2005 IEEE Engineering in Medicine and Biology 27th Annual Conference*, Shanghai, China, 2005.

[58] E. J. Costa and E. F. Cabral, Jr., "EEG-based discrimination between imagination of left and right hand movements using Adaptive Gaussian Representation," *Med Eng Phys,* vol. 22, pp. 345-8, Jun 2000.

[59] E. Gysels, P. Renevey, and P. Celka, "SVM-based recursive feature elimination to compare phase synchronization computed from broadband and narrowband EEG signals in Brain-Computer Interfaces," *Signal Processing,* vol. 85, pp. 2178-2189, Nov 2005.

[60] M. Thulasidas, C. Guan, and J. Wu, "Robust classification of EEG signal for brain-computer interface," *IEEE Trans Neural Syst Rehabil Eng,* vol. 14, pp. 24-9, Mar 2006.

[61] A. Vallabhaneni and B. He, "Motor imagery task classification for brain computer interface applications using spatiotemporal principle component analysis," *Neurol Res,* vol. 26, pp. 282-7, Apr 2004.

[62] N. Christianini and J. Shawe-Taylor, *An Introduction to Support Vector Machines and other kernel-based learning methods*: Cambridge University press, 2000.

[63] C. Cortes and V. Vapnik, "Support-vector networks," *Machine Learning,* vol. 20, pp. 273-297, Sep 1995.

[64] S. R. Gunn, "Support Vector Machines for classification and regression," University of Southampton, Technical report, May 1998.

[65] D. J. McFarland, W. A. Sarnacki, T. M. Vaughan, and J. R. Wolpaw, "Brain-computer interface (BCI) operation: signal and noise during early training sessions," *Clin Neurophysiol,* vol. 116, pp. 56-62, Jan 2005.

[66] B. Mahmoudi and A. Erfanian, "Electro-encephalogram based brain-computer interface: improved performance by mental practice and concentration skills," *Med Biol Eng Comput,* vol. 44, pp. 959-69, Nov 2006.

[67] M. R. Nuwer, G. Comi, R. Emerson, A. Fuglsang-Frederiksen, J. M. Guerit, H. Hinrichs, A. Ikeda, F. J. Luccas, and P. Rappelsburger, "IFCN standards for digital recording of clinical EEG. International Federation of Clinical Neurophysiology," *Electroencephalogr Clin Neurophysiol,* vol. 106, pp. 259-61, Mar 1998.

[68] H. Petsche, H. Pockberger, and P. Rappelsberger, "[Music perception, EEG and musical training]," *EEG EMG Z Elektroenzephalogr Elektromyogr Verwandte Geb,* vol. 16, pp. 183-90, Dec 1985.

[69] Watermark, "Enya," *Watermark,* 1988.

[70] The kids aren't alright, "Offspring," *Americana,* 1998.

[71] Physiology Software Tools, Inc., "E-prime ": http://www.pstnet.com/products/e-prime (last viewed: Nov 2006)

[72] Electrical Geodesics, Inc., "The Net-Station," http://www.egi.com/netstation.html. (last viewed: Nov 2006)

[73] C. Veigl, "BrainBay ": http://www.shifz.org/brainbay. (last viewed: Sep 2006)

[74] R. Likert, "A Technique for the Measurement of Attitudes," *Archives of Psychology* vol. 140, pp. 1-55, 1932.

[75] C. Thornton, "Separability is a learner's best friend," in *Proc. of the 4th Neural Computation and Psychology Workshop: Connectionist Representations*, London, 1997, pp. 40-47.

[76] A. Delorme and S. Makeig, "EEGLAB: an open source toolbox for analysis of single-trial EEG dynamics including independent component analysis," *J Neurosci Methods,* vol. 134, pp. 9-21, Mar 15 2004.

[77] Wikipedia, "Cross-validation," http://en.wikipedia.org/wiki/Cross-validation#_ref-Kohavi95_0, (last viewed: Feb 2007).

[78] C. Neuper, R. Scherer, M. Reiner, and G. Pfurtscheller, "Imagery of motor actions: differential effects of kinesthetic and visual-motor mode of imagery in single-trial EEG," *Brain Res Cogn Brain Res,* vol. 25, pp. 668-77, Dec 2005.

[79] J. B. Earle, "Task difficulty and EEG alpha asymmetry: an amplitude and frequency analysis," *Neuropsychobiology,* vol. 20, pp. 95-112, 1988.

[80] R. Kristeva, D. Cheyne, W. Lang, G. Lindinger, and L. Deecke, "Movement-related potentials accompanying unilateral and bilateral finger movements with different inertial loads," *Electroencephalogr Clin Neurophysiol,* vol. 75, pp. 410-8, May 1990.

[81] S. R. Benbadis and D. Rielo, "EEG Atlas: Focal (Nonepileptic) Abnormalities," eMedicine, WebMD, http://www.emedicine.com/neuro/topic688.htm (last viewed: Feb 2007).

[82] "Biology website reference for students and teachers," www.usm.maine.edu/psy/broida/101/neuron.JPG (last viewed: Oct 2005)

[83] K. M. V. D. Graaff, *Human Anatomy*, 6th ed. New York: McGraw-Hill, pp.271-273, 2002.

Appendix A Geodesic Sensor Net Specifications

The following specification is an extract from the GSN technical manual [13].

Overall System Specifications

System 200 has been designed for use under the environmental conditions given in Table A.1.

Table A.1: GSN system 200 overall operating environment

Storage temperature	0° to 47° C (32° to 116° F)
Operating temperature	10° to 35° C (50° to 95° F)
Relative humidity	5% to 95% non condensing
Maximum altitude	3,048 m (10,000 feet)

Dimensions, Weight

The following are approximate overall dimensions for the Net Amps box:

- Height: 27.9 cm (11 inches)
- Width: 43.2 cm (17 inches)
- Depth: 48.0 cm (18.9 inches)

The approximate weight of the Net Amps box is 16.8 kg (37 lb).

Dynamic Range

Maximum resolvable signal is ±2.5V/1000, or ±2.5 millivolts.

Precision

Minimum resolvable signal is ±2500 microvolts/±32,768, or 0.076 microvolts.

Inherent Noise

Amplifiers always have a certain amount of low-level noise inherent to the circuitry. This noise comes from a variety of sources, including thermal activity, leakage of digital signals to analog circuitry, and power supply noise. The Net Amps is a low-noise amplifier: Net Amps internal noise, measured with the analog inputs grounded, is tested to be less than 1 μV RMS, and typically falls below 0.6 μV RMS. Amplifier inherent noise is to be distinguished from noise that has an environmental origin.

Appendix B ModularEEG Specifications and Schematics

The following specification and schematics is an extract from the ModularEEG documentation in the OpenEEG website [12].

B.1 ModularEEG specification

General specification

Number of channels	2 - 6 (only 2 tested)
Resolution	four 10 bits, two 8 bits
Input Voltage Resolution	0.5 uV
Input Voltage Full Scale	+/-256 uV
Wideband noise	~ 1 uVp-p
Supply Current (5V or 9 - 12V supply)	70 mA (2 channels)
Isolation voltage *(note 2, 3)*	2500V (1 minute)
Continuous isolation voltage *(note 2, 3)*	480V

Notes:

1. On the ATmega8 microcontroller, channels 5 and 6 are only 8 bit due to noise problems. These channels cannot be used for EEG without increasing the EEG-amplifier gain four times.
2. The DCDC converter and optocoupler are certified to withstand 3000Vrms and 2500Vrms respectively, for one minute. The guaranteed working voltage under periods longer than one minute is 1100Vrms and 480Vrms respectively.
3. The ModularEEG is not IEC60601-1 certified. It will probably not handle lightning strikes and other extreme electrical conditions. Use with caution.

Supply Current

Digital board	52 mA
Digital board + serial cable connected	56 mA
Total current (including 2 channel amp)	73 mA
Estimated total for 4 channel setup	77 mA
DC/DC converter efficiency	~78% (=>15mA, 2 ch)

EEG Amplifier specification

Gain	7812.5 (nominally)
Offset handling capability	**TBD** > 200 mVdc
Low frequency CMRR	**TBD** > 100 dB
Highpass filter	2nd order, fc = 0.4Hz
Anti-aliasing filter	See filter document.
Extra features	250 uV(+/-10%) test signal. DRL circuit - adds > 40dB CMRR at 50/60Hz.

AD-converter specification (AT90S4433)

Number of channels	6
Resolution	10 bits
Effective number of bits *(note 1, 3)*	9.1 bits (< 100Hz)
Signal to Noise Ratio *(note 1, 3)*	58.7dB (max possible 60dB)
Integral Nonlinearity *(note 2)*	+/- 0.5 LSB (typ)
Differential Nonlinearity *(note 2)*	+/- 0.5 LSB (typ)
Offset Error *(note 2)*	1 LSB (typ)
Absolute Accuracy (ADC clock = 200kHz)	1 LSB (typ), 2 LSB max
Gain error (Voltage reference error)	1% (typ), 2.25% max

Notes

1. Dynamic characteristics are taken from *Holcher, R. et al., The Test of AD Converters Embedded on Two Microcontrollers, Measurement Science Review (Journal of the Institute of* ***Measurement Science,*** *Slovak Academy of Sciences,* http://www.measurement.sk/ *), Volume 1 Number 1 2001* http://www.measurement.sk/PAPERS/Holcer.pdf
2. INL, DNL, offset error and absolute accuracy numbers are taken from the manufacturer's data sheet. The article in note 1 specifies a higher INL: 1.4 LSB max (absolute value, not +/- 1.4 LSB). All values assume ADC clock <200 kHz. Yeah, these numbers could be better.
3. The article in note 1 discusses the AT90S8535 microcontroller. This is a bigger microcontroller in the same family as AT90S4433, so chances are they have very similar cores. The measurements were done at a higher sample rate (fs = 4800Hz) and with Vref = 2.5V which may degrade the results slightly compared to the fs = 256Hz and Vref = 4.0V used in the ModularEEG.

B.2 Analog board schematic

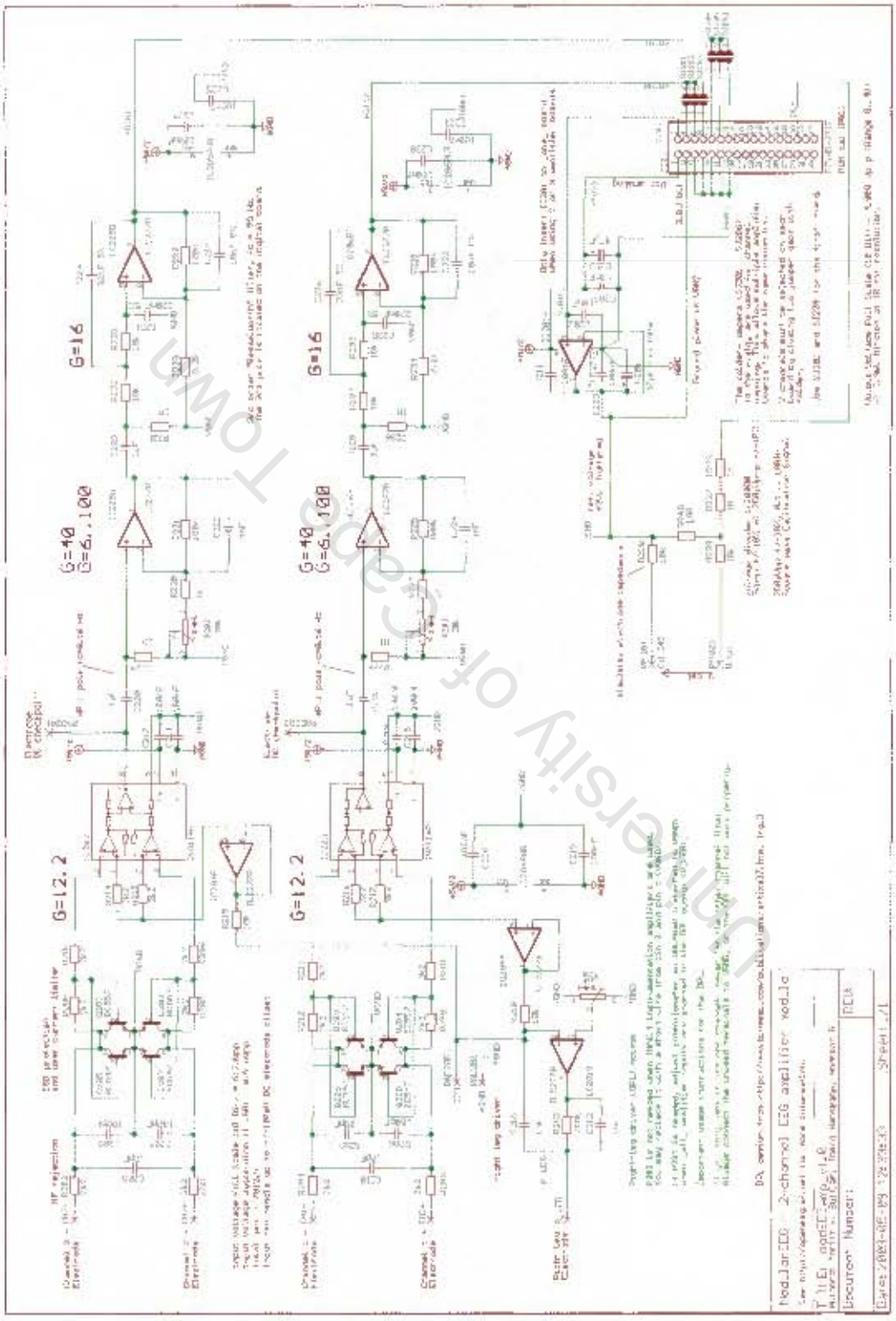

B.3 Digital board schematic

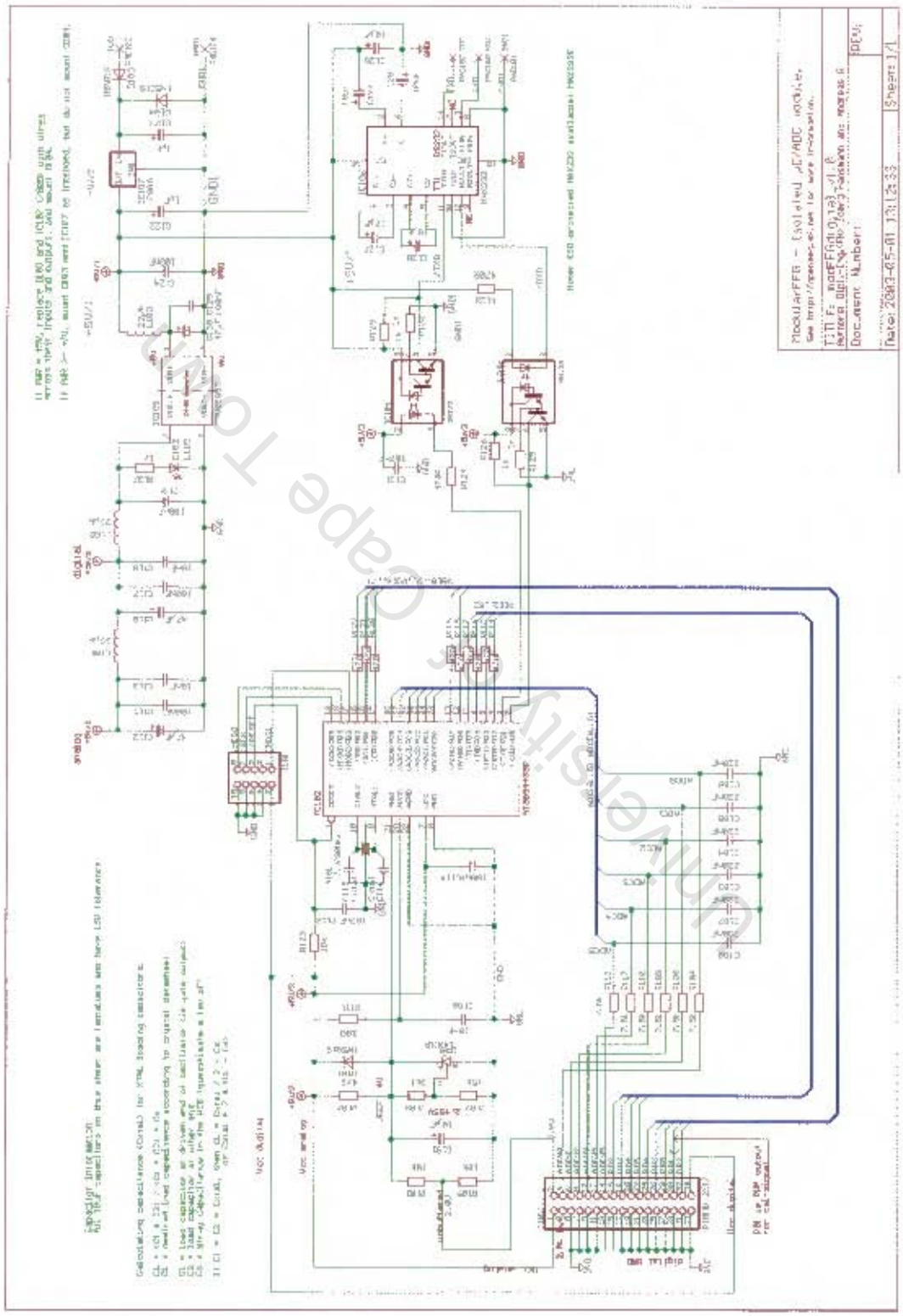

Appendix C Neuroanatomy and Muscles

C.1 The structure of the neuron

The human body contains more than 100 billion neurons, and most of them are concentrated in the brain. Neurons are cells that carry information in the brain and in the central nervous system, in the form of electro-chemical signals. The neurons have specialized projections called axons and dendrites, and a cell body shown in figure C.1.

The dendrites are branched processes that extend from the cytoplasm of the cell body, which respond to specific stimuli and conduct impulses to the cell body. The axon is a relatively long, cylindrical process that conducts impulses away from the cell body.

The signals are carried along axons (signal transmitter) and dendrites (signal receiver) of the neuron by changes in electrical properties called action potential.

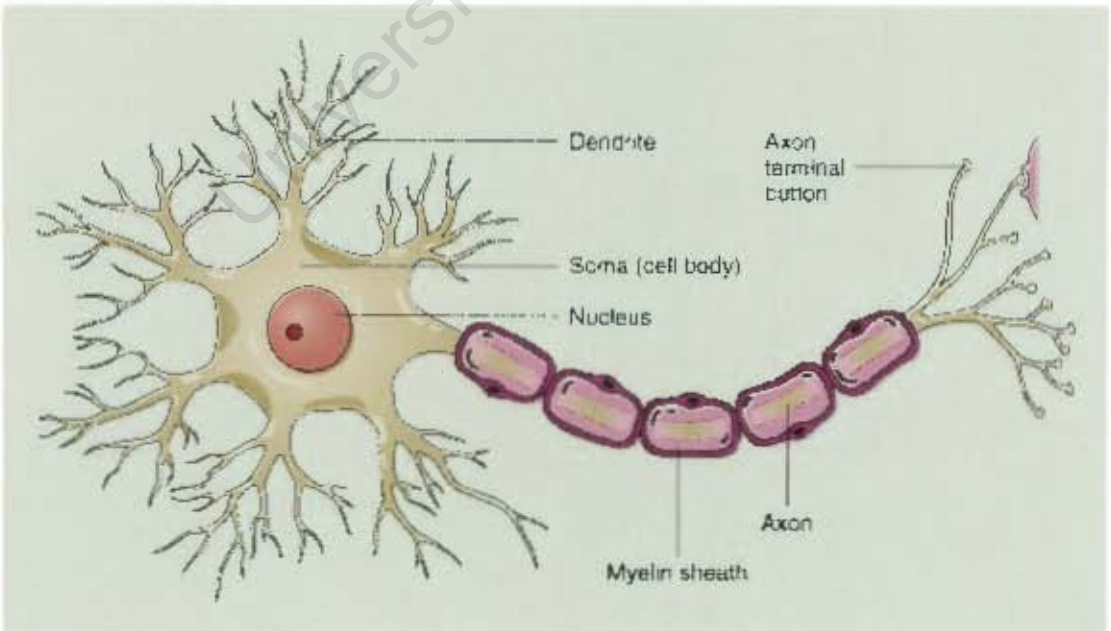

Figure C.1: The structure of a neuron [82].

C.2 The structure of the brain

"The cerebrum, consisting of five paired lobes within two convoluted hemispheres, is concerned with higher brain function, including the perception of sensory impulses, the instigation of voluntary movement, the storage of memory, thought processes and reasoning ability, the cerebrum is also concerned with instinctual and limbic (emotional) functions" [83].

"The left and right hemispheres of the cerebrum are incompletely separated by a longitudinal cerebral fissure, which is then subdivided into five lobes by deep sulci or fissures. Four of these lobes appear on the surface of the cerebrum and are named according to the overlying cranial bones" [83]. See figure C.2 for a lateral and superior view of the cerebrum.

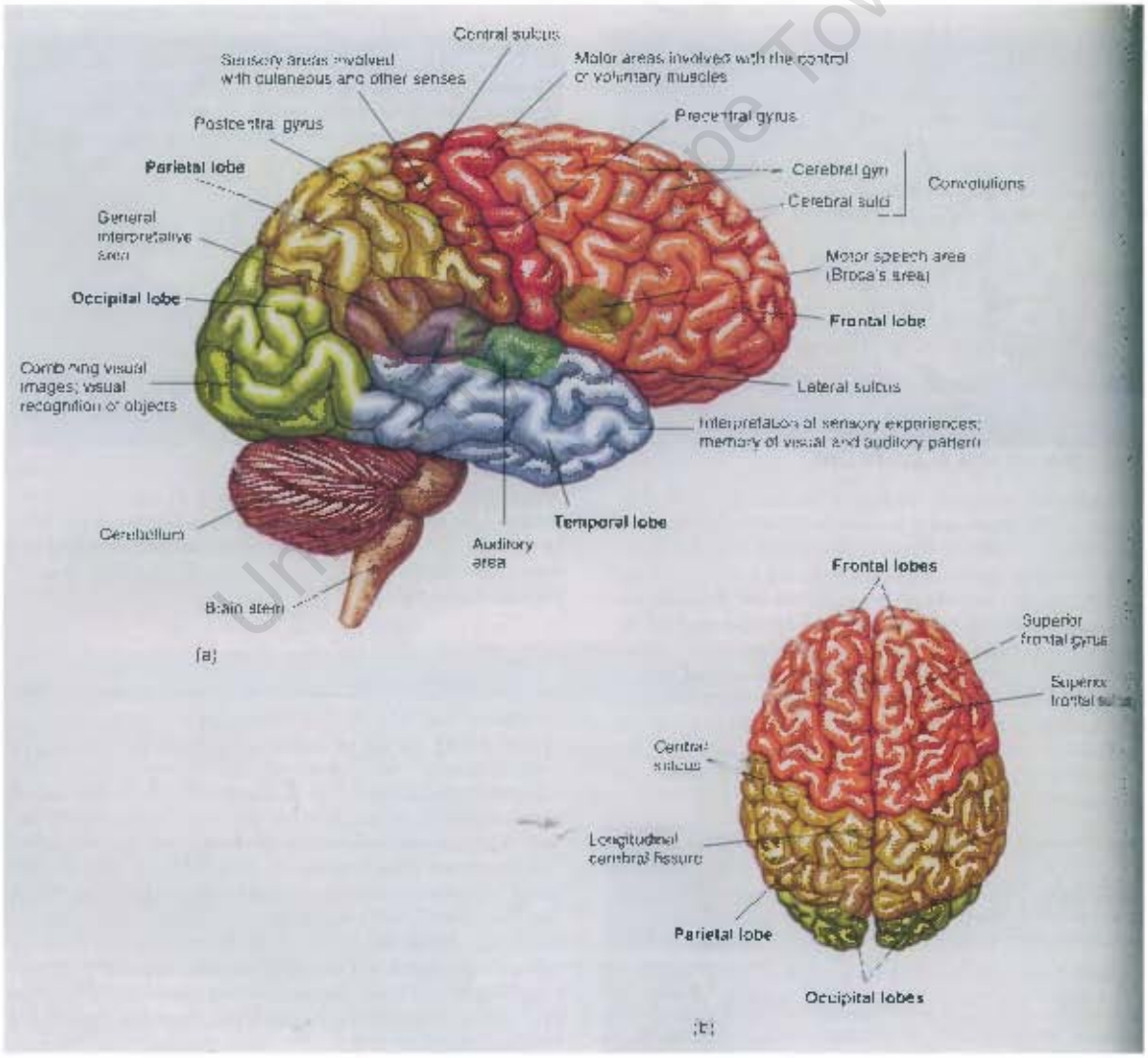

Figure C.2: The cerebrum. (a) a lateral view and (b) a superior view [83].

Eye blinks can be detected by increase in activity in the occipital lobe, where visual area is located. In the centre of the left and right hemisphere is where the auditory areas can be found. The motor and sensory motor areas of the cerebral cortex are shown in figure C.3, which are responsible for motor movement and sensory stimuli.

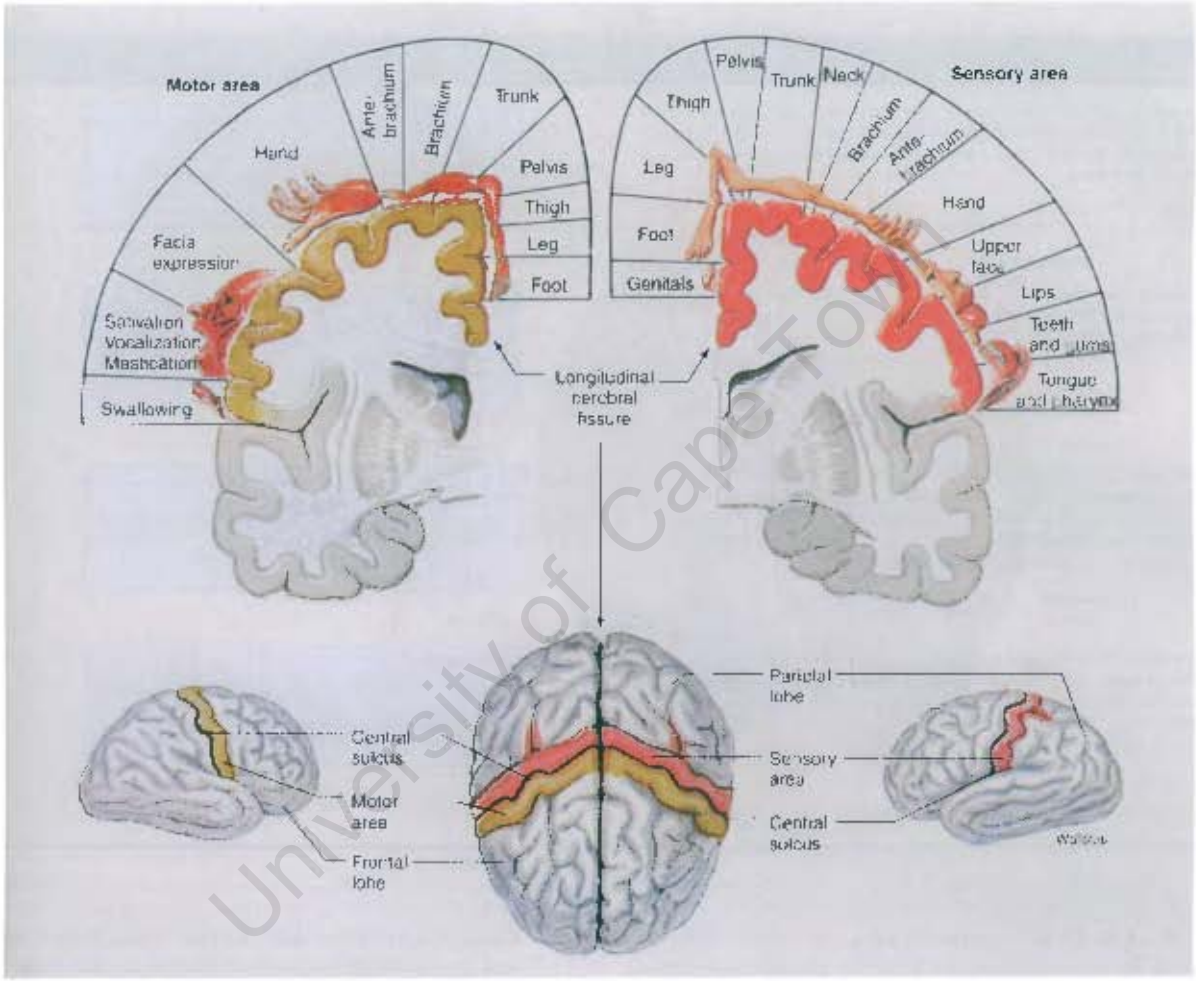

Figure C.3: Motor and sensory areas of the cerebral cortex. Motor areas control skeletal muscle and sensory areas receive somatesthetic sensations [83]

C.3 Flexor Carpi Ulnaris muscle

"The flexor carpi ulnaris muscle is positioned on the medial anterior side of the forearm, where it assists in flexing the wrist joints and adducting the hand" [83]. See figure C.4 for a diagram showing its position on the hand

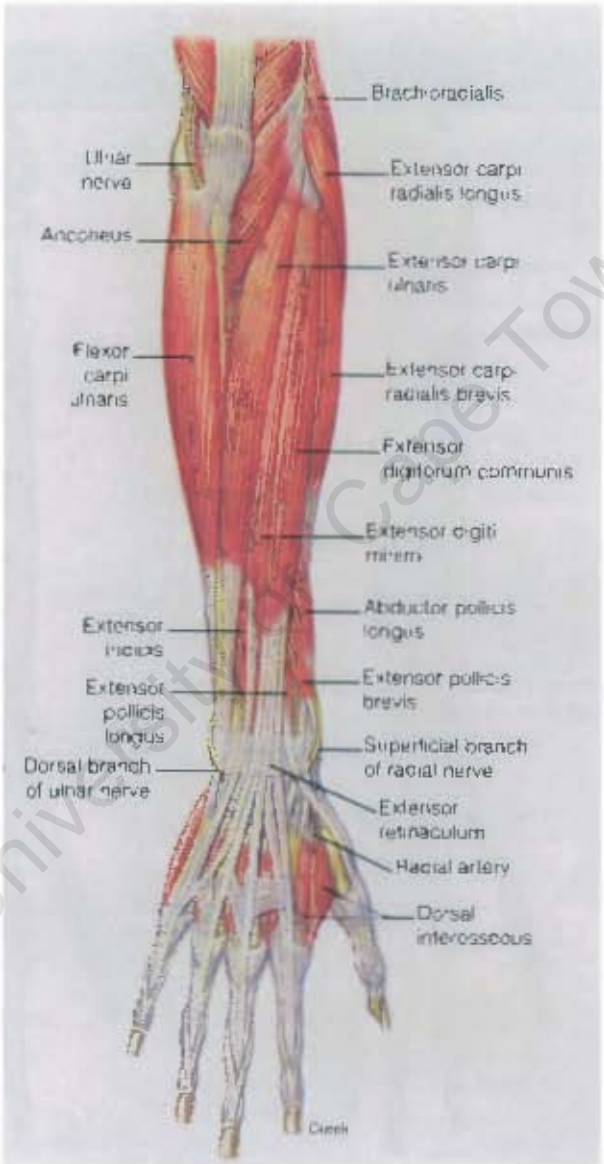

Figure C.4: Superficial muscles of right forearm: a posterior view [83]

Appendix D Ethics Approval

UNIVERSITY OF CAPE TOWN

Health Sciences Faculty
Research Ethics Committee
Room E52-24 Groote Schuur Hospital Old Main Building
Observatory 7925
Telephone [021] 406 6338 • Facsimile [021] 406 6411
e-mail [illegible]

27 November 2006

REC REF: 379/2006

Ms TA Lin
Electrical Engineering
Upper Campus

Dear Ms Lin

PROJECT TITLE: USING SCALP EEG TO IMPLEMENT A DIRECT BRAIN COMPUTER INTERFACE BASED ON MENTAL STATE.

Thank you for submitting your study to the Research Ethics Committee for review.

I have pleasure in informing you that the Ethics committee has **formally approved** the above mentioned study.

Please note that the ongoing ethical conduct of the study remains the responsibility of the principal investigator

This serves to confirm that the University of Cape Town Research Ethics Committee complies to the Ethics Standards for Clinical Research with a new drug in patients, based on the Medical Research Council (MRC-SA), Food and Drug Administration (FDA-USA), International Convention on Harmonisation Good Clinical Practice (ICH GCP) and Declaration of Helsinki guidelines.

The Research Ethics Committee granting this approval is in compliance with the ICH Harmonised Tripartite Guidelines E6: Note for Guidance on Good Clinical Practice (CPMP/ICH/135/95) and FDA Code Federal Regulation Part 50, 56 and 312

Please quote the REC. REF in all your correspondence.

Yours sincerely

Signed by candidate

PROF. M. BLOCKMAN
pp CHAIRPERSON, HSF HUMAN ETHICS

[illegible]

Appendix E Subject Consent forms

An investigation of EEG changes generated with mental tasks

Informed consent

Engineers from the University of Cape Town are developing a brain-computer interface that may be used to assist paralyzed people. A mental task based brain-computer interface is being investigated, this interface classifies the mental state of the subject, using neural network based on the frequency spectrum of EEG. Certain frequency components of EEG are modulated by the various mental states, therefore EEG recordings are required.

Health volunteers are required to perform a series of experimental tasks, during which EEG waveforms will be recorded. Each volunteer will be paid R50 on successful completion of the study. Aside from the payment, this testing will have no immediate benefit to the volunteers. However as part of a research and development process, it is envisaged that the end result of the research would be a brain-computer device.

Testing procedure

All testing will be carried out in the EEG laboratory, at the Anatomy Building (UCT Health Science Faculty)

The investigator will place the 128 channel Geodesic Sensor Net on the volunteers for the recording of EEG. 8 different experimental scenarios will be evaluated for their effect on the mental state. Each scenario will last 5 minutes. At the end of the experiment, the subjects will be asked to rate the level of mental fatigue of each mental task on a scale of 1 (least fatigue) -- 5 (most fatigue). Subjects are required to keep as still as possible during the 5 minutes recording sessions.

Possible risks associated with participation

The EEG equipment is inherently safe. Temporary mild skin sensitivity may results from the salt solution used with the electrode sponge. In the unlikely case of any subject experiencing discomfort, the subject should alert the investigator. The University of Cape Town has a public liability cover should some unforeseen event occur whilst you are participating in this study.

Statement of understanding and consent

I confirm that the exact procedure and techniques and the possible complications of the above tests have been thoroughly explained to me. I am free to withdraw from the study at any time should I choose to do so understand that I may ask questions at any time during the testing procedure. I know that the personal information required by the researchers and derived from the testing procedure will remain strictly confidential and will only be revealed as a number in classification analysis. I have carefully read this form and understand the nature, purpose and procedures of this study. I agree to participate in this research project conducted by the UCT Division of Biomedical Engineering.

Name of volunteer / guardian (if necessary): _____

Signature: _____

Name of Investigator: _____

Signature: _____

Date: _____

Research team

Postgraduate student: Ms T.A Lin (MSc student: UCT Electrical Engineering) Lnxtsu001@mail.uct.ac.za

Supervisors: Dr. L.R John (Lecturer, UCT MRC/Medical Imaging Unit) ljohn@cormack.uct.ac.za

Prof. J.C Tapson (Professor, UCT Electrical Engineering) jtapson@ebe.uct.ac.za

Appendix F Topographical plots

This section presents the topographical plots showing the individual channel classification accuracies for real tasks versus imagined tasks, and well as all other combinations of tasks not shown in the main text.

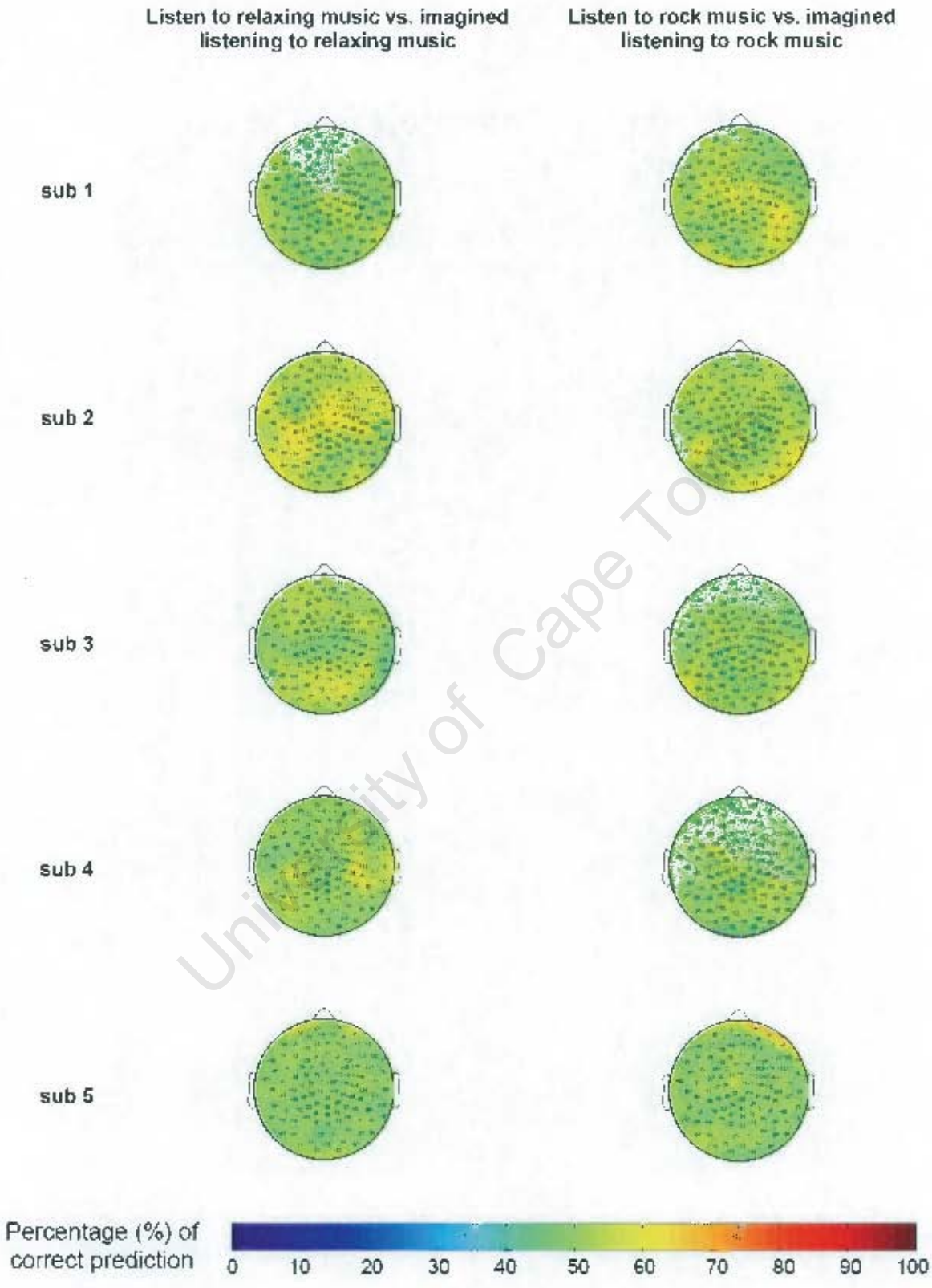

Figure F.1: Topographical plots showing SVM classification accuracy for real music tasks versus imagined music tasks.

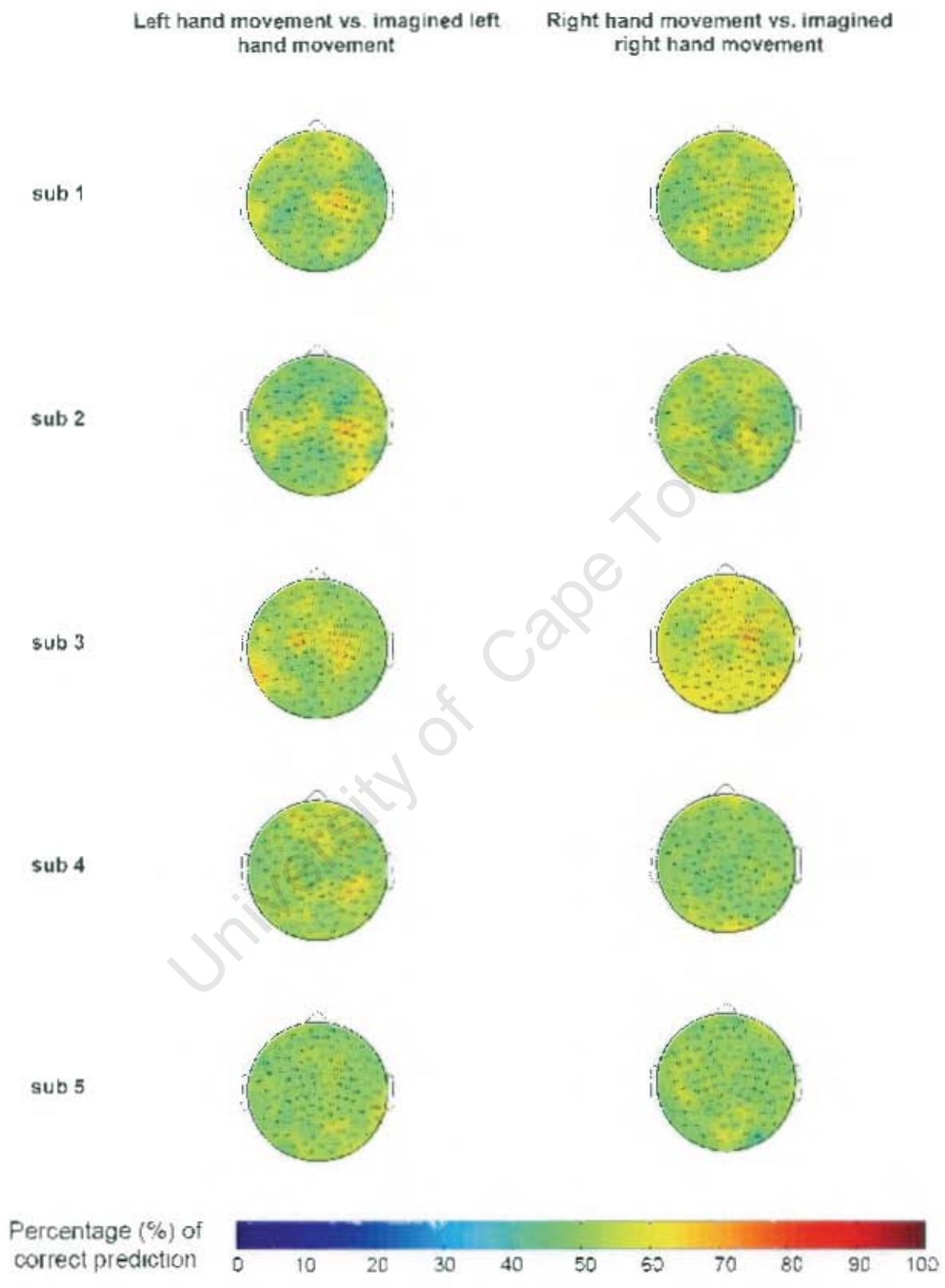

Figure F.2: Topographical plots showing SVM classification accuracy for real hand movement tasks versus imagined hand movement tasks

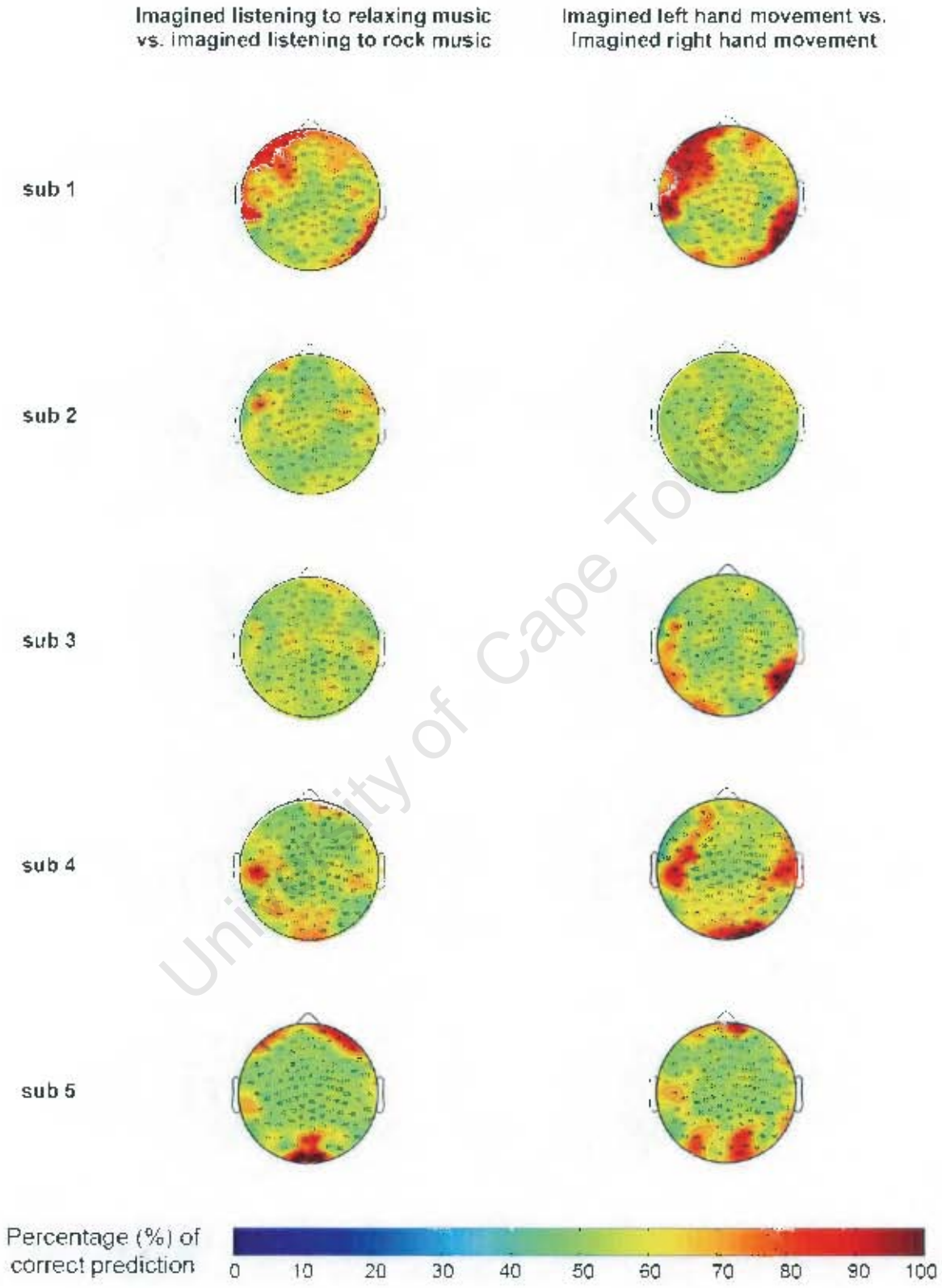

Figure F.3: Topographical plots showing SVM classification accuracy for imagined relax versus imagined rock music tasks and imagined left versus imagined right hand movement tasks.

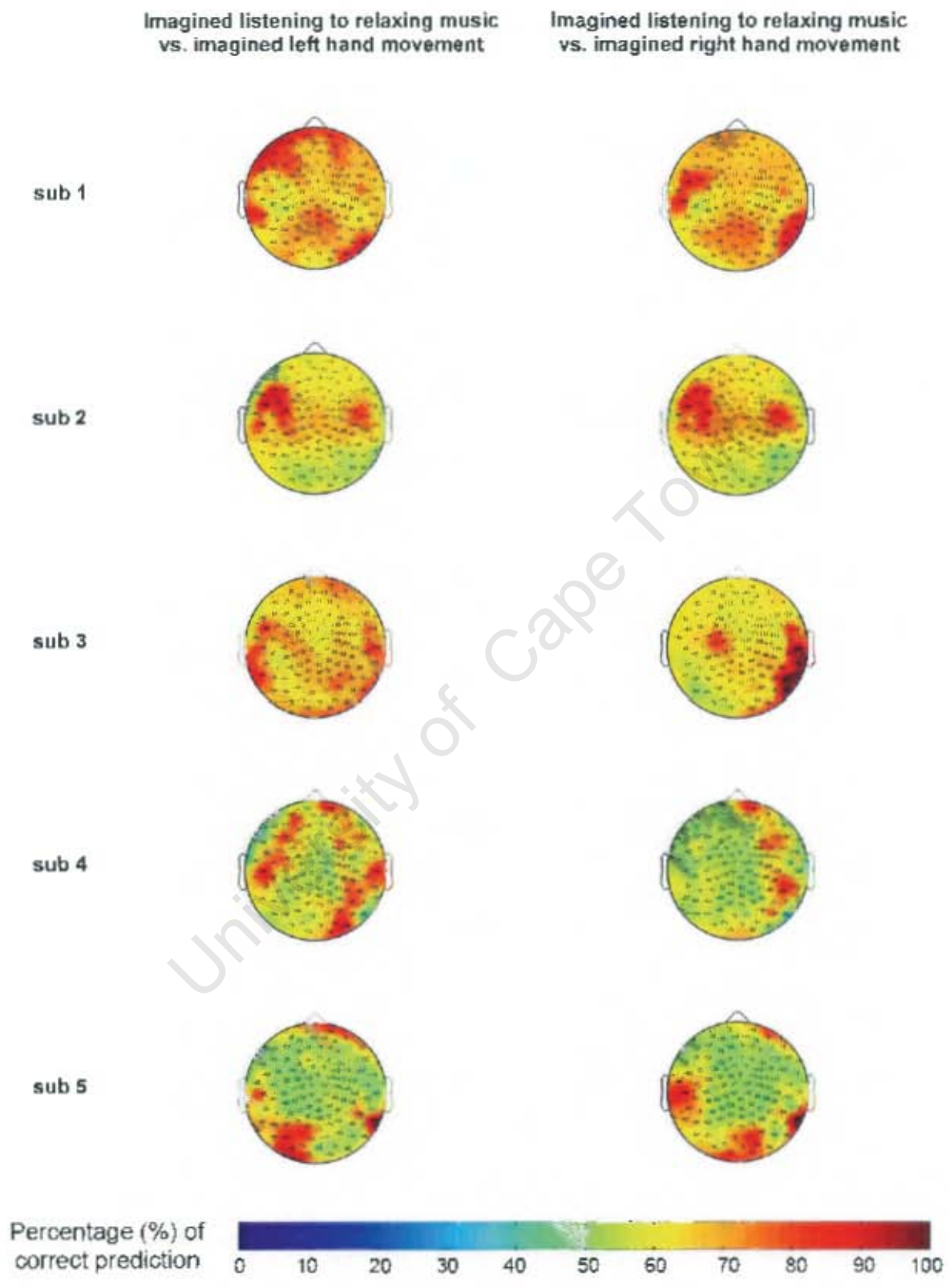

Figure F.4: Topographical plots showing SVM classification accuracy for imagined relaxing music task versus imagined left and right hand movement tasks.

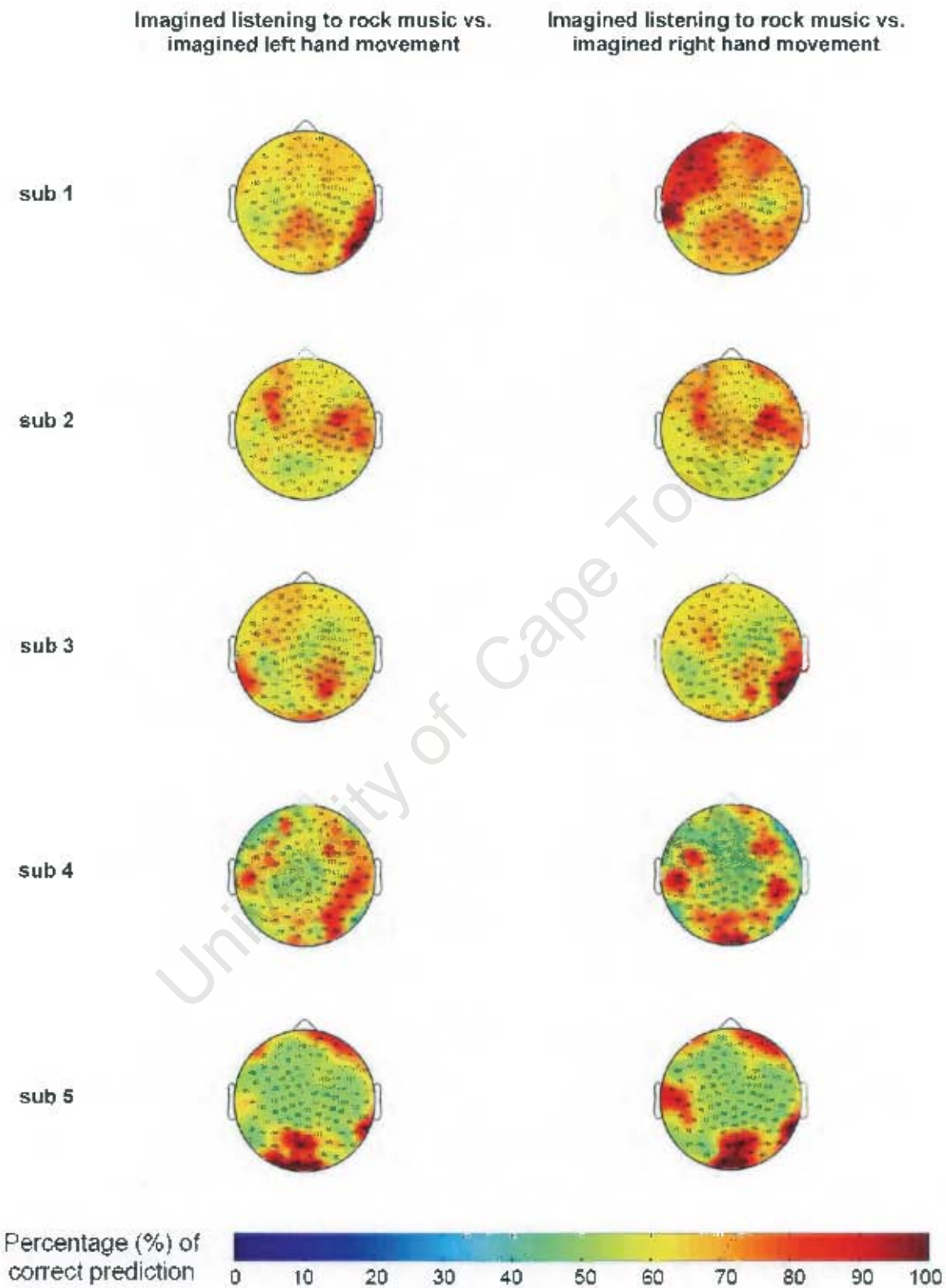

Figure F.5: Topographical plots showing SVM classification accuracy for imagined rock music task versus imagined left and right hand movement tasks.

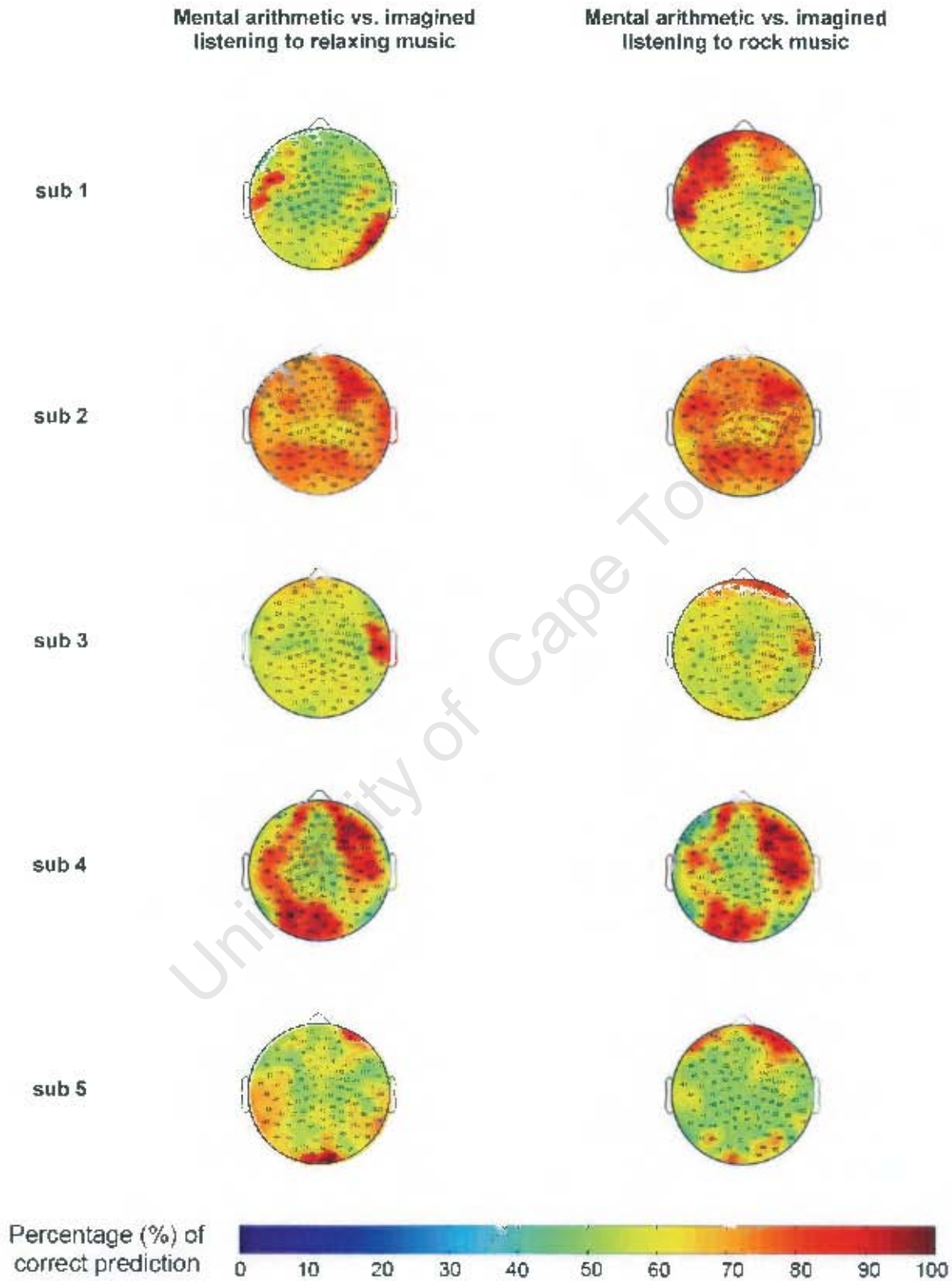

Figure F.6: Topographical plots showing SVM classification accuracy for mental arithmetic task versus imagined music tasks.

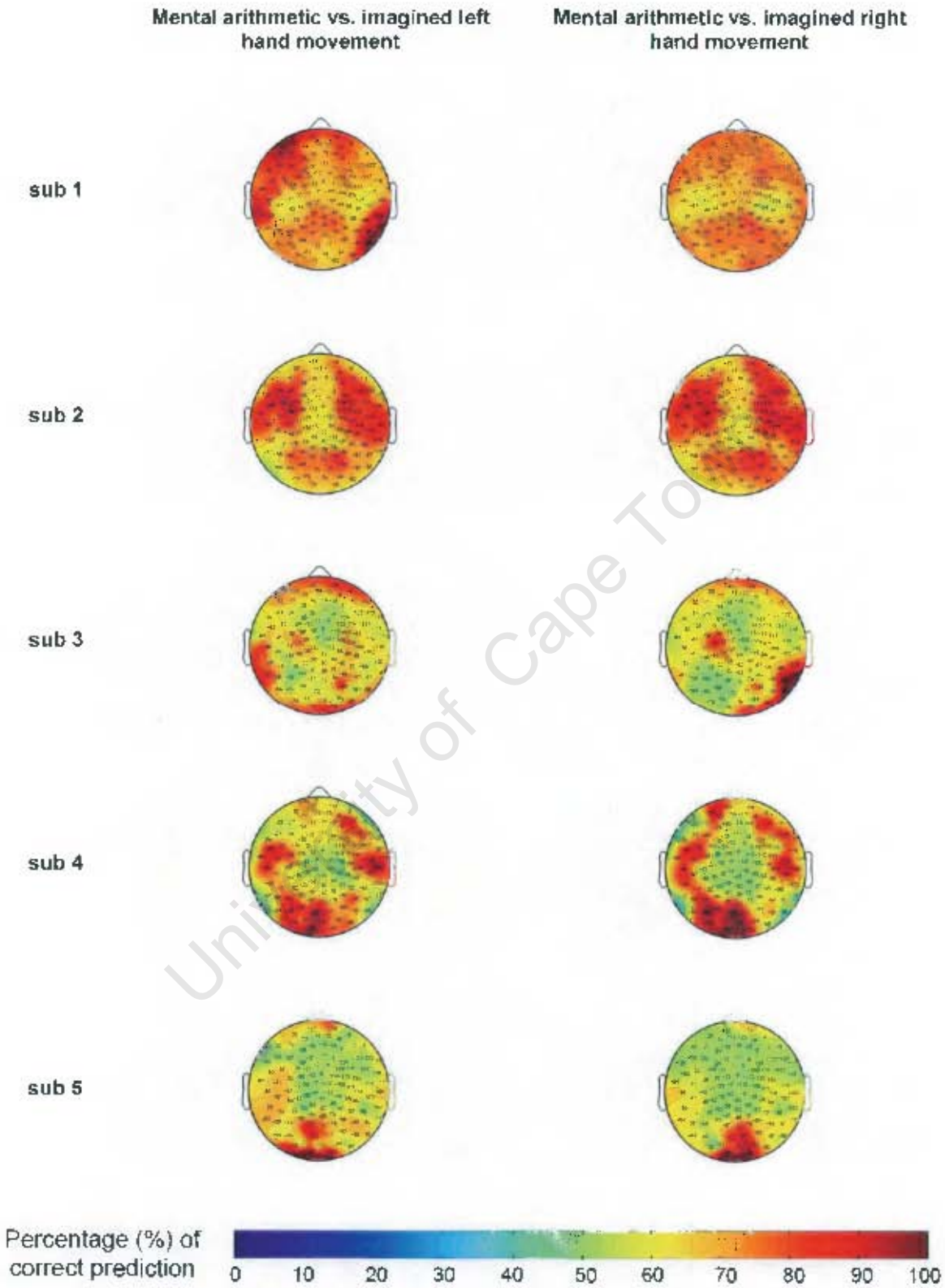

Figure F.7: Topographical plots showing SVM classification accuracy for mental arithmetic task versus imagined hand movement tasks.

Appendix G Examples of artifact removed from recorded data

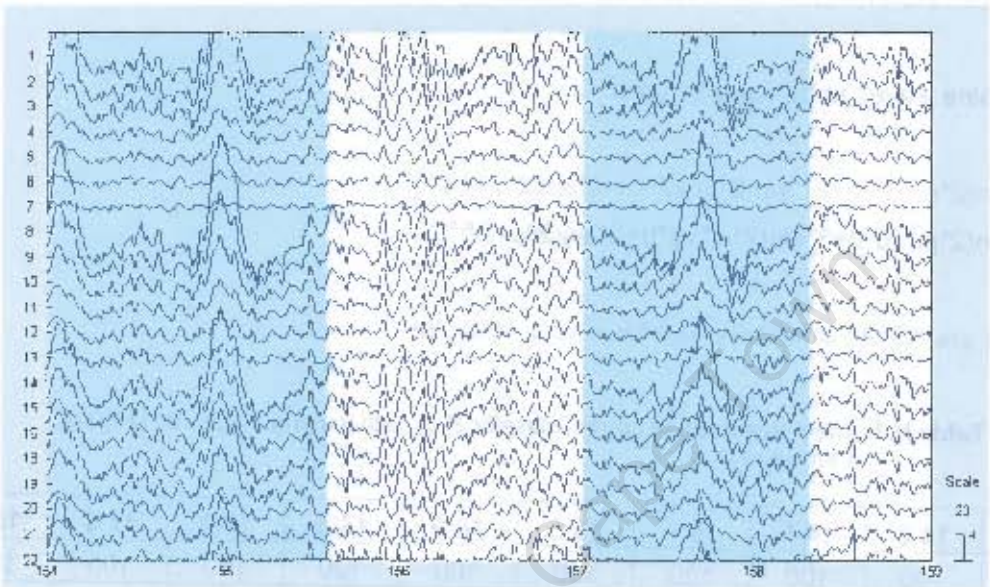

Figure G.1: Example of eye blink artifacts removed (highlight in blue) from the multi channel EEG data.

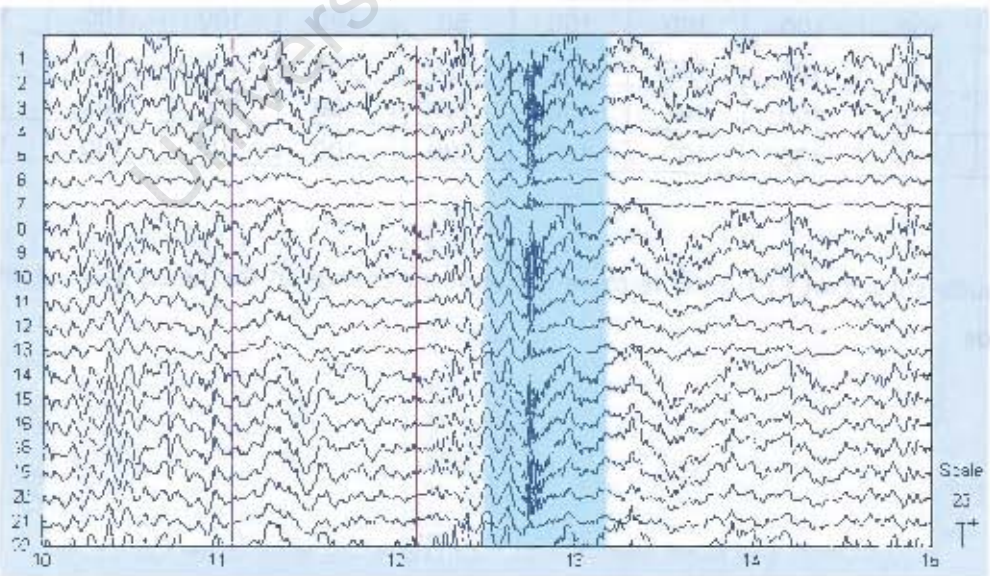

Figure G.2: Example of EMG artifacts removed (highlight in blue) from the multi-channel EEG data.

Appendix H SVM validation results

This classification results from SVM toolbox testing are shown in table H.1 below:

The two sine waves to be classified are:

s1 = 2*sin(2*pi*10*t)+k1*sin(2*pi*k2*t)+ 2*sin(2*pi*25*t);

s2 = 2*sin(2*pi*10*t)+3*sin(2*pi*16*t)+2*sin(2*pi*25*t);

where k1 and k2 are amplitude and frequency variables.

Table H.1: The percentage of correct classification with varying amplitude (k1) and frequency (k2).

k1 \ k2	14.0	14.5	15.0	15.5	16.0	16.5	17.0	17.5	18.0
1.0	100	100	100	100	100	100	100	100	100
1.5	100	100	100	100	100	100	100	100	100
2.0	100	100	100	100	50	100	100	100	100
2.5	100	100	100	100	50	100	100	100	100
3.0	100	100	100	50	50	50	100	100	100
3.5	100	100	100	100	50	100	100	100	100
4.0	100	100	100	100	50	100	100	100	100
4.5	100	100	100	100	100	100	100	100	100
5.0	100	100	100	100	100	100	100	100	100

The results show that FFT-SVM is more sensitive to change in frequency than change in amplitude.

Appendix I MATLAB Code

This section contains the MATLAB codes used for EEG data analysis. The files include:

- Read BrainBay archive file
- EEG data preprocessing
- Find frequency component of single channel data
- Compute classification results for each channel
- Append channel labels to results
- Plot topographical plots
- Test SVM toolbox

I.1 Read BrainBay archive file (ModularEEG)

```
%%%%%%% read ARC %%%%%%%%
%% read data from the BrainBay archive file %%

function readARC = readARC (testnum)

testfile = [testnum '.arc'];

fid = fopen(testfile,'r');

ch1_vector = [];
ch3_vector = [];
ch4_vector = [];


[test1_header, count]=fread(fid,255,'uint8');
[test1_discard, count]=fread(fid,7680,'uint8');  %% discard first 30s

for data_size = 1:84480      % 4mins = 61440%  5mins=76800  1min = 15360  30s = 7680

 for loop = 1:17
  [test1_data, count]=fread(fid,1,'uint8');

  if test1_data == 165
     [test1_data, count]=fread(fid,1,'uint8');
     if test1_data == 90
        break;
     end
  end
 end

  [test1_data, count]=fread(fid,15,'uint8');

  if count < 15
     break;
  end

  ch1_sample = test1_data(3)*256 + test1_data(4) - 512;
  ch3_sample = test1_data(7)*256 + test1_data(8) - 512;
  ch4_sample = test1_data(9)*256 + test1_data(10) - 512;
  ch1_vector = [ch1_vector; ch1_sample];
  ch3_vector = [ch3_vector; ch3_sample];
  ch4_vector = [ch4_vector; ch4_sample];

end

fclose(fid)

eval(['save sub17_r_' testnum '.mat']);

return;

%%%%%%%%%%%%%%%%%%%%%
```

I.2 EEG data pre-processing (GSN - EEGLAB)

```
%%%%% EEG pre-process  %%%%%%%%%%

clear all; close all;
eeglab;

%% t1
eegfile = 'sub17_r_t1';
```

```
eval(['EEG = pop_importdata( "dataformat", "matlab", "data", "C:\Documents and
Settings\Administrator\Desktop\EEG experiment oct 2006\subject17 (aadil)\' eegfile '.mat", "setname","' eegfile '",
"srate",256, "pnts",0, "xmin",0, "nbchan",3);']);
EEG = eeg_checkset( EEG );
EEG = pop_eegfilt( EEG, 1, 0, [], [0]);
EEG.setname='sub17_f1';
EEG = eeg_checkset( EEG );
EEG = pop_eegfilt( EEG, 0, 40, [], [0]);
EEG = eeg_checkset( EEG );

%%% save set
eval(['EEGsetname = "' eegfile '_bpf.set"']);
EEG = pop_saveset( EEG, EEGsetname, 'C:\Documents and Settings\Administrator\Desktop\EEG experiment
oct 2006\subject17 (aadil)\');

%% t2
eegfile = 'sub17_r_t2';

eval(['EEG = pop_importdata( "dataformat", "matlab", "data", "C:\Documents and
Settings\Administrator\Desktop\EEG experiment oct 2006\subject17 (aadil)\' eegfile '.mat", "setname","' eegfile '",
"srate",256, "pnts",0, "xmin",0, "nbchan",3);']);
EEG = eeg_checkset( EEG );
EEG = pop_eegfilt( EEG, 1, 0, [], [0]);
EEG.setname='sub17_f1';
EEG = eeg_checkset( EEG );
EEG = pop_eegfilt( EEG, 0, 40, [], [0]);
EEG = eeg_checkset( EEG );

%%% save set
eval(['EEGsetname = "' eegfile '_bpf.set"']);
EEG = pop_saveset( EEG, EEGsetname, 'C:\Documents and Settings\Administrator\Desktop\EEG experiment
oct 2006\subject17 (aadil)\');

%%%%%%%%%%%%%%%%%%%%%%%%
```

I.3 Find frequency component of single channel EEG data

```
%%%%%%%% find frequency vector  %%%%%%%%


function freq_m = find_freq_vector(raw_vector, fft_length, slide_pt, sum_bands)  %% take in raw_eeg, fft_length
and sliding window percentage in decimals (0.2 for 20%)

sample_rate = 200;

epoch_size = fft_length*sample_rate;
index_vector = [1:epoch_size];
freq_vector = (index_vector-1)*sample_rate/epoch_size;
freq_vector = freq_vector';

matrix_ch = [];

sliding = round(slide_pt*epoch_size);
num_epoch = round(length(raw_vector)/sliding - epoch_size/sliding) -1;

for k = 0:num_epoch-1
   current_epoch1 = raw_vector(k*sliding+1 : k*sliding+1 + epoch_size-1);
   current_epoch1 = hanning(epoch_size).*current_epoch1;
   current_epoch1 = current_epoch1';
   fft_epoch = abs(fft(current_epoch1)*2/epoch_size);
   matrix_ch = [matrix_ch; fft_epoch];
end

%%%%%%%%%%%%%%%%%%%%%%%%%%%%%%%%%%%%%%%%%%%%%%%%%%%% filter bank
freq_v = [];
```

```
freq_m = [];


if sum_bands == 0  %%%%%%%%%%%%%%%%%%%%%%%%%%% no summing of bands
   for epoch = 1:num_epoch
      for freq = 1:30

         freq_v(freq) = matrix_ch(epoch,freq+4);
      end
      freq_m = [freq_m, freq_v'];
   end

   sum_bands
elseif sum_bands == 1  %%%%%%%%%%%%%%%%%%%%%%%%%%% sum the bands
   for epoch = 1:num_epoch
      for freq = 4:7
        theta(freq-3) = matrix_ch(epoch,freq);
      end

      for freq = 8:13
        alpha(freq-7) = matrix_ch(epoch,freq);
      end

      for freq = 14:30
        beta(freq-13) = matrix_ch(epoch,freq);
      end
      freq_v = [freq_v, mean(theta)];
      freq_v = [freq_v, mean(alpha)];
      freq_v = [freq_v, mean(beta)];

      freq_m = [freq_m, freq_v'];
      freq_v = [];
   end

   sum_bands
elseif sum_bands == 2  %%%%%%%%%%%%%%%%%%%%%%%%%%% beta band only

   for epoch = 1:num_epoch
      for freq = 14:30
        beta(freq-13) = matrix_ch(epoch,freq);
      end
      freq_m = [freq_m, beta'];
      beta = [];
   end

   sum_bands
elseif sum_bands == 3  %%%%%%%%%%%%%%%%%%%%%%%%%%% alpha band only

   for epoch = 1:num_epoch
      for freq = 8:13
        alpha(freq-7) = matrix_ch(epoch,freq);
      end
      freq_m = [freq_m, alpha'];
      alpha = [];
   end

   sum_bands
elseif sum_bands == 4   %%%%%%%%%%%%%%%%%%%%%%%%%%% theta band only

   for epoch = 1:num_epoch
      for freq = 4:7
        theta(freq-3) = matrix_ch(epoch,freq);
      end
      freq_m = [freq_m, theta'];
      theta = [];
   end
```

```
   sum_bands

elseif sum_bands == 5  %%%%%%%%%%%%%%%%%%%%%%%%%%%%%%%%%%%%%%%alpha & beta
   for epoch = 1:num_epoch
      for freq = 8:30
        a_b(freq-7) = matrix_ch(epoch,freq);
      end
      freq_m = [freq_m, a_b'];
      a_b = [];
   end

   sum_bands

elseif sum_bands == 6  %%%%%%%%%%%%%%%%%%%%%%%%%%%%%%%%%%%%%%%%%  alpha & theta
   for epoch = 1:num_epoch
      for freq = 4:13
        a_t(freq-3) = matrix_ch(epoch,freq);
      end
      freq_m = [freq_m, a_t'];
      a_t = [];
   end

   sum_bands


elseif sum_bands == 8  %%%%%%%%%%%%%%%%%%%%%%%%%%%%%%%%%%%%%%%%%%%%beta1 band only

   for epoch = 1:num_epoch
      for freq = 14:20
        beta(freq-13) = matrix_ch(epoch,freq);
      end
      freq_m = [freq_m, beta'];
      beta = [];
   end

   sum_bands

elseif sum_bands == 9  %%%%%%%%%%%%%%%%%%%%%%%%%%%%%%%%%%%%%%%%%%%%beta2 band only

   for epoch = 1:num_epoch
      for freq = 21:30
        beta(freq-20) = matrix_ch(epoch,freq);
      end
      freq_m = [freq_m, beta'];
      beta = [];
   end

   sum_bands

elseif sum_bands == 10  %%%%%%%%%%%%%%%%%%%%%%%%%%%%%%%%%% test sig gen
   for epoch = 1:num_epoch
      for freq = 1:30

         freq_v(freq) = matrix_ch(epoch,freq);
      end
      freq_m = [freq_m, freq_v'];
   end

   sum_bands

end

return;

%%%%%%%%%%%%%%%
```

I.4 Loop through all the channels, compute classification results for each channel

```
%%%%%%%% loop all ch %%%%%%%%

function svm_ch = loop_all_ch(sub, t1, t2, sum_bands)

ss = 1; fft = 1;
eval(['load sub' num2str(sub) '_tst' num2str(t1) '.mat']);
eval(['load sub' num2str(sub) '_tst' num2str(t2) '.mat']);
svm_ch = [];
%tic

eval(['load sub' num2str(sub) '_chanlocs']);
for k = 1:length(this_chanlocs);

eval(['freq_m1 = find_freq_vector(tst' num2str(t1) '(' num2str(k) ',:)" ,' num2str(fft) ',' num2str(ss) ','
num2str(sum_bands) ');']);
eval(['freq_m2 = find_freq_vector(tst' num2str(t2) '(' num2str(k) ',:)" ,' num2str(fft) ',' num2str(ss) ','
num2str(sum_bands) ');']);

m1 = freq_m1';
m2 = freq_m2';

len = min(length(m1), length(m2))
random_v = randperm(len);

m1_tm = [];
m2_trn = [];
m1_tst = [];
m2_tst = [];

for i = 1:round(len/2)              %%%% training set %%%%
   data1 = m1(random_v(i), :);
   m1_tm = [m1_tm; data1];
end

for i = 1:round(len/2)
   data1 = m2(random_v(i), :);
   m2_trn = [m2_tm; data1];
end

for i = round(len/2)+1:len          %%%% testing set %%%%
   data1 = m1(random_v(i), :);
   m1_tst = [m1_tst; data1];
end

for i = round(len/2)+1:len
   data1 = m2(random_v(i), :);
   m2_tst = [m2_tst; data1];
end

tp_trn = ones(round(len/2), 1);
tn_trn = -ones(round(len/2), 1);
tp_tst = ones(len-round(len/2), 1);
tn_tst = -ones(len-round(len/2), 1);

%%%%%%%%%%%%%%%%%%%%%%%%%%%%%%%%


X_trn = [m1_trn; m2_tm];
X_tst = [m1_tst; m2_tst];
t_tm = [tp_tm;tn_trn];
t_tst = [tp_tst;tn_tst];

[nsv, alpha, b0] = svc(X_trn,t_trn, 'linear', 0.1);
predictedY = svcoutput(X_trn,t_tm,X_tst,'linear',alpha,b0,1);
```

```
e = abs(predictedY - t_tst);

mce = mean(e)

t_correct = 0;
for i = 1:length(predictedY)
   if predictedY(i) < 0 && t_tst(i) == -1
      t_correct = t_correct + 1;
   elseif predictedY(i) > 0 && t_tst(i) == 1
      t_correct = t_correct + 1;
   end
end

percent_correct = t_correct/length(predictedY)

ch = [sub, t1, t2, sum_bands, mce, percent_correct, k];
svm_ch = [svm_ch; ch];
end

return;

%%%%%%%%%%%%%%%%%%%%%
```

I.5 Append channel labels to results

```
%%%%%% add channel label  %%%%%%%%%%

%%%%%% add ch_labels %%%%

clear;
for sub = 16:16;
   eval(['load sub' num2str(sub) '_svm_beta_ave']);
   eval(['load sub' num2str(sub) '_labels']);
   k = length(ave_svm)/length(ch_label);
   ch_label_all = [];
   for n = 1:k
      ch_label_all = [ch_label_all; ch_label];
   end

   ave_svm = [ave_svm, ch_label_all];

   eval(['save sub' num2str(sub) '_svm_beta_ave_ch ave_svm']);
end


%%%%%%%%%%%%%%%%%%
```

I.6 Plot topographical plots

```
%%%%%%%%%%% plot topoplot %%%%%%%%%%%%%%

clear all
sub = 17;
eval(['load sub' num2str(sub) '_svm_alpha_ave']);
eval(['load sub' num2str(sub) '_chanlocs']);
k = length(this_chanlocs);
n = 0;
for t1 = 1:1
   for t2 = t1+1:11
                  figure;
                  topoplot(ave_svm(n*k+1:n*k+k, 6), this_chanlocs, 'maplimits',[0,1], 'electrodes', 'labelpoint');
                  eval(['title("sub' num2str(sub) ':  t' num2str(t1) '  t' num2str(t2) '","fontsize", 16 )']);
                  colorbar;
      pic = ['sub' num2str(sub) '_' num2str(t1) '_0' num2str(t2) '_alpha_ave_topo'];
                  eval(['print(gcf, "-dpng","' pic '")']);
      close all;
```

```
    n = n+1;
  end
end

%%%%%
```

I.7 Test SVM toolbox

```
%%%% test SVM toolbox %%%

clear all;

t = 0.005:0.005:60;

% s1 = 2*sin(2*pi*10*t)+3*sin(2*pi*15*t)+4*sin(2*pi*30*t);
% s2 = 2*sin(2*pi*20*t)+5*sin(2*pi*15*t)+1*sin(2*pi*25*t);

test_correct = [];

for k1 = 1:0.5:5
  correct = [];
  for k2 = 14:0.5:18
                s1 = 2*sin(2*pi*10*t)+k1*sin(2*pi*k2*t)+ 2*sin(2*pi*25*t);
                s2 = 2*sin(2*pi*10*t)+3*sin(2*pi*16*t)+2*sin(2*pi*25*t);
                ss = 1; fft = 1; sum_bands = 5;

                eval(['freq_m1 = find_freq_vector_testsvm(s1,' num2str(fft) ',' num2str(ss) ','
num2str(sum_bands) ');']);
                eval(['freq_m2 = find_freq_vector_testsvm(s2,' num2str(fft) ',' num2str(ss) ','
num2str(sum_bands) ');']);

                m1 = freq_m1';
                m2 = freq_m2';

                len = min(length(m1), length(m2))
                random_v = randperm(len);

                m1_tm = [];
                m2_tm = [];
                m1_tst = [];
                m2_tst = [];

                for i = 1:round(len/2)          %%%% training set %%%%
        data1 = m1(random_v(i), :);
        m1_tm = [m1_tm; data1];
                end

                for i = 1:round(len/2)
        data1 = m2(random_v(i), :);
        m2_tm = [m2_tm; data1];
                end

                for i = round(len/2)+1:len          %%%% testing set %%%%
        data1 = m1(random_v(i), :);
        m1_tst = [m1_tst; data1];
                end

                for i = round(len/2)+1:len
        data1 = m2(random_v(i), :);
        m2_tst = [m2_tst; data1];
                end

                tp_trn = ones(round(len/2), 1);
```

```
                tn_trn = -ones(round(len/2), 1);
                tp_tst = ones(len-round(len/2), 1);
                tn_tst = -ones(len-round(len/2), 1);

                %%%%%%%%%%%%%%%%%%%%%%%%%%%%%

                X_trn = [m1_trn; m2_trn];
                X_tst = [m1_tst; m2_tst];
                t_trn = [tp_trn;tn_trn];
                t_tst = [tp_tst;tn_tst];

                %%%%%%%%%%%%%

                [nsv, alpha, b0] = svc(X_trn,t_trn, 'linear', 0.1);
                predictedY = svcoutput(X_trn,t_trn,X_tst,'linear',alpha,b0,1);
                e = abs(predictedY - t_tst);

                mce = mean(e)

                t_correct = 0;
                for i = 1:length(predictedY)
        if predictedY(i) < 0 && t_tst(i) == -1
           t_correct = t_correct + 1;
        elseif predictedY(i) > 0 && t_tst(i) == 1
           t_correct = t_correct + 1;
        end
                end

                percent_correct = t_correct/length(predictedY)

%%%%
   correct = [correct, percent_correct];
   end
   test_correct = [test_correct; correct];
end

%%%%%%%%%%%%%%%%%%
```